ELECTROMAGNETIC THEORY OF DISTRIBUTED FEEDBACK LASERS IN PERIODIC DIELECTRIC WAVEGUIDES

Thesis by

Gary Alan Evans

In Partial Fulfillment of the Requirements

For the Degree of

Doctor of Philosophy

California Institute of Technology

Pasadena, California

1975

(Submitted July 22, 1974)

To Judy Kirk,

who has been good to me

and good for me

Acknowledgments

I would like to express my sincere appreciation to my adviser Professor Charles H. Papas for his encouragement and understanding during the course of this work and throughout my studies at Caltech.

My friend and colleague Dr. Charles Elachi of the Jet Propulsion Laboratory provided me with hours of fruitful discussions and critically read the manuscript. I have enjoyed collaborating with both Dr. Charles Elachi and Professor Cavour Yeh of the University of California at Los Angeles and have benefited from their scientific and technical expertise.

I am happy to acknowledge discussions of the mathematical and numerical aspects of this thesis with Professor Robert McCarty of the University of Santa Clara. Many years ago, he told me about derivatives and integrals when I was working at Chet's Auto Service in Omak, Washington.

Both the Physics section and the Planetology and Oceanography section at the Jet Propulsion Laboratory provided me with computer time and a pleasant, comfortable atmosphere in which to work. Dr. Fred T. Krogh and Dr. Edward W. Ng of the Science and Engineering Computing Section at the Jet Propulsion Laboratory provided valuable information and assistance with the numerical computations.

Financial assistance during my graduate studies was provided at various times by the National Science Foundation and by the California Institute of Technology.

Mrs. Ruth Stratton, Miss Dian Rapchak, and Mrs. Kathy Ellison typed the manuscript. Thanks to all of you.

ABSTRACT

A theory for distributed feedback lasers in transversely bounded structures is developed. The space harmonics approach is used to discuss the general properties of periodic structures. The coupled mode approach is used to develop expressions for the threshold gain, longitudinal mode structure, and electromagnetic field distribution for distributed feedback lasers.

Three basic structures are considered for distributed feedback lasers--thin film waveguides, diffusion waveguides, and fiber waveguides.

Equations for the amplification of a waveguide mode that extends transversely over both regions with and without gain are derived.

Analytical expressions are derived for coupling between modes in periodically perturbed dielectric waveguides. Sinusoidal perturbations of the electric permittivity and of the waveguide boundary are considered.

Theoretical results indicate that an optimum design of distributed feedback lasers can be achieved by an appropriate choice of geometrical parameters. Regions of optimum design are illustrated in numerous plots of normalized threshold gain versus normalized laser frequency.

TABLE OF CONTENTS

Chapter I

INTRODUCTION

This dissertation is a theoretical investigation of active periodic dielectric waveguides. Such structures are known as distributed feedback (DFB) lasers. The principal requirements of any laser source are an optical cavity, feedback, and an active medium to provide optical gain. Conventional laser sources sandwich a material with gain between mirrors. The mirrors provide feedback and the optical cavity is the resulting Fabré-Perot etalon.

For distributed feedback lasers, the optical cavity is a section of a waveguide. The feedback is provided by a periodic perturbation of a waveguide parameter such as the waveguide width or dielectric constant. The periodic perturbation provides a distributed scattering mechanism that couples a forward waveguide mode to a backward waveguide mode. The gain medium can be included inside the waveguide or in the substrate or cladding adjacent to the guiding region. A gain medium is a material that amplifies an electromagnetic wave propagating in the medium. The gain of a medium is defined (see Chapter III) as the natural logarithm of the amplitude growth of the electromagnetic field per unit length.

Distributed feedback lasing structures offer several advantages over conventional lasers. The small size of the optical waveguiding structure reduces pump power and facilitates heat transfer. Additionally, this efficient, stable, compact device is capable of being constructed along with other optical elements on a single block of semiconductor material. The field of integrated optics is concerned

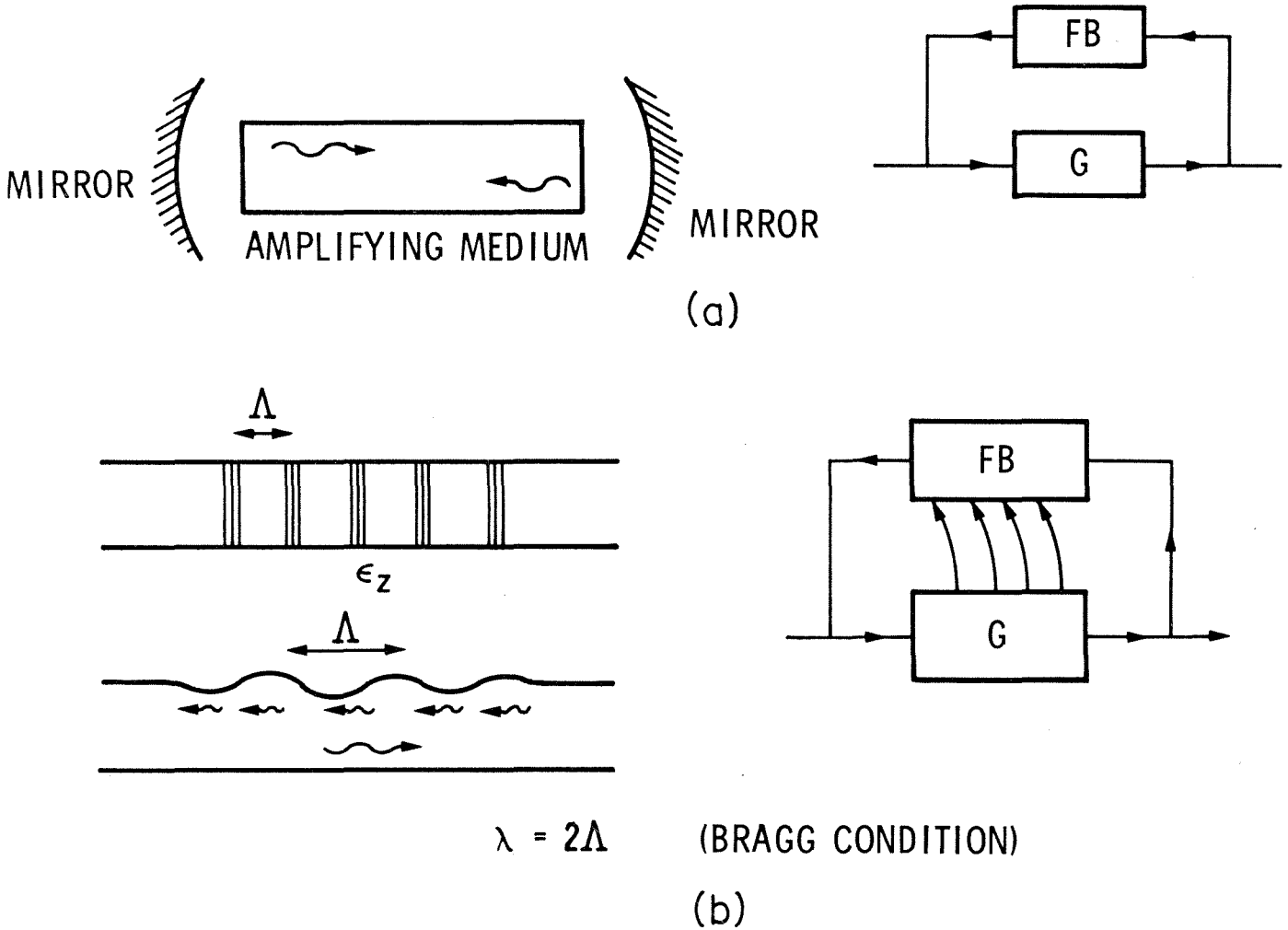

Fig. 1.1 (a) Conventional laser with single feedback path.
(b) Distributed feedback laser with multiple feedback paths.

with the development and fabrication of such optical circuits.

DFB structures also have important applications in high power and high frequency lasers. A serious problem with several high power conventional lasers is mirror burning[13,14] due to high energy density at the mirrors. DFB lasers do away with mirrors, as thousands of periodic perturbations provide the feedback. High frequency lasers, such as a proposed vacuum ultraviolet 800Å superfluid helium laser under consideration at the Jet Propulsion Laboratory, may require mirrors with reflectivity greater than present day materials can provide at the desired lasing wavelength. Of course it is only natural to consider periodic crystals as a cavity for future X-ray lasers, since periodic crystals played a large role in the development of X-rays. In particular, the utilization of naturally occurring minerals and new synthetic analogues of the zeolite class have been proposed as DFB laser and monochromator cavities[15]. The zeolite class has a porous honeycomb structure of long channels with atomic spacing from 7-8Å. Such structures appear ideal for neon K_α radiation at 14.61Å.

The first DFB laser was developed by Kogelnik and Shank[68] in 1971, and since then a number of researchers have reported the development of different types of distributed feedback lasers[59,69-73].

The first theoretical analysis of DFB lasers was that of Kogelnik and Shank[1] for a transversely infinite and homogeneous medium. Marcuse[2] then suggested using distributed feedback in capillary gas lasers, and calculated coupling coefficients between "guided" modes of a hollow dielectric waveguide to estimate the laser threshold based on the analysis of Kogelnik and Shank. The optical cavity of a capillary

gas laser is unlike a conventional dielectric waveguide where the refractive index is larger in the core than in the surrounding medium. In a conventional optical waveguide it is possible to confine light to the core region by making use of total internal reflection of rays that are reflected from the core-cladding interface. In capillary lasers the core region is a gas with a low index of refraction relative to the refractive index of the surrounding medium. No total internal reflection is possible at the core cladding interface and all modes of such a structure are radiation modes. In Chapter V, a scheme to support conventional guided modes in a capillary laser by diffusing impurities into the cladding to provide a guiding structure is studied[4].

Other researchers have proposed analyses for dielectric slab waveguide DFB lasers. Wang[5,6] considered thin film waveguides and used the waveguide structure to calculate a reduced value of the coupling constant derived by Kogelnik and Shank. DeWames and Hall[7] used a space harmonics method and derived solutions identical to those of Kogelnik and Shank with analytic expressions for the reduction of both the coupling and threshold gain coefficients due to field penetration beyond the active medium.

Both the above analyses require the forward and backward waves to be the same mode, and the active medium is considered to be in the guide.

Applications of the distributed feedback principle have been theoretically applied to hybrid laser structures. Chinn[8] has extended

the analysis of Kogelnik and Shank for the case of mirror reflectivity at the end faces of a DFB structure. Shubert and Anderson[9], Wang[6], and Shubert[10,25] have considered nonuniform distributed feedback lasers where the distributed feedback and gain regions are nonuniform over the laser structure.

The treatment in this dissertation begins in Chapter II with a different formulation of the coupled mode theory for DFB lasers that allows the forward and backward waves to experience different gain (or attenuation) and travel with different group velocities. This approach is especially applicable to cases where the forward and backward waves are different modes of the guiding structure.

The third chapter calculates the effective gain of a waveguide mode. For practical DFB devices, the gain medium is either in the guiding region or in the substrate or cladding surrounding the guiding medium. The energy of a waveguide mode, however, is spread over portions of both regions. Solving the dispersion relations of the waveguide with complex dielectric constants allows solving for an effective gain for the mode. The effective gain is a function of mode number and frequency and is used to calculate the gain of the forward and backward waves considered in Chapter II.

The fourth chapter treats coupling between modes of a waveguide due to a periodic perturbation of a waveguide parameter. The analytical expressions derived for the coupling coefficients are good for all frequencies and waveguide dimensions with the constraints that the periodic boundary perturbation (ηW) be small ($\leq 10\%$) compared to the laser oscillation wavelength, and the permittivity perturbation ($\eta\varepsilon$)

be much less than ε.

In Chapter V, theoretical results are obtained for three basic types of DFB dielectric waveguide lasers. The first waveguide structure considered is a thin film or dielectric slab. A thin film DFB laser would be an ideal source of radiation for planar waveguide optics in the emerging field of integrated optics.

The next structures considered are optical waveguides formed by diffusion. Considerable interest has been expressed recently in such waveguides, as the diffusion process circumvents the difficulty of growing suitable thin single-crystal layers.

The final structure analyzed is an optical fiber waveguide. If a region of a fiber incorporated a laser source, the complicated problem of coupling light from an external source vanishes.

A major result of Chapter V is that for a given waveguide structure and lasing wavelength there is usually an optimum choice of geometric parameters that result in a minimum required threshold gain[11].

Chapter II

Distributed Feedback Laser Theory

The study of distributed feedback lasers is in large part a study of electromagnetic wave propagation in periodic structures. Propagation of waves in periodic media was discussed as early as 1887 by Lord Rayleigh[48] and later by Strutt[49] and Van der Pol and Strutt[50]. A detailed and comprehensive review of the work on waves in periodic structures as of the late 1940's can be found in Wave Propagation in Periodic Structures[47] by Leon Brillouin. The work concerning waves in periodic structures has not been limited to optical waves, but covers the electromagnetic spectrum from microwaves to X-rays as well as mechanical waves, vibrational waves, and electrons in crystals[51].

Two major approaches are used in the study of periodic structures: the exact space harmonics (Floquet) approach and the approximate coupled mode approach. In this chapter we begin with a review of the space harmonics approach to discuss the general properties of periodic structures.

The space harmonics formalism provides exact solutions but is somewhat cumbersome. For this reason, in Section B we use the coupled mode approach to obtain coupled wave equations for DFB lasers in guiding structures. The coupled wave equations are then solved in Section C to obtain general equations for the required threshold gain (i.e., the gain the material is required to have before there is any oscillation or light output), longitudinal mode distribution, and longitudinal field distribution.

In Appendix D, the relation between space harmonics and coupled mode theory is explored. We find that for the applications considered in this dissertation, the approximations required by the coupled mode approach are valid. This result is not surprising because coupled wave formalism has been successfully employed to describe X-ray diffraction[16], light diffraction by acoustic waves[17,33], and electro-optic gratings[18], and the properties of thick film holograms[19,52].

A. Space Harmonics

To illustrate the principles of the space harmonics formalism, we consider the problem of propagation of a transverse electric wave ($\underline{E} = \underline{e}_y E_y$ and $\underline{H} = \underline{e}_x H_x + \underline{e}_z H_z$) along a dielectric waveguide where the permittivity in the guiding region is periodically perturbed (see Fig. 21b).

We begin with Maxwell's equations:

$$\nabla \times \underline{E} = -\mu \frac{\partial \underline{H}}{\partial t} \tag{2.1a}$$

$$\nabla \times \underline{H} = \frac{\partial}{\partial t}(\varepsilon \underline{E}) + \underline{J} \tag{2.1b}$$

$$\nabla \cdot \underline{H} = 0 \tag{2.1c}$$

$$\nabla \cdot \varepsilon \underline{E} = \rho \tag{2.1d}$$

and the medium constants are

$$\mu = \mu_o \quad , \text{ the free space magnetic permeability}$$

$$\varepsilon(z) = \varepsilon_o \varepsilon_1 (1 + \eta \cos Kz) \qquad \text{(perturbation region)} \tag{2.2a}$$

SURFACE PERTURBATION

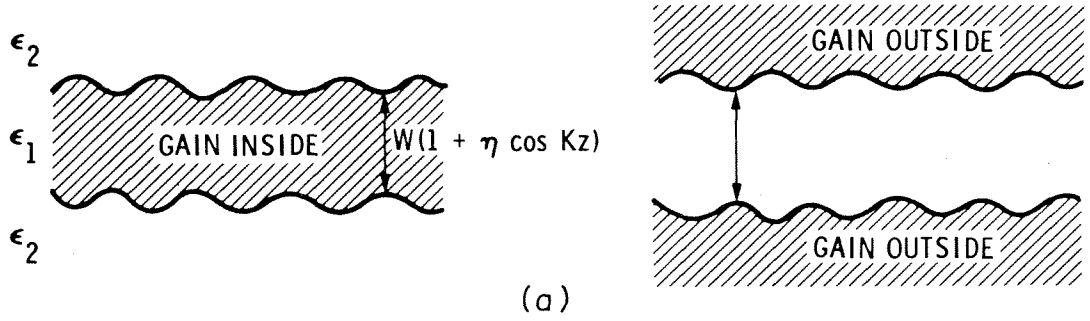

(a)

VOLUME PERTURBATION OF DIELECTRIC CONSTANT INSIDE GUIDE

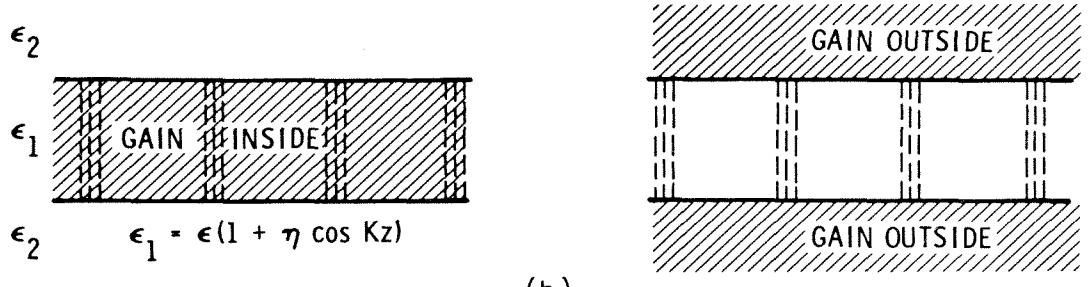

(b)

VOLUME PERTURBATION OF DIELECTRIC CONSTANT OUTSIDE GUIDE

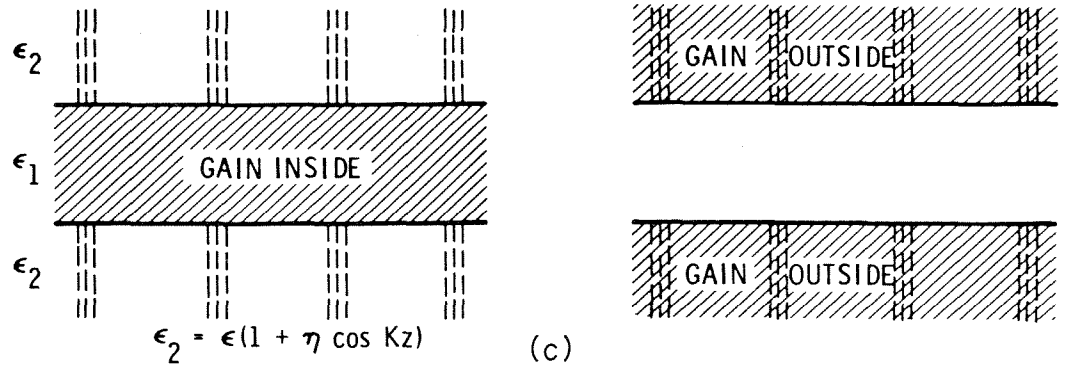

(c)

Fig. 2.1 Possible configurations for DFB lasers: (a) waveguide boundary perturbation, (b) periodic permittivity inside the waveguide, (c) periodic permittivity in the substrate. The active medium can be either in the waveguide or in the substrate.

$$\varepsilon(z) = \varepsilon_o \varepsilon_2 \qquad \text{(homogeneous region)} \qquad (2.2b)$$

where

ε_o = free space electric permittivity

$\varepsilon_1, \varepsilon_2$ = relative permittivity of the undisturbed dielectric in the perturbation region or homogeneous region

η = amplitude of the relative permeability change

$K = 2\pi/\Lambda$, the wave vector of the periodic disturbance

Λ = the wavelength of the periodic disturbance

Equation (2.2a) is the expression for the electric permittivity in the guiding region, and (2.2b) the expression outside the guiding region.

We reduce Maxwell's equations to the monochromatic state[36] by choosing $\exp(-i\omega t)$ for the time dependence.

Maxwell's equations give the wave equation in a current and source-free periodic medium for TE waves as

$$\frac{\partial^2 E_y}{\partial x^2} + \frac{\partial^2 E_y}{\partial y^2} + \frac{\partial^2 E_y}{\partial z^2} + \varepsilon_{rel}(z)\, k^2 E_y = 0 \qquad (2.3)$$

where

$$k^2 = \omega^2 \mu_o \varepsilon_o = \omega^2/c^2 \qquad (2.4)$$

c is the speed of light in vacuum, and

$$\varepsilon_{rel}(z) = \varepsilon(z)/\varepsilon_o$$

By (2.2a)

$$\varepsilon(z + \Lambda) = \varepsilon(z) \qquad (2.5)$$

and therefore (2.3) is a partial differential equation with periodic

coefficient $\varepsilon(z)$ and can be solved with the help of a representation commonly referred to as Floquet's theorem[37-40]. This theorem is actually a generalization to linear partial differential equations of a theorem in ordinary linear differential equations with periodic coefficients established by Floquet[42]. Such generalizations have been carried out by Bloch[43], and more recently by Odeh and Keller[41]. Applied to (2.3), Floquet's theorem may be stated as follows[37]: A time harmonic electromagnetic field $E_y(x,y,z)$ of a normal mode guided along an axially periodic structure possesses the property

$$E_y(x,y,z+\Lambda) = e^{i\beta\Lambda} E_y(x,y,z) \tag{2.6}$$

The Floquet wave vector β is referred to as the fundamental propagation constant.

For the sake of simplicity, we consider the guiding structure to depend transversely only on the x coordinate, and assume the structure infinitely homgeneous in the y coordinate. We can therefore assume no E_y dependence on y.

If we define $P(x,z)$ by

$$E_y(x,z) = e^{i\beta z} P(x,z) \tag{2.7}$$

we verify from (2.6) that

$$P(x,z+\Lambda) = P(x,z) \tag{2.8}$$

Equations (2.7) and (2.8) constitute an equivalent statement of Floquet's theorem for axially periodic structures, and says that the cross sectional field distribution of a periodic structure remains

unchanged under an axial translation of the observation point through a distance Λ, while the mode amplitude multiplies itself by a constant $e^{i\beta\Lambda}$.

Hessel[37] distinguishes $P(x,z)$ as the local "microscopic" field structure within a period, and $E_y(x,z)$ given by (2.7) as the guided-wave field at any point on an infinite periodic structure.

We now expand $P(x,z)$ in a Fourier series

$$P(x,z) = \sum_{n=-\infty}^{\infty} d_n a_n(x)\, e^{inKz} \tag{2.9}$$

and substitute into (2.7):

$$E_y(x,z) = e^{i\beta z} \sum_{n=-\infty}^{\infty} d_n a_n(x)\, e^{inKz} = \sum_{n=-\infty}^{\infty} d_n a_n(x)\, e^{i(\beta+nK)z} \tag{2.10}$$

The expansion (2.10) indicates the field is expressible as an infinite sum of travelling waves of the form $d_n a_n(x) \exp[i(\beta + nK)z]$. These travelling waves are commonly called space harmonics. The wave vectors $\beta+nK$ represent the spatial harmonic longitudinal propagation constants while d_n denotes the corresponding spatial harmonic amplitudes, and $a_n(x)$ denotes the normalized (at the boundary) transverse dependence.

If we write (2.2a) in the exponential form

$$\varepsilon(z) = \varepsilon_o\varepsilon_1\left[1 + \frac{\eta}{2} e^{iKz} + \frac{\eta}{2} e^{-iKz}\right] \tag{2.11}$$

we can insert (2.10) into (2.3) and obtain

$$\sum_{n=-\infty}^{\infty} \{d_n \frac{d^2 a_n(x)}{dx^2} + [-(\beta+nK)^2 + \varepsilon_1 k^2]\, d_n a_n(x)$$

$$+ \varepsilon_1 \frac{\eta}{2} k^2 d_{n+1} a_{n+1}(x) + \varepsilon_1 \frac{\eta}{2} k^2 d_{n-1} a_{n-1}(x)\} e^{i(\beta+nK)z} = 0 \tag{2.12}$$

inside the perturbation region and

$$\sum_{n=-\infty}^{\infty} \{d_n \frac{d^2 a_n(x)}{dx^2} + [-(\beta+nK)^2 + \varepsilon_2 k^2]\, d_n a_n(x)\} e^{i(\beta+nK)z} = 0 \tag{2.13}$$

outside the perturbation region.

Solutions of equations of the form (2.12) and (2.13) with boundary conditions have been discussed by Chu and Tamir[33], Elachi and Yeh[20,22], Dabby et al[53], and others[37,38,39,40]. The method requires the variables $a_n(x)$ and d_n to be solutions of the infinite set of homogeneous equations

$$D_n a_n(x) d_n + a_{n+1}(x) d_{n+1} + a_{n-1}(x)\, d_{n-1} = 0 \tag{2.14a}$$

where

$$D_n = 2 \frac{\dfrac{d^2 a_n(x)}{dx^2} \Big/ a_n(x) - (\beta+nK)^2 + \varepsilon_1 k^2}{\varepsilon_1 \eta k^2} \tag{2.14b}$$

inside the guiding region, and

$$\frac{d^2 a_n(x)}{dx^2} \Big/ a_n(x) - (\beta+nK)^2 + \varepsilon_2 k^2 = 0 \tag{2.15}$$

outside the guiding region. Equations (2.14a,b) and (2.15) follow by requiring (2.12) and (2.13) to be satisfied for all values of z. In principle, the ratios d_n/d_o, the $a_n(x)$ and the dispersion relation

for the guiding structure may be determined from the infinite set of three-term recurrence relations resulting from (2.12) and (2.13) and the requirement at the boundary between the perturbation region and the homogeneous region that the tangential electric and magnetic fields be continuous. For the case of distributed feedback lasers in a periodic guiding structure, the term d_o is ultimately determined from the incident pumping power that provides population inversion in the gain medium.

For clarity, let us consider the simple case of a wave propagating in a transversely unbounded periodic medium[21] (Fig. 2.2). Equations (2.14a,b) become

$$D_n d_n + d_{n+1} + d_{n-1} = 0 \tag{2.16a}$$

and

$$D_n = \frac{2}{\eta}\left[1 - \left(\frac{\beta + nK}{k\sqrt{\varepsilon_1}}\right)^2\right] \tag{2.16b}$$

This system of equations is the basic result of the space harmonics approach. It shows that each space harmonic n is coupled to the two neighboring space harmonics $n-1$ and $n+1$. Using matrix notation, we can write

$$\underline{\underline{D}} \cdot \underline{\underline{A}} = 0 \tag{2.17a}$$

where

$$\underline{\underline{A}} = \begin{pmatrix} \vdots \\ d_{-1} \\ d_o \\ d_1 \\ \vdots \end{pmatrix} \tag{2.17b}$$

and

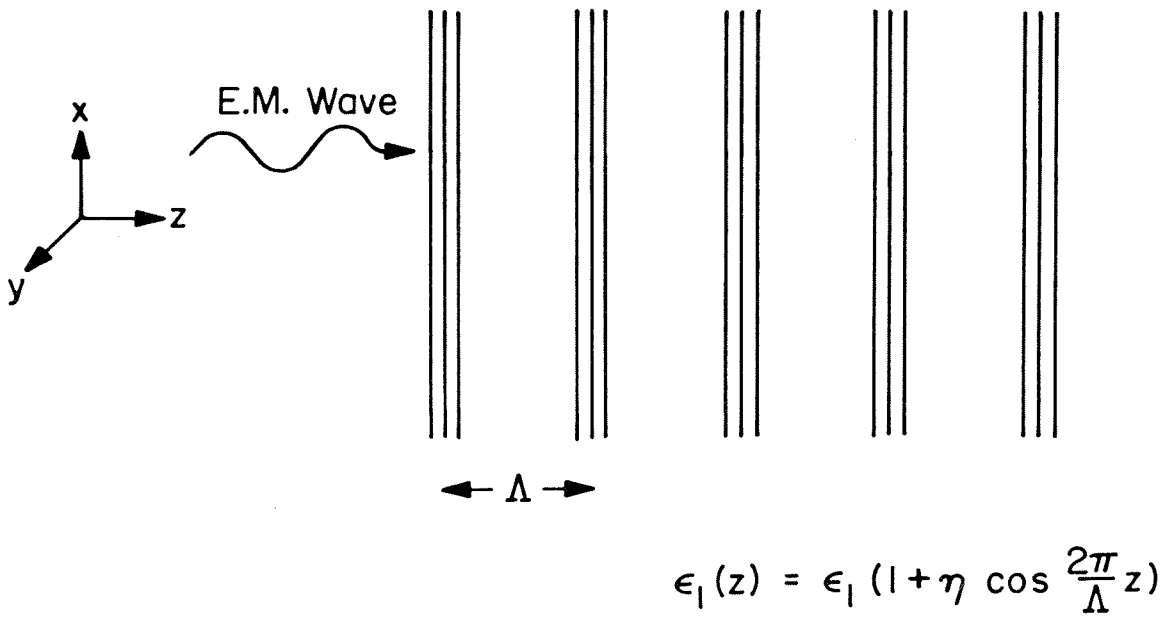

Fig. 2.2 Electromagnetic wave propagating in an infinite, unbounded periodic medium.

$$\underline{\underline{D}} = \begin{pmatrix} 1 & D_{-1} & 1 & 0 & 0 \\ 0 & 1 & D_0 & 1 & 0 \\ 0 & 0 & 1 & D_1 & 1 \end{pmatrix} \qquad (2.17c)$$

As there are no boundaries in our simple infinite periodic media case, the relative amplitudes d_n/d_o can be determined from (2.17a)[21]. The nontriviality condition

$$\det(D) = 0 \qquad (2.18)$$

is the dispersion relation and gives the value of β as a function of k or ω.

Equation (2.18) in general must be solved numerically. However, we can obtain an understanding of the properties of the solution by introducing the periodic perturbation in an infinitesimal fashion so that the original guiding structure is really unperturbed. The effect of these negligible periodic perturbations is to introduce the infinite number of space harmonics but to leave undisturbed the shape of the initial dispersion curve.

For η infinitesimally small, equation (2.16b) reduces to

$$\eta D_n = 0 \Longrightarrow \quad \beta = \pm\sqrt{\varepsilon_1}\, k - nK \qquad (2.19)$$

The corresponding Brillouin diagram (Fig. 2.3) consists of an infinite number of "subdiagrams" which correspond to the different space harmonics, and each is identical to the diagram of the homogeneous case.

If we take η finite but small ($\eta << 1$), we can write the electric field expression approximately as[21]

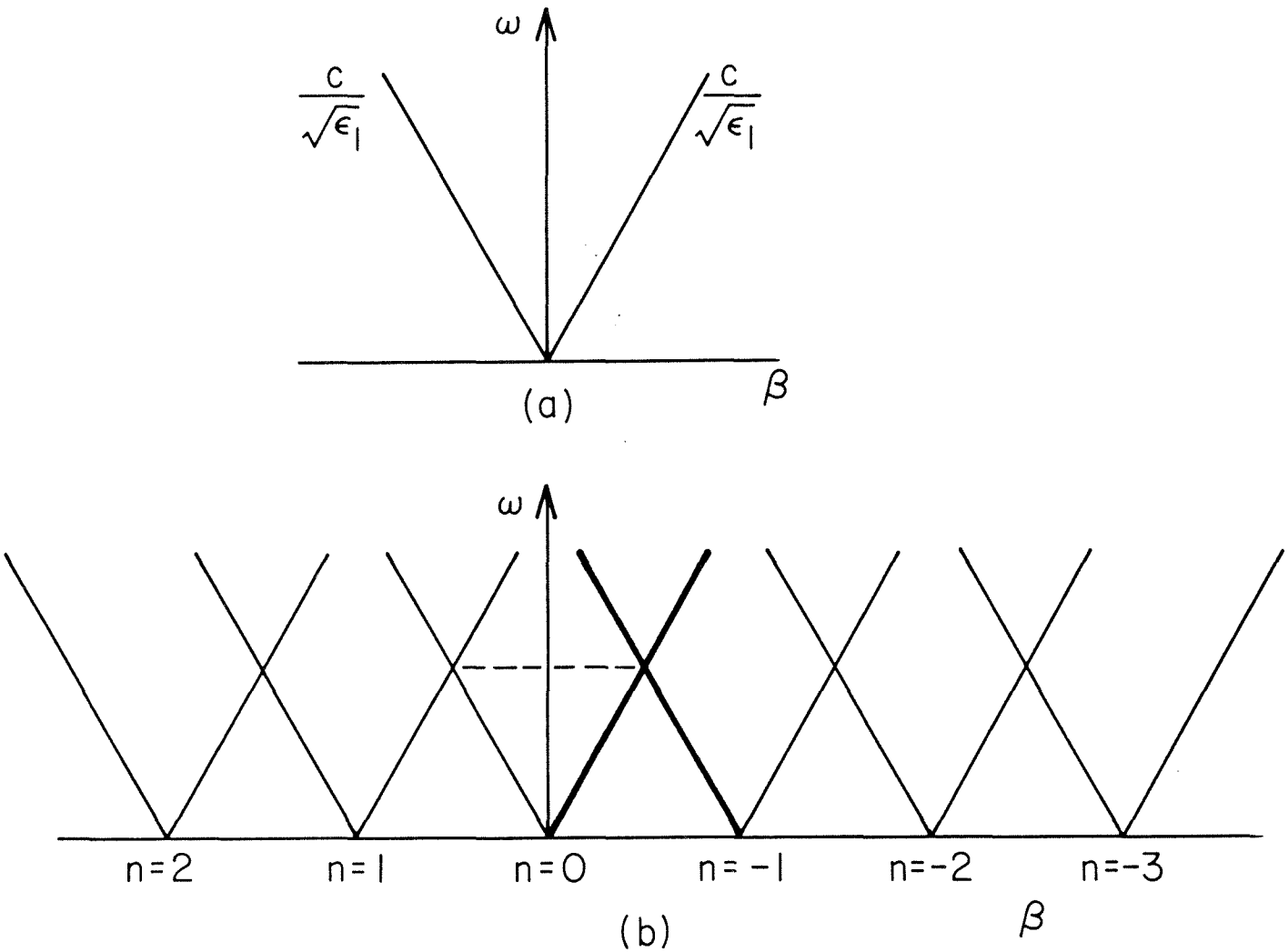

Fig. 2.3 (a) ω-β diagram for an unperturbed, homogeneous, infinite medium. (b) ω-β diagram for an infinite medium after introduction of a period perturbation.

$$E_y = (d_o + d_1 e^{iKz} + d_{-1} e^{-iKz}) e^{i\beta z} \tag{2.20}$$

where we neglect all other space harmonics. The system of equations (2.16a) becomes

$$D_o' d_o + \frac{\eta}{2} d_1 + \frac{\eta}{2} d_{-1} = 0 \tag{2.21a}$$

$$D_1' d_1 + \frac{\eta}{2} d_o = 0 \tag{2.21b}$$

$$D_{-1}' d_{-1} + \frac{\eta}{2} d_o = 0 \tag{2.21c}$$

where

$$D_n' = \frac{\eta}{2} D_n = 1 - \left(\frac{\beta + nK}{k\sqrt{\varepsilon_1}}\right)^2 \tag{2.22}$$

For most values of k, D_{-1}' and D_1' are large compared to η, and therefore from (2.21b,c) we see that d_1 and d_{-1} are small compared with d_o, and to satisfy (2.21a) we must have

$$D_o' \simeq 0 \tag{2.23}$$

which gives the same dispersion equation as in the unperturbed medium:

$$\beta = \sqrt{\varepsilon_1}\ k \tag{2.24}$$

However, it is possible that not only $D_o' \simeq 0$, but simultaneously D_1' or $D_{-1}' \simeq 0$. Let us suppose the parameters of the problem are such that

$$D_o' \simeq 0 \implies \beta^2 = k^2 \varepsilon_1 \tag{2.25}$$

and

$$D'_{-1} \simeq 0 \implies (\beta-K)^2 = k^2\varepsilon_1 \tag{2.26}$$

From (2.25) and (2.26) this occurs if

$$\beta^2 - 2\beta K + K^2 \simeq \beta^2 \tag{2.27}$$

which requires

$$\beta \simeq K/2 \tag{2.28}$$

In this case we still have $d_1 << d_o$, but we can no longer say $d_{-1} << d_o$. The system of equations for the region around the interaction point ($k_o = \omega_o/c$, $\beta_o = \sqrt{\varepsilon_1}\, k_o$, $\beta_o = K/2$) becomes

$$D'_o\, d_o + \frac{\eta}{2} d_{-1} = 0 \tag{2.29a}$$

$$D'_{-1} d_{-1} + \frac{\eta}{2} d_o = 0 \tag{2.29b}$$

The nontrivial solution of (2.29a,b) requires

$$D'_o D'_{-1} = \frac{\eta^2}{4} \tag{2.30}$$

In the neighborhood of the intersection point we can write

$$\beta = \beta_o + \Delta\beta \tag{2.31a}$$

$$k = k_o + \Delta k \tag{2.31b}$$

to give

$$D_0'D_{-1}' = [1 - (\frac{\beta_o + \Delta\beta}{(k_o+\Delta k)\sqrt{\varepsilon_1}})^2][1 - (\frac{-\beta_o + \Delta\beta}{(k_o+\Delta k)\sqrt{\varepsilon_1}})^2] = \frac{\eta^2}{4} \qquad (2.32)$$

Expanding and using

$$(1 + \xi_1)\Big/(1 + \xi_2) = 1 + \xi_1 - \xi_2 \qquad (2.33)$$

for ξ_1, ξ_2 small, we obtain

$$(\frac{\Delta\omega}{\omega_o})^2 - (\frac{\Delta\beta}{\beta_o})^2 = (\frac{\eta}{4})^2 \qquad (2.34)$$

For $|\Delta\omega/\omega_o| < \eta/4$, we write equation (2.34) as

$$\frac{\Delta\beta}{\beta_o} = \pm i \sqrt{(\frac{\eta}{4})^2 - (\frac{\Delta\omega}{\omega_o})^2} \qquad (2.35)$$

which is the equation of an ellipse. This region is called a stop-band interaction and it corresponds to an exponential energy transfer between the two interacting waves as $\Delta\beta$ is imaginary. For $|\Delta\omega/\omega_o| > \eta/4$, equation (2.34) may be written as

$$\frac{\Delta\beta}{\beta_o} = \pm \sqrt{(\frac{\Delta\omega}{\omega_o})^2 - (\frac{\eta}{4})^2} \qquad (2.36)$$

which corresponds to a hyperbola with asymptotes corresponding to the unperturbed ($\eta = 0$) medium. The Brillouin diagram near an intersection region is shown in Fig. 2.4.

Using equation (2.29a), we can calculate the ratios of the amplitudes of the space harmonics:

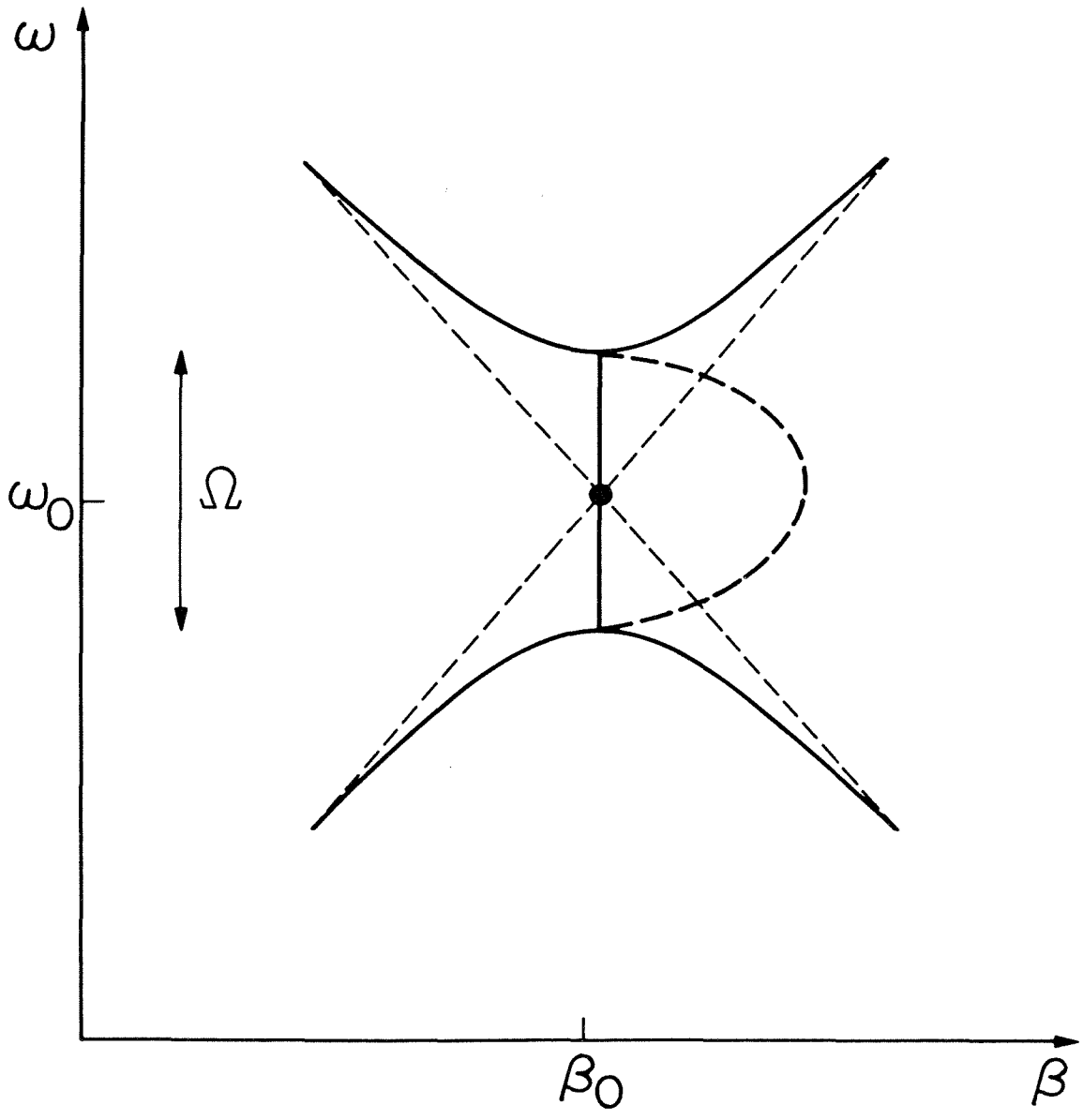

Fig. 2.4 ω-β diagram near an interaction region. The solution for β is complex. The dashed curve is the imaginary part of β and the solid curve is the real part of β.

$$\left|\frac{d_{-1}}{d_0}\right| = \left|\frac{2}{\eta} D_0'\right| = \left|\frac{4}{\eta}\left[\frac{\Delta\beta}{\beta_0} - \frac{\Delta\omega}{\omega_0}\right]\right| \tag{2.37}$$

Using (2.34), we see that for $\Delta\omega = 0$

$$\left|\frac{d_{-1}}{d_0}\right| = 1 \tag{2.38}$$

To summarize our discussion of a plane wave propagating in an infinite, unbounded periodic medium, we conclude that the complete field solution is seen to consist of an infinite number of space harmonics, and the complete dispersion curve of an infinite number of branches. Except near the stop bands, the amplitude of the $n = 0$ space harmonic is dominant. At the stop bands, the amplitudes of the two space harmonics which cross to produce the stop band are large and equal, and can be physically interpreted as producing the standing wave ($d\omega/d\beta = 0$ at the band edges) associated with the stop band. Near the stop bands, the amplitudes of the other space harmonics generally increase. Cassedy[38] and Hessel[54] have computed numerically the relative harmonic amplitudes d_n/d_0 in and around the stop band regions. For $\eta = 0.4$, $|d_{-1}|/|d_0| \simeq 1$, throughout the stop band region, and the next largest ratio $|d_1|/|d_0|$ is about 0.1. Of the remaining harmonics, only the d_2, d_{-2}, d_3, d_{-3} have amplitude ratios greater than 10^{-4}.

If we now consider the case of a bounded periodic medium, by analogy with the unbounded case, the Brillouin diagram for a periodic dielectric waveguide consists of an infinite number of "subdiagrams" as illustrated in Fig. 2.5. Strong coupling occurs at the intersection

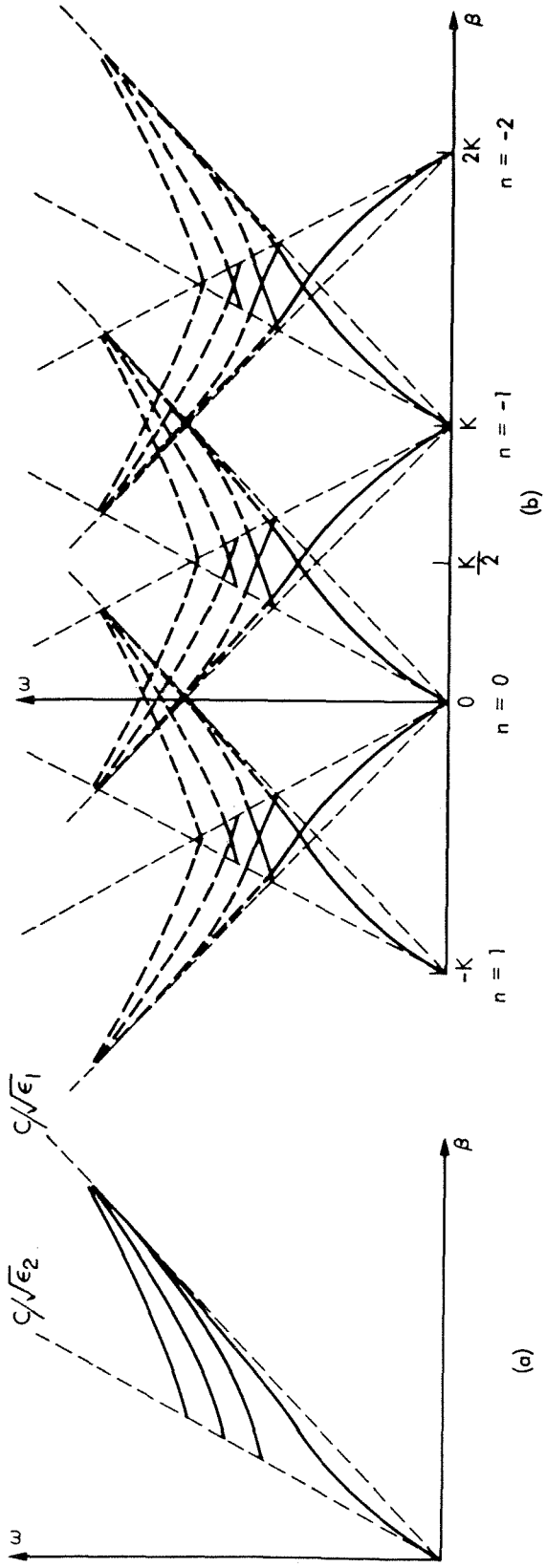

Fig. 2.5 (a) ω-β diagram (Brillouin diagram) for a typical dielectric waveguide. (b) ω-β diagram for a typical periodic dielectric waveguide.

points between different harmonics, leading to energy transfer between modes. Two types of coupling can occur, depending on the choice of K, the wave vector of the perturbation (Fig. 2.6). As illustrated in Fig. 2.6a, the group velocities of the two coupled harmonics can be parallel. In this case the energy is transferred back and forth between two harmonics propagating in the same direction. This type of coupling is termed codirectional. Contradirectional coupling, where the group velocities are antiparallel (Fig. 2.6b) provides the feedback mechanism for DFB lasers. In Chapter IV the contradirectional mode coupling indicated in Fig. 2.6b is calculated using an approximate analytical method rather than the numerical method of space harmonics.

In the infinite medium case only a forward and backward mode exists in the $n = 0$ or central curve of the Brillouin diagram. A dielectric waveguide can support several discrete guided modes and a continuum of radiation modes[20,33]. [For a discussion of the radiation modes of a dielectric waveguide, see the treatment by Collin [29] and Marcuse[34].] An exact solution[20,33] of the dispersion relations for a periodic dielectric waveguide gives rise to guided and radiation modes as in the homogeneous dielectric guide, as expected. We are concerned only with perturbations which couple guided modes and therefore the radiation modes are neglected. As illustrated in Fig. 2.7, when the wave vector K of the perturbation is chosen to couple guided modes, there is no interaction with the region of radiation modes. With this consideration, the field expression given by (2.10) can be written to show explicitly the guided mode behavior:

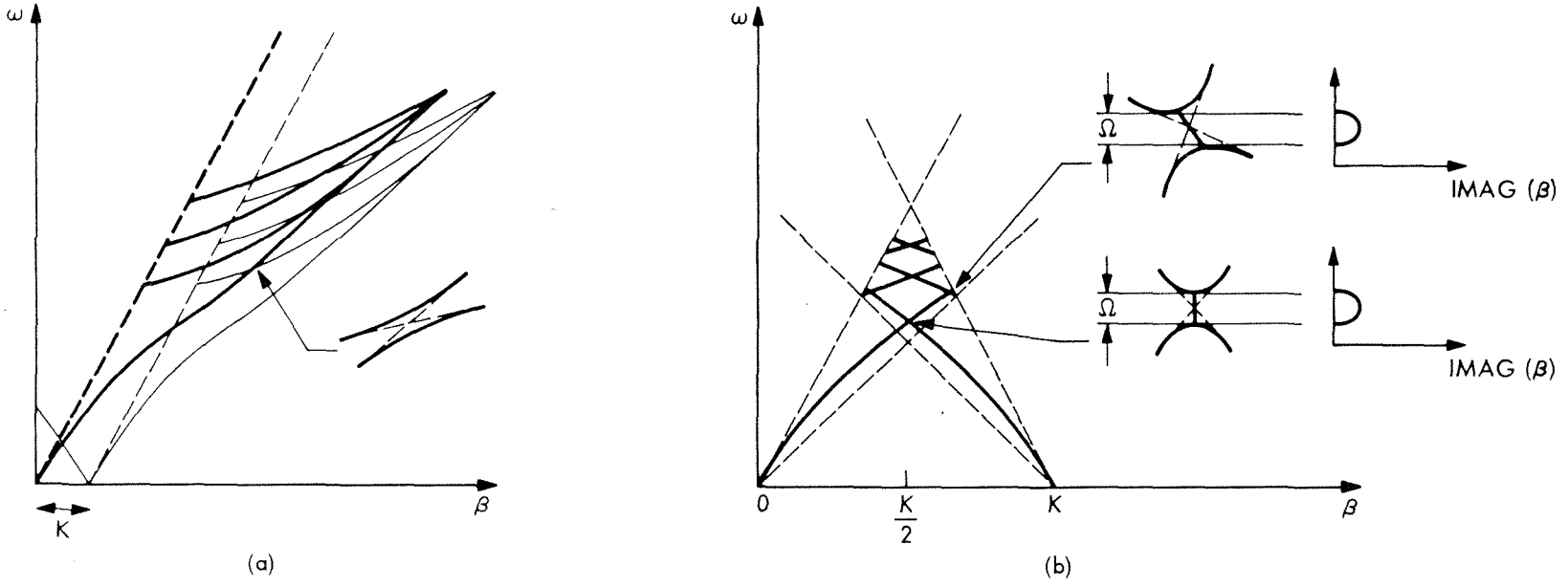

Fig. 2.6 Interaction regions between two space harmonics, (a) codirectional interaction, (b) contradirectional symmetric and nonsymmetric interaction.

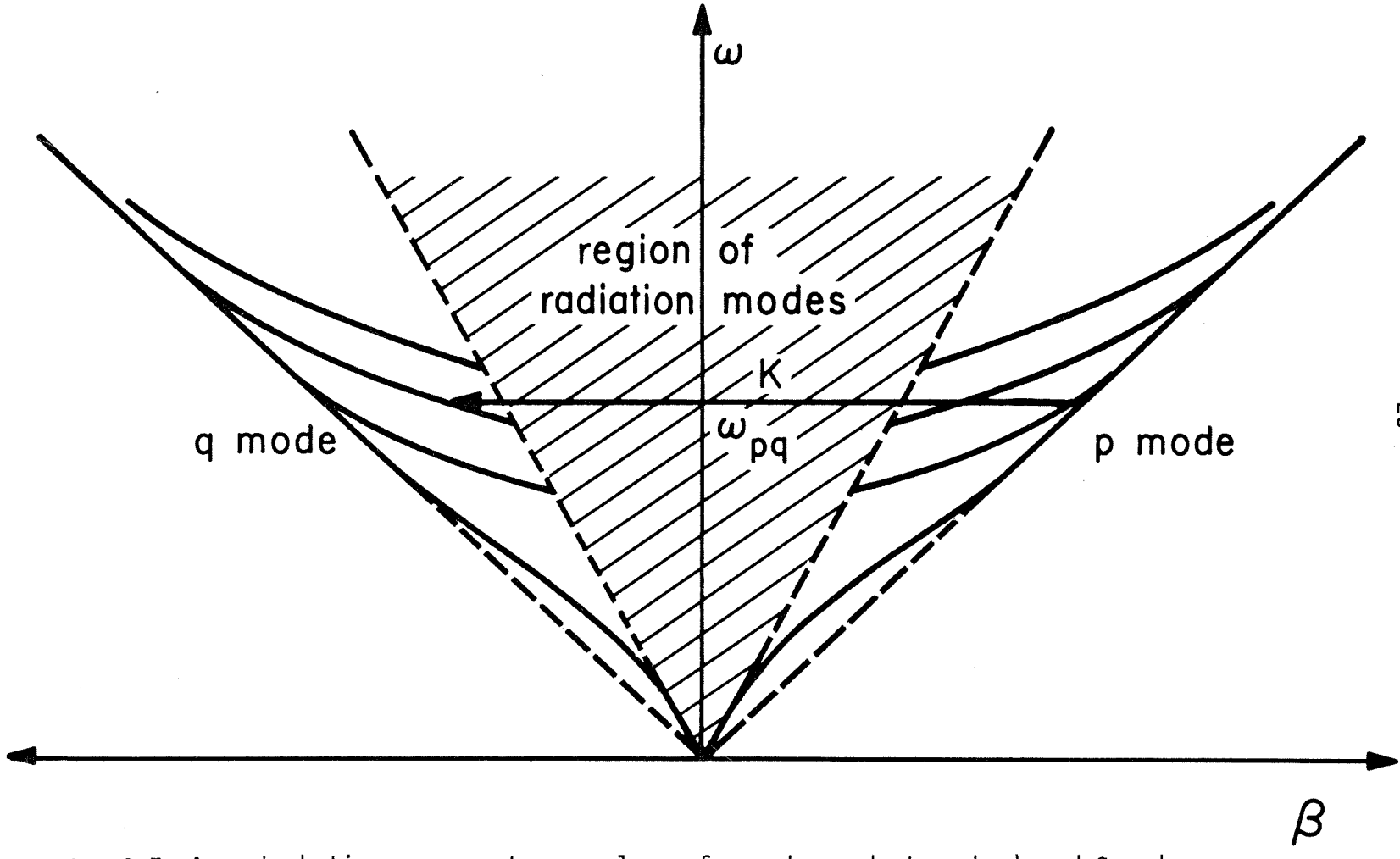

Fig. 2.7 A perturbation wave vector couples a forward p mode to a backward q mode.

$$E_y(x,z) = \sum_{n=-\infty}^{\infty} \sum_{r=-R}^{R} d_{n,r} a_{n,r}(x)\, e^{i(\beta_r + nK)z} \tag{2.39}$$

where β_r is the $(r-1)^{th}$ solution of the dispersion relations discussed previously, $d_{n,r}$ is the corresponding amplitude of the n^{th} harmonic of the r^{th} guided mode, and $a_{n,r}(x)$ the corresponding transverse dependence of the n^{th} harmonic of the r^{th} guided mode. The summation over r extends over the $2R$ guided modes (counting a forward and the corresponding backward wave as two modes) that exist at a given frequency ω.

In this section we have only discussed periodic perturbations of the dielectric constant. Dielectric waveguides having periodically corrugated surfaces follow a similar space harmonics analysis[20,53] and have the same characteristic stop bands and pass bands. In Chapter IV the stop band regions due to periodic surface perturbations of dielectric waveguides are analyzed.

B. Coupled Mode Theory

We consider a forward wave $a_p(x)\, d_p(z)\, e^{i\beta_{po}z}$ and a backward wave $a_q(x)\, d_q(z)\, e^{-i\beta_{qo}z}$ to be travelling in a dielectric waveguide with a periodic perturbation of the electric permittivity. In this section we deviate from the convention in other sections and consider both β_{po} and β_{qo} to be positive. The coefficient $a_r(x)$ is the transverse field distribution of the r^{th} guided mode, $d_r(z)$ is the amplitude of the r^{th} guided mode, and β_{ro} is the longitudinal wave vector of the r^{th} mode at the Bragg frequency ω_o (see Fig. 2.5a). The

resulting electric field can thus be written

$$E_{pq}(x,z) = a_p(x)\, d_p(z)\, e^{i\beta_{po}z} + a_q(x)\, d_q(z)\, e^{-i\beta_{qo}z} \qquad (2.40)$$

To formulate the coupled mode theory, we begin by ignoring the effect of the electric permittivity perturbation on the transverse mode behavior. This effect is later considered in Chapter IV where first order correction terms to the transverse mode functions are calculated.

From our discussion of space harmonics we know that strong contradirectional mode coupling due to Bragg scattering can occur if $K = \beta_{po} + \beta_{qo}$. Since we desire the coupled mode theory for distributed feedback lasers, we must consider the dielectric waveguide medium to be active. Thus a wave travelling in this medium is amplified (or "experiences gain"). Mathematically we can represent an active medium with an imaginary component of the dielectric constant. Physically, the relative imaginary component is very small, only as large as 10^{-3} for high gain lasers (see Chapter III), and because the relative real component of the dielectric constant is always greater than or equal to one, the effect of gain can be treated as a perturbation. If we consider the region of inhomogeneous permittivity and the active region to be in the guiding region of a waveguide structure, equations (2.2a,b) become

$$\varepsilon(z) = \begin{cases} \varepsilon_o\varepsilon_1(1 + \eta \cos Kz) - i\varepsilon_o\varepsilon_i & \text{(guiding region)} \\ \varepsilon_o\varepsilon_2 & \text{(homogeneous region)} \end{cases} \qquad (2.41)$$

Using (2.40), (2.41a,b) in the wave equation (2.3), and defining

$$\varepsilon_{1,2} = \varepsilon_1 h(x) + \varepsilon_2(1 - h(x)) \tag{2.42}$$

where

$$h(x) = \begin{cases} 1 & \text{guiding region} \\ 0 & \text{homogeneous region} \end{cases} \tag{2.43}$$

we obtain

$$\frac{d^2a_p(x)}{dx^2} d_p(z)\, e^{i\beta_{po}z} + \frac{d^2a_q(z)}{dx^2} d_q(z)\, e^{-i\beta_{qo}z}$$

$$+ a_p(x)\left[-\beta_{po}^2 d_p(z) + 2i\beta_{po} \frac{d\, d_p(z)}{dz} + \frac{d^2 d_q(z)}{dz^2}\right] e^{i\beta_{po}z}$$

$$+ a_q(x)\left[-\beta_{qo}^2 d_q(z) - 2i\beta_{qo} \frac{d\, d_q(z)}{dz} + \frac{d^2 d_q(z)}{dz^2}\right] e^{-i\beta_{qo}z}$$

$$+ k^2[\varepsilon_{1,2} - i\varepsilon_i h(x)][a_p(x)d_p(z)e^{i\beta_{po}z} + a_q(x)d_q(z)e^{-i\beta_{qo}z}]$$

$$+ \frac{\varepsilon_1 \eta\, h(x)\, k^2}{2}[\, a_p(x)d_p(z)(e^{i(\beta_{po}+K)z} + e^{i(\beta_{po}-K)z})$$

$$+ a_q(x)\, d_q(z)(e^{-i(\beta_{qo}-K)z} + e^{-i(\beta_{qo}+K)z})] = 0 \tag{2.44}$$

From the solutions of the unperturbed waveguides (see Appendices A,B,C)

$$\frac{d^2a_r(x)}{dx^2} \Big/ a_r(x) + k^2(\varepsilon_{1,2}) = \beta_r^2 \tag{2.45}$$

and using

$$\beta_{po} + \beta_{qo} = K \tag{2.46}$$

$$F_p(x,z) = a_p(x)\, d_p(z) \tag{2.47a}$$

$$B_q(x,z) = a_q(x)\, d_q(z) \tag{2.47b}$$

we can write (2.44) as

$$\left[\frac{\partial^2 F_p}{\partial z^2} + [-i\varepsilon_i h(x)k^2 + (\beta_p^2 - \beta_{po}^2)]F_p + 2i\beta_{po}\frac{\partial F}{\partial z} + \frac{\varepsilon_1 \eta h(x)}{2} k^2 B_q\right] e^{i\beta_{po}z}$$

$$+ \left[\frac{\partial^2 B_q}{\partial z^2} + [-i\varepsilon_i h(x)k^2 + (\beta_q^2 - \beta_{qo}^2)]B_q - 2i\beta_{qo}\frac{\partial B_q}{\partial z} + \frac{\varepsilon_1 \eta h(x)}{2} k^2 F_p\right] e^{-i\beta_{qo}z}$$

$$+ \varepsilon_1 \frac{\eta}{2} h(x)k^2 F_p e^{i(2\beta_{po}+\beta_{qo})z} + \varepsilon_1 \frac{\eta}{2} h(x)k^2 B_q e^{-i(2\beta_{qo}+\beta_{po})z} = 0 \tag{2.48}$$

The last two terms in (2.48) correspond to higher order (n=2) space harmonics and are neglected[1,19,28]. This point is discussed further in Appendix D. For even high gain lasers, the wave amplitude growth per wavelength only approaches 2% [26,27]. Additionally, we consider $\eta << 1$. Therefore the wave amplitudes $F_p(x,z)$ and $B_q(x,z)$ are expected to vary slowly along z so that their second derivatives $\partial^2 F_p/\partial z^2$ and $\partial^2 B_q/\partial z^2$ can be neglected compared to terms of order $\lambda^{-1}\partial F_r/\partial z$, $\lambda^{-2}\eta F_r$, and $\lambda^{-2}\varepsilon_i F_r$ appearing in (2.48). With these approximations, we can write a set of coupled wave equations by equating terms of equal z dependence:

$$\frac{\partial F_p}{\partial z} + \left[-\frac{\varepsilon_i h(x)k^2}{2\beta_{po}} - i\frac{\beta_p^2 - \beta_{po}^2}{2\beta_{po}}\right]F_p = \frac{i\varepsilon_1 \eta h(x)}{4\beta_{po}} k^2 B_q \tag{2.49a}$$

$$-\frac{\partial B_q}{\partial z} + \left[\frac{\varepsilon_i h(x)k^2}{2\beta_{qo}} - i\frac{\beta_q^2 - \beta_{qo}^2}{2\beta_{qo}}\right]B_q = \frac{i\varepsilon_1 \eta h(x)}{4\beta_{qo}} k^2 F_p \tag{2.49b}$$

Considering the term $(\beta_r^2 - \beta_{ro}^2)/2\beta_{ro}$ in (2.49a,b), we write

$$\frac{\beta_r^2 - \beta_{ro}^2}{2\beta_{ro}} = \frac{(\beta_r - \beta_{ro})(\beta_r + \beta_{ro})}{2\beta_{ro}} \simeq \beta_r - \beta_{ro} \simeq c\psi_r(k)\,\Delta k \qquad (2.50)$$

where $\psi_r(k)$ is the reciprocal of the group velocity ($\psi_r(k) = \frac{\partial \beta_r}{c\,\partial k} = \frac{\partial \beta_r}{\partial \omega}$) for the r^{th} mode of the waveguide, and Δk is related to the departure of the oscillation frequency ω from the Bragg frequency ω_o:

$$\Delta k = k - k_o = \frac{\omega - \omega_o}{c} \qquad (2.51)$$

where c is the speed of light in vacuum. As the frequency departures are assumed to be small we have put $\beta_r/\beta_{ro} \simeq 1$ and $\psi_r(k) \simeq \psi_r(k_o)$ in the derivation of (2.50).

The gain term $\varepsilon_i h(x)k^2/(2\beta_{ro})$ and the coupling term $\varepsilon_1 \eta h(x)k^2/(4\beta_{ro})$ in (2.49a,b) are nonzero by (2.43) only in the guiding region where the gain medium and periodic perturbation are assumed located. We can generalize (2.49a,b) to be coupled wave equations independent of x if we introduce the concepts of effective gain and effective coupling. G_{eff}, the effective gain per unit length experienced by the waveguide modes F_r and B_r can be related to the actual gain per unit length of the active material in the guiding region by an efficiency coefficient $c_r(k)$:

$$G_{eff} = C_r(k)\, G \qquad (2.52)$$

The coefficient $C_r(k)$ is frequency dependent as the efficiency is almost zero near the cutoff frequency of the dielectric waveguide (the mode energy is mostly in the substrate or cladding) and approaches one well above cutoff as all the mode energy becomes confined to the guiding

region that contains the active medium. Chapter III is devoted to calculating the $c_r(k)$'s for the various waveguide configurations.

Similar considerations apply to the coupling term. The detailed coupling between modes F_p and B_q is solved in Chapter IV using the perturbed transverse mode functions. The coupling term $\varepsilon_1 h(x)k^2 / (4\beta_{ro})$ in (2.49a,b) can therefore be replaced by a coupling coefficient $\chi_{pq}(k)$. Expressions for $\chi_{pq}(k)$ and the reciprocal of the group velocity $\psi_r(k)$ for the various waveguide configurations are given in Chapter IV.

Incorporating all of the above considerations, and using $\chi_{pq} = \chi_{qp}$ (see Chapter IV), we write the coupled wave equations in their final form:

$$\frac{\partial F_p(x,z)}{\partial z} - [c_p(k)G + ic\psi_p(k)\Delta k]F_p(x,z) = i\chi_{pq}(k)\, B_q(x,z) \qquad (2.53a)$$

$$-\frac{\partial B_q(x,z)}{\partial z} - [c_q(k)G + ic\psi_q(k)\Delta k]B_q(x,z) = i\chi_{pq}(k)\, F_p(x,z) \qquad (2.53b)$$

The derivation of (2.53a,b) considers both the active material and the periodic dielectric constant to be in the guiding region. However, the coupled wave equations have a general physical interpretation. A wave changes in amplitude along z because of coupling to the other wave ($\chi_{pq}B_q, \chi_{pq}F_p$) or gain ($c_p(k)GF_p$, $c_q(k)G\,B_q$). For small deviations from the Bragg condition, the feedback due to mode coupling in the stop band region remains significant and the phase term ($c\psi_p(k)\Delta kF_p$, $c\psi_q(k)\Delta kB_q$) is required in calculating the oscillation condition. Pierce[45,46] has shown the concept of coupled modes to apply to

various systems where the coupled wave equations are of the general form of (2.53a,b). Based on the physical interpretation of (2.53a,b) we can generalize our coupled equations to general structures with periodic perturbations and regions of gain if we calculate the $c_r(k)$'s, $\chi_{pq}(k)$'s, and $\psi_r(k)$'s specifically for each configuration (as we do in Chapters III and IV). Different combinations of gain regions and parameter perturbations to be considered in this thesis are illustrated in Fig. 2.1.

C. Solutions of the Coupled Wave Equations

The coupled wave equations (2.53a,b) describe wave propagation in a guiding structure in the presence of gain and a periodic perturbation of a waveguide parameter. Because our model is that of a self oscillating device, the internal waves F_p and B_q start with zero amplitudes at their corresponding longitudinal boundaries, receiving their initial energy via scattering from the counterruning wave. This is illustrated in Fig. 2.8. Considering a structure of length L extending from $z = -L/2$ to $z = L/2$, the boundary conditions for the wave amplitudes become

$$B_q(x,L/2) = F_p(x,-L/2) = 0 \tag{2.54}$$

The solutions to the coupled wave equations with the boundary conditions (2.54) give the laser oscillation conditions. A finite signal output results with no signal input, which is the definition of an oscillator.

If we now take the partial derivative with respect to z of (2.53a) and use (2.53b), we obtain

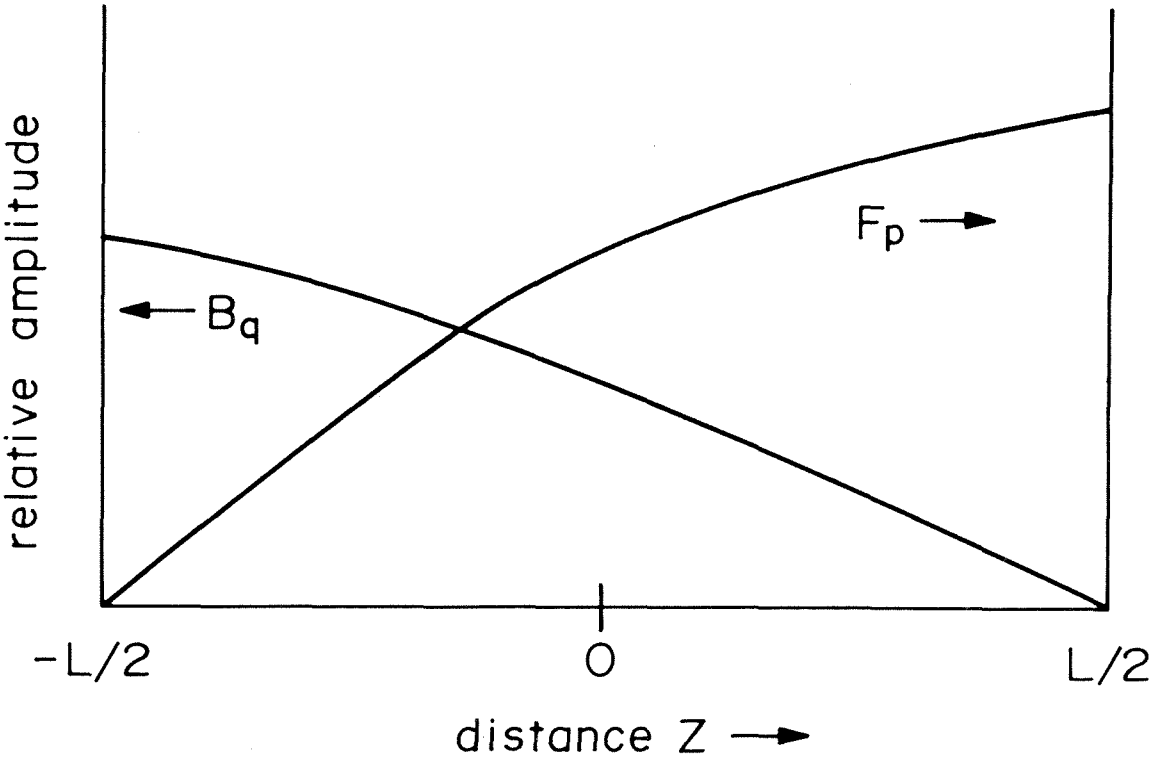

Fig. 2.8 Sketch of the amplitudes of the left traveling wave B_q and the right traveling wave F_p versus distance.

$$-\frac{\partial^2 F_p(x,z)}{\partial z^2} + \{(c_p(k) - c_q(k))G + ic(\psi_p(k) - \psi_q(k)\ \Delta k\}\frac{\partial F_p(x,z)}{\partial z}$$

$$+ \{\chi_{pq}^2(k) + (c_q(k)G + ic\psi_q(k)\Delta k)(c_p(k)G + ic\psi_p(k)\Delta k)\}\ F_p(x,z) = 0 \tag{2.55}$$

$F_p(x,z)$ and $B_q(x,z)$ are defined in (2.47a,b) as a product $a_r(x)d_r(z)$. Dividing (2.55) through by $a_p(x)$ we obtain an ordinary linear differential equation and the solutions to (2.53a,b) become[23]

$$F_p(x,z) = a_p(x)\ d_p(z) \tag{2.56a}$$

$$B_q(x,z) = a_q(x)\ d_q(z) \tag{2.56b}$$

where

$$d_p(z) = f_1\ e^{\gamma_1 z} + f_2\ e^{\gamma_2 z} \tag{2.56c}$$

$$d_q(z) = b_1\ e^{\gamma_1 z} + b_2\ e^{\gamma_2 z} \tag{2.56d}$$

and

$$\gamma_{1,2} = \left(\frac{c_p(k) - c_q(k)}{2}\right)G + ic\left(\frac{\psi_p(k) - \psi_q(k)}{2}\right)\Delta k$$

$$\pm\sqrt{\chi_{pq}^2(k) + \left[\left(\frac{c_p(k) + c_q(k)}{2}\right)G + ic\left(\frac{\psi_p(k) + \psi_q(k)}{2}\right)\Delta k\right]^2} \tag{2.57}$$

The transverse field distributions $a_r(x)$ in (2.56a,b) are closely approximated by the corresponding unperturbed approximations given in Appendices A, B, and C. Corrections to the unperturbed transverse field distributions are used in Chapter IV in the derivation of coupling

coefficients

Writing

$$a_{pq} = \left(\frac{c_p(k) - c_q(k)}{2}\right)G + ic\left(\frac{\psi_p(k) - \psi_q(k)}{2}\right)\Delta k \tag{2.58a}$$

$$b_{pq} = \sqrt{\chi^2_{pq}(k) + \left[\left(\frac{c_p(k) + c_q(k)}{2}\right)G + ic\left(\frac{\psi_p(k) + \psi_q(k)}{2}\right)\Delta k\right]^2} \tag{2.58b}$$

the boundary conditions give

$$f_2 = -f_1\, e^{-b_{pq}L} \tag{2.59a}$$

$$b_2 = -b_1\, e^{b_{pq}L} \tag{2.59b}$$

Substituting (2.56c,d) and (2.59a,b) into (2.53a,b) and comparing terms of equal exponential z dependence we find

$$f_1(-Y_{pq} + b_{pq}) = i\chi_{pq}(k)\, b_1 \tag{2.60a}$$

$$f_1 e^{-b_{pq}L}(Y_{pq} + b_{pq}) = -i\chi_{pq}(k)\, b_1\, e^{b_{pq}L} \tag{2.60b}$$

Multiplying (2.60a) and (2.60b), and using (2.58b), we have

$$b_1 = f_1\, e^{-b_{pq}L} \tag{2.61}$$

We can now write (2.56c,d) as

$$d_p(z) = \pm f_1\, e^{-b_{pq}\, L/2}\, e^{a_{pq}z} \sinh b_{pq}(z + L/2) \tag{2.62a}$$

$$d_q(z) = \pm f_1\, e^{-b_{pq}\, L/2}\, e^{a_{pq}z} \sinh b_{pq}(z - L/2) \tag{2.62b}$$

To solve for the required threshold gain G and phase mismatch Δk from the exact Bragg frequency, we use (2.53a) to write

$$d_q(z) = \frac{f_1 e^{-b_{pq}L/2} e^{a_{pq}z}}{i\chi_{pq}} [\{a_{pq} - (c_p(k)G + ic\,\psi_p(k)\Delta k)\} \sinh b_{pq}(z+\tfrac{L}{2}) + b_{pq} \cosh b_{pq}(z+\tfrac{L}{2})] \qquad (2.63)$$

The boundary condition $B_q(x,-L/2) = 0$ requires

$$Y_{pq} = \sqrt{\chi_{pq}^2(k) + Y_{pq}^2} \coth\sqrt{\chi_{pq}^2(k) + Y_{pq}^2}\, L \qquad (2.64)$$

where

$$Y_{pq} = \frac{c_p(k) + c_q(k)}{2} G + ic(\frac{\psi_p(k) + \psi_q(k)}{2})\,\Delta k \qquad (2.65)$$

The required threshold gain for laser oscillation is given by

$$G = \frac{2}{c_p(k) + c_q(k)} \text{Re}\,\{Y_{pq}\} \qquad (2.66a)$$

and the corresponding phase mismatch by

$$\Delta k = \frac{2}{c(\psi_p(k) + \psi_q(k))} \text{Im}\,\{Y_{pq}\} \qquad (2.66b)$$

The Y_{pq} that solve (2.64) are generally complex valued, with different values corresponding to different branches of the complex hyperbolic cotangent function. The various Y_{pq} correspond to the different longitudinal modes of the DFB resonator, just as a conventional Fabre-Perot interferometer has longitudinal modes spaced at $\Delta k = \pi/(nL)$

where L is the mirror spacing and n the index of refraction[24]. Since

$$\coth(z + im\pi) = \coth(z) \qquad m \text{ any integer} \tag{2.67}$$

we see from (2.64) and (2.66b) that the DFB resonator modes are spaced approximately $\pi/(n_{av}L)$ for small coupling $\chi_{pq}(k)$, where we have defined an average index of refraction as

$$n_{av} = \frac{c(\psi_p(k) + \psi_q(k))}{2} \tag{2.68}$$

The coupling coefficient $\chi_{pq}(k)$, gain efficiencies $c_p(k)$, $c_q(k)$, and reciprocals of the group velocities $\psi_p(k)$, $\psi_q(k)$ are fixed by the waveguide geometry. Therefore the transcendental equation (2.64) can be solved for Y_{pq} given the waveguide parameters, and (2.66a,b) can be used to obtain the required threshold gains and corresponding longitudinal mode spacings for a waveguide of length L. G and Δk, along with the parameters $c_p(k)$, $c_q(k)$, $\psi_p(k)$, $\psi_q(k)$, and $\chi_{pq}(k)$ determine γ_1 and γ_2 from equation (2.57), or similarly, a_{pq} and b_{pq} from equations (2.58a,b). Thus the mode amplitudes $d_r(z)$ are specified by (2.62a,b) and the electric field for the p-q configuration is given by

$$E_{pq}(z) = F_p(x,z)\, e^{i\beta_{po}z} + B_q(x,z)\, e^{-i\beta_{qo}z} \tag{2.67}$$

As this is a linear threshold calculation, the absolute field amplitudes remain unspecified. An accounting of the "pump" or input power and the nonlinear effect of gain saturation[77,78] would allow specifying f_1 in (2.6a,b).

We have now obtained general equations for the threshold gain, longitudinal mode distribution, and longitudinal field distribution. In Chapter V, these general equations are applied to specific guiding structures.

D. Comments

In (2.40) of Section C, we arbitrarily chose a forward p mode coupled to a backward q mode. However, as our model is symmetric, an equally valid choice would be a forward q mode coupled to a backward p mode. By equations (2.64)-(2.68), both configurations have the same threshold gain and phase mismatch. This point is also discussed in Appendix D, and is illustrated in Fig. 2.5 and Fig. D.1, where operation at a frequency ω_{pq} corresponding to the interaction region of a p and a q mode is shown to generate forward and backward waves of both modes.

The analysis up to this point and in the rest of this thesis considers only transverse electric waves. For isotropic media the theory of periodic perturbations of dielectric waveguides predicts[28] that there is no scattering from transverse electric (TE) to transverse magnetic (TM) modes, and vice versa. Thus in isotropic media, DFB lasing could occur between corresponding pairs of TM modes or corresponding pairs of TE modes depending upon the choice of parameters[56]. For a laser oscillation frequency ω_{pq}, and a fixed perturbation wave vector K, only one pair of modes are strongly coupled (see Fig. 2.5). However, if a medium exhibits gain over a relatively broad frequency region, it is possible that a perturbation wave vector K could couple two pairs of modes at various frequencies as indicated in Fig. 2.9.

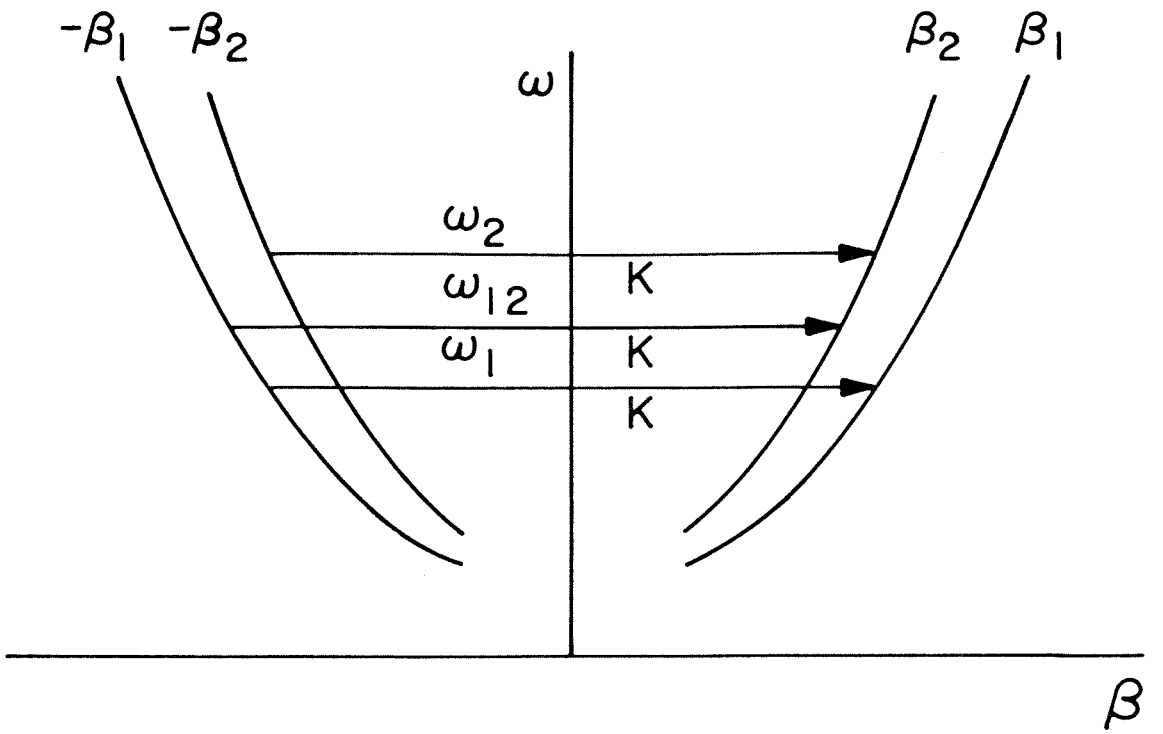

Fig. 2.9 ω-β diagram illustrating three scattering processes. The perturbing wave vector K has the same length for each process. Backward scattering between modes 1-1, 1-2, and 2-2 occurs at frequencies ω_1, ω_{12}, and ω_2, respectively.

In this case the active region must have significant gain over the frequency range $\omega_1 < \omega < \omega_2$, where ω_1 and ω_2 are frequencies indicated in Fig. 2.9.

If DFB lasers are constructed using anisotropic material, it is possible to orient the optic axis so as to guide only TE modes or only TM modes. Additionally, it is possible to orient the optic axis to allow coupling of TE to TM modes[57,58,59,60]. DFB lasers have been constructed by Bjorkholm et al.[59] using an organic dye gain medium (which characteristically exhibits gain over a relatively broad frequency spectrum[61]) on anisotropic substrates. Simultaneously, the three frequencies indicated in Fig. 2.9 were observed. In this experiment the modes corresponding to $\pm\beta_1$ were TE-like modes and those corresponding to $\pm\beta_2$ were TM-like modes and the frequencies observed indicated that all three processes shown in Fig. 2.9 occurred due to the broad gain spectrum. The analysis presented in this thesis could be extended in a straightforward manner to apply to TM-TM and TE-TM mode interactions.

A method of obtaining a periodic medium remains, which has not been discussed. If a medium is pumped by two coherent beams, the interference fringes generate a periodicity of the gain in the medium. This gain periodicity can be accounted for if η in (2.41) is considered imaginary[1]. However, for the purposes of this thesis, only perturbations of the real part of the dielectric constant and surface perturbations are considered, and η remains real.

Finally, it should be mentioned that the results of this chapter could be extended to any type of periodicity which can be

expanded in a Fourier series. The waveguide parameters could be written as

$$\varepsilon(z) = \varepsilon_0\varepsilon_1(1 + \eta\, f_1(z))$$

or

$$W(z) = W(1 + \eta\, f_2(z))$$

In this case, η has to be multiplied by the coefficient of the Fourier component of $f_1(z)$ or $f_2(z)$ used for phase matching. A complication arises, however, in that other existing Fourier components could couple competing processes at the same frequency.

Chapter III

The Effective Gain Coefficients

The purpose of this chapter is to calculate the effective gain (or gain efficiency) of a waveguide mode for the case where the mode energy is spread transversely over both regions with and regions without gain. Figure 3.1a illustrates such a case. In practical distributed feedback lasers, it is expected that the gain medium will be either in the guiding region or outside the guiding region in the cladding of a fiber or substrate of a thin film or diffusion waveguide.

The method employed to calculate the effective gain is that of solving the dispersion relations of the guiding structure with complex dielectric constants ($\varepsilon_{rel} = \varepsilon_{re} - i\varepsilon_i$) and solving for the resulting complex transverse and longitudinal wave vectors. The complex wave vectors of the guiding structure are then related to the gain of the mode.

The task of solving the dispersion relations with complex dielectric constants can be simplified by realizing $\varepsilon_i^{(1,2)} << \varepsilon_{re}^{(1,2)}$ even for high gain lasers. (We use the notation $\varepsilon^{(m)}$ to designate the relative dielectric constant in the guiding region (m=1) or in the substrate or cladding (m=2). $\varepsilon_i^{(1,2)}$ can be shown to be much smaller than $\varepsilon_{re}^{(1,2)}$ if we represent a gain medium of infinite extent with a complex index of refraction $n = n_{re} - in_i$ ($\varepsilon = n^2$) and a consider a plane wave propagating in the medium to experience gain G :

$$E_p e^{i(n_{re} - in_i)kz} = E_p e^{in_{re}kz} e^{n_i kz} \tag{3.1}$$

where E_p is the amplitude of the plane wave at $z = 0$ and by

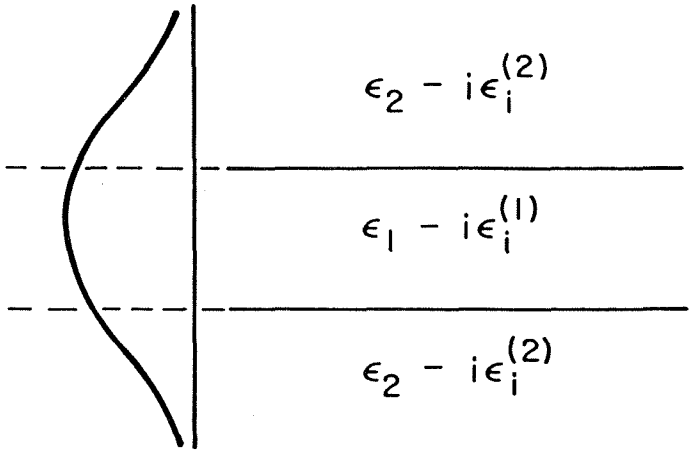

(a)

$$C = \frac{P_i}{P_t} \times \frac{T}{t}$$

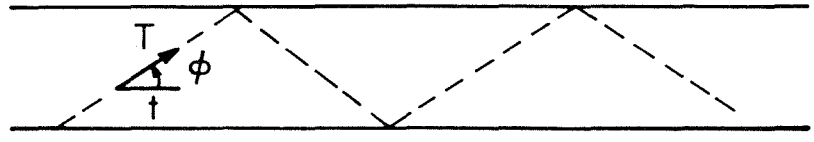

(b)

Fig. 3.1 (a) Representation of an active waveguide with gain in the guiding region (1) and gain in the substrate region (2). (b) The effective gain of a thin film waveguide mode is the ratio of the power inside the waveguide mode to the total mode power, multiplied by the ray trajectory length (T) per unit length of the waveguide (t).

definition

$$G = n_i \frac{2\pi}{\lambda} \tag{3.2}$$

so that

$$n_i = G\lambda/2\pi \tag{3.3}$$

Typically, the highest gain lasers are semiconductor lasers where G can approach 200 cm^{-1} at wavelengths around 0.9 microns[26,27]. For such a case, $n_i \simeq 3 \times 10^{-3}$ and is in general much smaller. Values of n_{re} are always greater than or equal to one, so the condition $n_i << n_{re}$ or equivalently $\varepsilon_i << \varepsilon_{re}$ is always satisfied.

A. Effective Gain Coefficients for Thin Film Waveguides

We consider the dielectric waveguide of width $2w$ illustrated in Fig. A.1 of Appendix A. From Appendix A where ε_1 and ε_2 were assumed real,

$$s^2 = \varepsilon_1 k^2 - \beta^2 \tag{3.4}$$

$$\delta^2 = -\varepsilon_2 k^2 + \beta^2 \tag{3.5}$$

$$\delta = s \begin{cases} \tan(sw) & \text{(even modes)} \\ -\cot an(sw) & \text{(odd modes)} \end{cases} \tag{3.6}$$

If the dielectric constants become complex

$$\varepsilon_1 = \varepsilon_{re}^{(1)} - i\varepsilon_i^{(1)} \tag{3.7a}$$

$$\varepsilon_2 = \varepsilon_{re}^{(2)} - i\varepsilon_i^{(2)} \tag{3.7b}$$

the transverse and longitudinal wave vectors in the guiding structure

become complex. As $\varepsilon_i^{(1,2)} << \varepsilon_{re}^{(1,2)}$, we can consider $\varepsilon_i^{(1,2)}$ to be a small perturbation giving rise to imaginary wave vector correction terms s_i, δ_i, and β_i, where

$$s = s_{re} + is_i \tag{3.8a}$$

$$\delta = \delta_{re} + i\delta_i \tag{3.8b}$$

$$\beta = \beta_{re} + i\beta_i \tag{3.8c}$$

and s_{re}, δ_{re}, and β_{re} are the unperturbed real wave vectors. Expanding (3.4) and (3.5) and keeping only first order terms in s_i, δ_i, and β_i, we have

$$s_{re}^2 = \varepsilon_{re}^{(1)}k^2 - \beta_{re}^2 \tag{3.9a}$$

$$s_i = -\frac{1}{2s_{re}}[\varepsilon_i^{(1)}k^2 + 2i\beta_{re}\beta_i] \tag{3.9b}$$

$$\delta_{re}^2 = -\varepsilon_{re}^{(2)}k^2 + \beta_{re}^2 \tag{3.10a}$$

$$\delta_i = \frac{1}{2\delta_{re}}[\varepsilon_i^{(2)}k^2 + 2\beta_{re}\beta_i] \tag{3.10b}$$

Expanding (3.6) in a Taylor series and again retaining only first order terms,

$$\delta_{re} = s_{re}\begin{cases}\tan(s_{re}w)\\ -\text{cotan}(s_{re}w)\end{cases} \tag{3.11a}$$

$$\delta_i = s_i \begin{cases} \tan(s_{re}w)[1 + \dfrac{2s_{re}w}{\sin(2s_{re}w)}] \\ -\text{cotan}(s_{re}w)[1 - \dfrac{2s_{re}w}{\sin(2s_{re}w)} \end{cases} \tag{3.11b}$$

From (3.10b)

$$\frac{\beta_i}{\beta_{re}} = \frac{\delta_i \delta_{re}}{\beta_{re}^2} - \frac{\varepsilon_i^{(2)} k^2}{2\beta_{re}^2} \tag{3.12b}$$

and with (3.11a,b) and (3.9b),

$$\frac{\beta_i}{\beta_{re}} = \frac{1}{2} \frac{k^2}{\beta_{re}^2} \left(\frac{-\varepsilon_i^{(2)} - \alpha_{t.f.} \varepsilon_i^{(1)}}{1 - \alpha_{t.f.}}\right) \tag{3.13}$$

where

$$\alpha_{t.f.} = \begin{cases} \tan^2(s_{re}w)[1 + \dfrac{2s_{re}w}{\sin(2s_{re}w)}] \\ -\text{cotan}^2(s_{re}w)[1 - \dfrac{2s_{re}w}{\sin(2s_{re}w)}] \end{cases} \tag{3.14}$$

The unperturbed wave vectors s_{re}, δ_{re}, and β_{re} are the multiple solutions of the dispersion relations (A.6) and (A.7). We therefore use the notation $\beta_i^{(r)}$ and $\beta_{re}^{(r)}$ to indicate the imaginary component of the longitudinal wave vector and the real component of the longitudinal wave vector of the r^{th} waveguide mode.

A plane wave travelling in an unbounded medium with gain ($\varepsilon = \varepsilon_{re} - i\varepsilon_i$) propagates as

$$e^{i\beta z} = e^{ik\sqrt{\varepsilon_{re}}z}\, e^{\varepsilon_i k/(2\sqrt{\varepsilon_r})z} = e^{i(\beta_{re} + i\beta_i)z} \tag{3.15}$$

where we have used $\varepsilon_i << \varepsilon_{re}$ so that $\sqrt{\varepsilon_{re} - i\varepsilon_i} \simeq \sqrt{\varepsilon_{re}}(1 - i\varepsilon_i/2\varepsilon_{re})$. From (3.15), we see that the gain or growth of the plane wave is given by $-\beta_i$ and is equal to the gain constant G of the unbounded medium, where

$$G = \frac{\varepsilon_i k}{2\sqrt{\varepsilon_{re}}} \tag{3.16}$$

However, in a waveguide structure where the simple relation $\beta = \sqrt{\varepsilon}\, k$ no longer holds, and the gain is localized to a specific region of the structure, we can define a function $C_r(k)$ called the effective gain as the gain of the r^{th} waveguide mode $-\beta_i^{(r)}$ divided by the medium gain:

$$C_r(k) = -\beta_i^{(r)}/G = -\frac{2\sqrt{\varepsilon_{re}}}{\varepsilon_i}\,\frac{\beta_i^{(r)}}{k} \tag{3.17}$$

From (3.17) we can also define the effective gain as the ratio of an effective imaginary part of the dielectric constant to the actual imaginary part of the dielectric constant

$$C_r(k) = \frac{(\varepsilon_i)_{eff}}{\varepsilon_i} \tag{3.18}$$

where

$$-(\varepsilon_i)_{eff} = 2\sqrt{\varepsilon_{re}}\,\frac{\beta_i^{(r)}}{k} = 2\sqrt{\varepsilon_r}\,\frac{\beta_{re}}{k}\,\frac{\beta_i^{(r)}}{\beta_{re}^{(r)}} \tag{3.19}$$

Using the expression for $\beta_i^{(r)}/\beta_{re}^{(r)}$ in (3.13), we write the gain

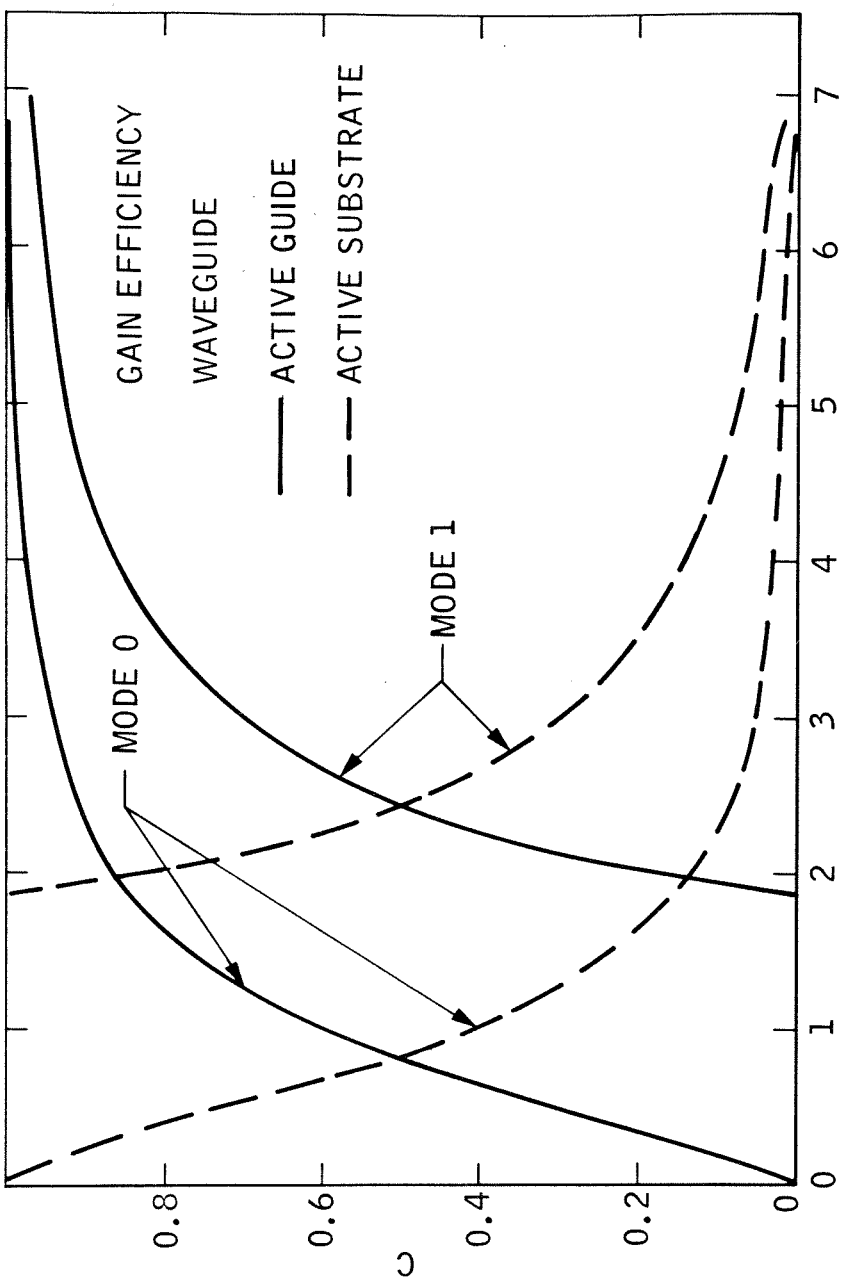

Fig. 3.2 Effective gain coefficients for the 0 and 1 modes of a thin film waveguide for the dielectric constants $\varepsilon_1 = (3.6)^2$ and $\varepsilon_2 = (3.5)^2$.

efficiency for the case of an active guide ($\varepsilon_i^{(2)} = 0$) as

$$C_r(k) = \sqrt{\varepsilon_{re}^{(1)}}\ \frac{k}{\beta_{re}^{(r)}}\ \frac{\alpha_{t.f.}}{1+\alpha_{t.f.}} \tag{3.20}$$

and for the case of an active substrate ($\varepsilon_i^{(1)} = 0$),

$$C_r(k) = \sqrt{\varepsilon_{re}^{(2)}}\ \frac{k}{\beta_{re}^{(r)}}\ \frac{1}{1+\alpha_{t.f.}} \tag{3.21}$$

We note from equation (A.15a,b) of Appendix A that the term $\alpha_{t.f}/(1+\alpha_{t.f})$ in (3.20) is the ratio of the mode power inside the guide to the total mode power. The factor $\sqrt{\varepsilon_{re}^{(1)}}\ k/\beta_{re}$ can be interpreted as $1/(\cos\phi)$ where ϕ is the angle between the optical ray representing the waveguide mode and the z axis. As illustrated in Fig. 3.1b, the gain efficiency coefficient given by (3.20) can be physically explained as the ratio of the mode power in the guide to the total mode power multiplied by $1/(\cos\phi)$. The factor $1/(\cos\phi)$ accounts for the longer path length in the gain medium due to the zig-zag path the mode follows compared to a straight line path down the guide.

Figure 3.2 is a plot of equations (3.20) and (3.21) for the first two waveguide modes as a function of the normalized free space wave vector.

B. Effective Gain Coefficients for Diffusion Waveguides

In this section we derive the gain efficiency coefficients for the two diffusion waveguides shown in Fig. B.1a,b of Appendix B. W is

the channel half-width of the channel diffusion guide, and d_o is the diffusion depth for both waveguide structures.

From Appendix B, we find for both geometries

$$\nu^2 = (2d_o)^2 (\beta^2 - \varepsilon_1 k^2) \tag{3.22}$$

$$\delta^2 = \beta^2 - \varepsilon_2 k^2 \tag{3.23}$$

and for the channel diffusion geometry,

$$\delta \begin{cases} \tanh(\delta W) \\ \text{cotanh}(\delta W) \end{cases} = -\sqrt{\alpha}\, k \frac{J_\nu'(2\sqrt{\alpha}\, kd_o)}{J_\nu(2\sqrt{\alpha}\, kd_o)} \qquad \begin{matrix} \text{(even modes)} \\ \text{(odd modes)} \end{matrix} \tag{3.24a}$$

and for the half-space diffusion geometry,

$$\delta = -\sqrt{\alpha}\, k \frac{J_\nu'(2\sqrt{\alpha}\, kd_o)}{J_\nu(2\sqrt{\alpha}\, kd_o)} \tag{3.24b}$$

The primes in (3.24a,b) indicate differentiation with respect to the argument $2\sqrt{\alpha}\, kd$ of the Bessel function. As in Section IIIA, we let ε_1 and ε_2 become complex (see (3.7a,b)) creating complex transverse and longitudinal wave vectors in the guiding structure. Again we consider $\varepsilon_i^{(1,2)}$ to be small perturbations giving rise to imaginary correction terms ν_i, δ_i, and β_i, where

$$\nu = \nu_{re} + i\nu_i \tag{3.25a}$$

$$\delta = \delta_{re} + i\delta_i \tag{3.25b}$$

$$\beta = \beta_{re} + i\beta_i \tag{3.25c}$$

and $\nu_{re}(2d_o), \delta_{re}$, and β_{re} are the unperturbed wave vectors.

Expanding (3.24a,b) in a Taylor series and keeping terms only up to first order in ν_i and δ_i,

$$\delta_{re}\begin{cases}\tanh(\delta_{re}w)\\ \text{cotanh}(\delta_{re}w)\end{cases} = -\sqrt{\alpha}\,k\,\frac{J'_{\nu_{re}}(2\sqrt{\alpha}\,kd_o)}{J_{\nu_{re}}(2\sqrt{\alpha}\,kd_o)} \quad \begin{matrix}\text{(channel}\\ \text{guide)}\end{matrix} \tag{3.26a}$$

$$\delta_{re} = -\sqrt{\alpha}\,k\,\frac{J'_{\nu_{re}}(2\sqrt{\alpha}\,kd_o)}{J_{\nu_{re}}(2\sqrt{\alpha}\,kd_o)} \quad \text{(half-space diffusion)} \tag{3.26b}$$

and

$$\delta_i = -\nu_i\sqrt{\alpha}\,k\;\; S(J) \qquad \text{(channel guide)} \tag{3.27a}$$

$$\delta_i = -\nu_i\sqrt{\alpha}\,k\;\; F(J) \qquad \text{(half-space diffusion)} \tag{3.27b}$$

where

$$S(J) = F(J)\left[\begin{cases}\tanh(\delta_{re}w)\\ \text{cotanh}(\delta_{re}w)\end{cases} + \delta_{re}w\begin{cases}\text{sech}^2(\delta_{re}w)\\ -\text{csch}^2(\delta_{re}w)\end{cases}\right]^{-1} \tag{3.28}$$

and

$$F(J) = \frac{\left(\frac{\partial J_{\nu_{re}-1}}{\partial\nu_{re}} - \frac{\partial J_{\nu_{re}+1}}{\partial\nu_{re}}\right)J_{\nu_{re}} - \frac{\partial J_{\nu_{re}}}{\partial\nu_{re}}\left(\left(J_{\nu_{re}-1} - J_{\nu_{re}+1}\right)\right)}{2J^2_{\nu_{re}}} \tag{3.29}$$

In general, we can write (3.26a,b) as

$$\delta_i = -\nu_i\sqrt{\alpha}\,kA(J) \tag{3.30}$$

where $A(J) = S(J)$ for the channel diffusion waveguide and $A(J) = F(J)$ for the half space diffusion waveguide.

We now expand (3.22) keeping only first order terms in ν_i and β_i

$$\nu_{re}^2 = (2d_o)^2 (\beta_{re}^2 - \varepsilon_{re}^{(1)} k^2) \tag{3.31a}$$

$$\nu_i = \frac{(2d_o)^2}{\nu_{re}} [\beta_i \beta_{re} + \varepsilon_i^{(1)} \frac{k^2}{2}] \tag{3.31b}$$

Subtracting (3.23) from (3.22) we obtain

$$\nu^2 = (2d_o)^2 [\delta^2 - (\varepsilon_1 - \varepsilon_2) k^2) \tag{3.32}$$

and expanding as before

$$\nu_{re}^2 = (2d_o)^2 [\delta_{re}^2 - (\varepsilon_{re}^{(1)} - \varepsilon_{re}^{(2)}) k^2] \tag{3.33a}$$

$$\nu_i = \frac{(2d_o)^2}{\nu_{re}} [\delta_{re} \delta_i - (\varepsilon_i^{(2)} - \varepsilon_i^{(1)}) \frac{k^2}{2}] \tag{3.33b}$$

Using (3.30) in (3.33b),

$$\nu_i = \frac{(2d_o)^2}{\nu_{re}} [-\delta_{re} \nu_i \sqrt{\alpha}\, k\, A(J) - (\varepsilon_i^{(2)} - \varepsilon_i^{(1)}) \frac{k^2}{2}] \tag{3.34}$$

and simplifying,

$$\nu_i = \frac{-(\varepsilon_i^{(2)} - \varepsilon_i^{(1)}) k^2 (2d_o)^2}{2\nu_{re}(1 + \alpha_D)} \tag{3.35}$$

where we define

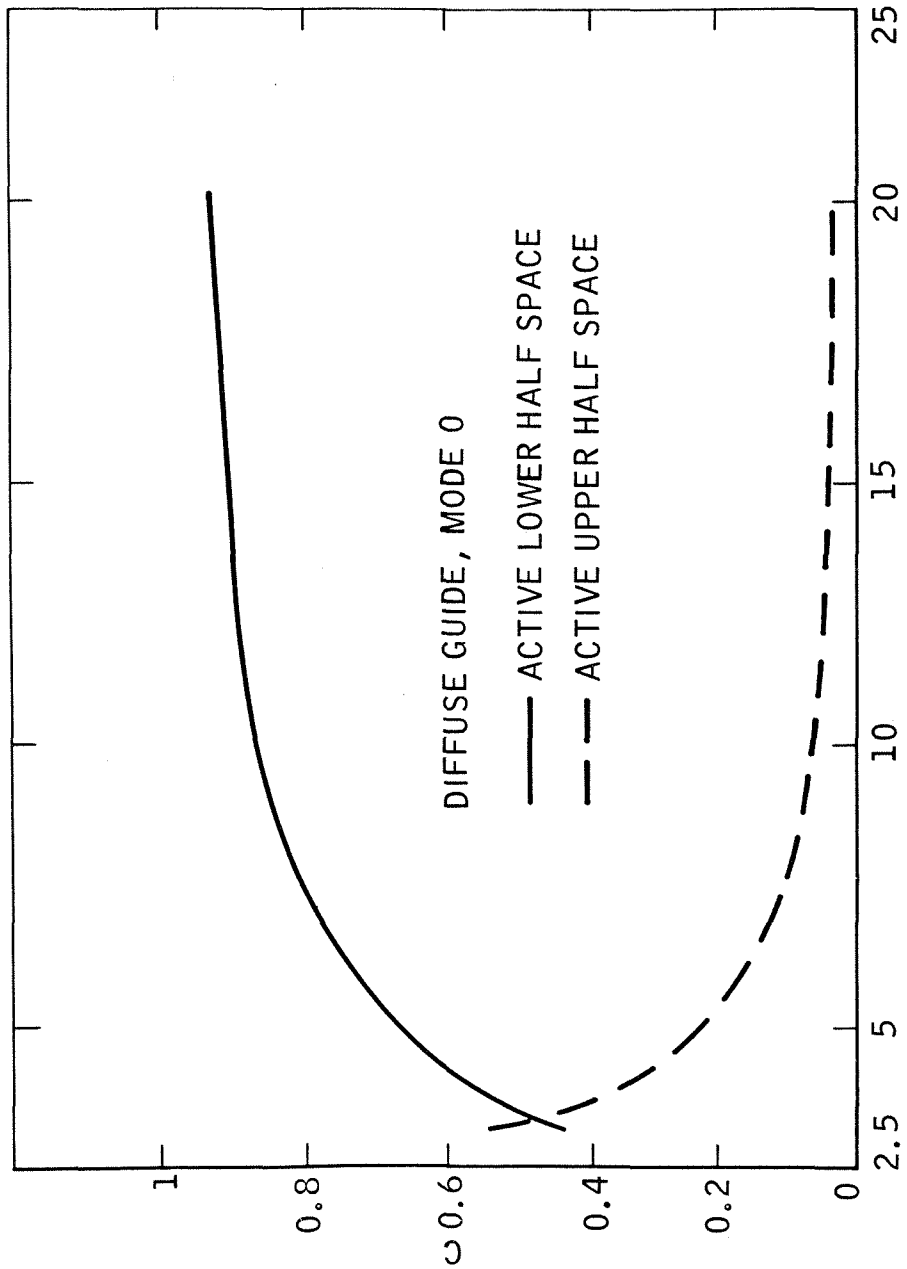

Fig. 3.3 Effective gain coefficients for the 0 mode of a diffusion waveguide for the parameter $\alpha = 0.1$, $\varepsilon_1 = (1.5)^2$, $\varepsilon_2 = 1$.

$$\alpha_D = \frac{4\sqrt{\alpha}\, k\, \delta_{re} d_o^2}{\nu_{re}} A(J) \tag{3.36}$$

From (3.31b) and (3.35)

$$\frac{\beta_i}{\beta_{re}} = \frac{-(\varepsilon_i^{(2)} - \varepsilon_i^{(1)} k^2}{2\beta_{re}^2(1 + \alpha_D)} - \frac{\varepsilon_i^{(1)} k^2}{2\beta_{re}^2} \tag{3.37}$$

Using (3.37) in (3.19) and (3.18) of Section IIIA, we write the gain efficiency for the case of gain in the inhomogeneous regions ($\varepsilon_i^{(2)} = 0$) as

$$C_r(k) = \sqrt{\varepsilon_{re}^{(1)}}\, \frac{k}{\beta_{re}^{(r)}}\, \frac{\alpha_D}{1 + \alpha_D} \tag{3.38}$$

Similarly, for the case of gain in the channel of a channel diffusion guide or gain in the homogeneous half space of a half space diffusion guide ($\varepsilon_i^{(1)} = 0$), the gain efficiency is

$$C_r(k) = \sqrt{\varepsilon_{re}^{(2)}}\, \frac{k}{\beta_{re}^{(r)}}\, \frac{1}{1 + \alpha_D} \tag{3.39}$$

Equations (3.38) and (3.39) are the gain efficiency coefficients for the diffusion waveguides and are plotted as a function of the normalized free space wave vector for the case of a half-space diffusion waveguide in Fig. 3.3.

C. Effective Gain Coefficients for Fiber Waveguides

In this section we derive the gain efficiency coefficients for the fiber waveguide of radius w shown in Fig. C.1 in Appendix C. From Appendix C,

$$sw \frac{J_0(sw)}{J_1(sw)} = - \delta w \frac{K_0(\delta w)}{K_1(\delta w)} \tag{3.40}$$

$$s^2 = \varepsilon_1 k^2 - \beta^2 \tag{3.41}$$

and

$$\delta^2 = \beta^2 - \varepsilon_2 k^2 \tag{3.42}$$

As in previous sections, we let ε_1 and ε_2 become complex (see (3.7a,b)) creating complex transverse and longitudinal wave vectors in the guiding structure. The small perturbations $\varepsilon_i^{(1,2)}$ give rise to imaginary wave vector correction terms s_i, δ_i, and β_i, as defined by equations (3.8a,b,c) in Section IIIA. As (3.41) and (3.42) are the same equations as (3.4) and (3.5) of Section IIIA, equations (3.9a,b) and (3.10a,b) are valid for both dielectric slab and fiber waveguides. Expanding (3.40) in a Taylor series and keeping only first order terms in s_i and δ_i,

$$s_{re} \frac{J_0(s_{re}w)}{J_1(s_{re}w)} = -\delta_{re}w \frac{K_0(\delta_{re}w)}{K_1(\delta_{re}w)} \tag{3.43a}$$

$$s_i w \, B(J) = - \delta_i w \, D(K) \tag{3.43b}$$

where

$$B(J) = \frac{J_0(s_{re}w)}{J_1(s_{re}w)} + s_{re}w \frac{J_1(s_{re}w)J_0'(s_{re}w) - J_0(s_{re}w)J_1'(s_{re}w)}{J_1^2(s_{re}w)} \tag{3.44}$$

and

$$D(K) = \frac{K_0(\delta_{re}w)}{K_1(\delta_{re}w)} + \delta_{re}w \frac{K_1(\delta_{re}w)K_0'(\delta_{re}w) - K_0(\delta_{re}w)K_1'(\delta_{re}w)}{K_1^2(\delta_{re}w)} \tag{3.45}$$

The primes in (3.44) and (3.45) indicate differentiation with respect

to the arguments $s_{re}w$ and $\delta_{re}w$ of the Bessel functions J and K.

Subtracting (3.10b) and (3.9b) and using (3.43b)

$$\delta_i = - \frac{B(J)}{\delta_{re} B(J) - s_{re} D(K)} \tag{3.46}$$

From (3.10b)

$$\beta_{re}\beta_i = - \frac{\varepsilon_i^{(2)}}{2} k^2 + \delta_{re}\delta_i \tag{3.47}$$

and we can write

$$\frac{\beta_i}{\beta_{re}} = \frac{1}{2} \left(\frac{k}{\beta_{re}}\right)^2 \left(\frac{-\varepsilon_i^{(1)}\alpha_F - \varepsilon_i^{(2)}}{1 + \alpha_F}\right) \tag{3.48}$$

where we define

$$\alpha_F = - \frac{\delta_{re} B(J)}{s_{re} D(K)} \tag{3.49}$$

Using (3.48) in (3.19) and (3.18) of Section IIIA, we write the gain efficiency for the case of gain in the fiber ($\varepsilon_i^{(2)} = 0$) as

$$C_r(k) = \sqrt{\varepsilon_{re}^{(1)}} \left(\frac{k}{\beta_{re}^{(r)}}\right) \frac{\alpha_F}{1 + \alpha_F} \tag{3.50}$$

For the case of gain in the cladding surrounding the fiber ($\varepsilon_i^{(1)} = 0$) the gain efficiency becomes

$$C_r(k) = \sqrt{\varepsilon_{re}^{(2)}} \left(\frac{k}{\beta_{re}^{(r)}}\right) \frac{1}{1 + \alpha_F} \tag{3.51}$$

The gain efficiency coefficients given by (3.50) and (3.51) are plotted in Fig. 3.4 as a function of the normalized free space wave vector.

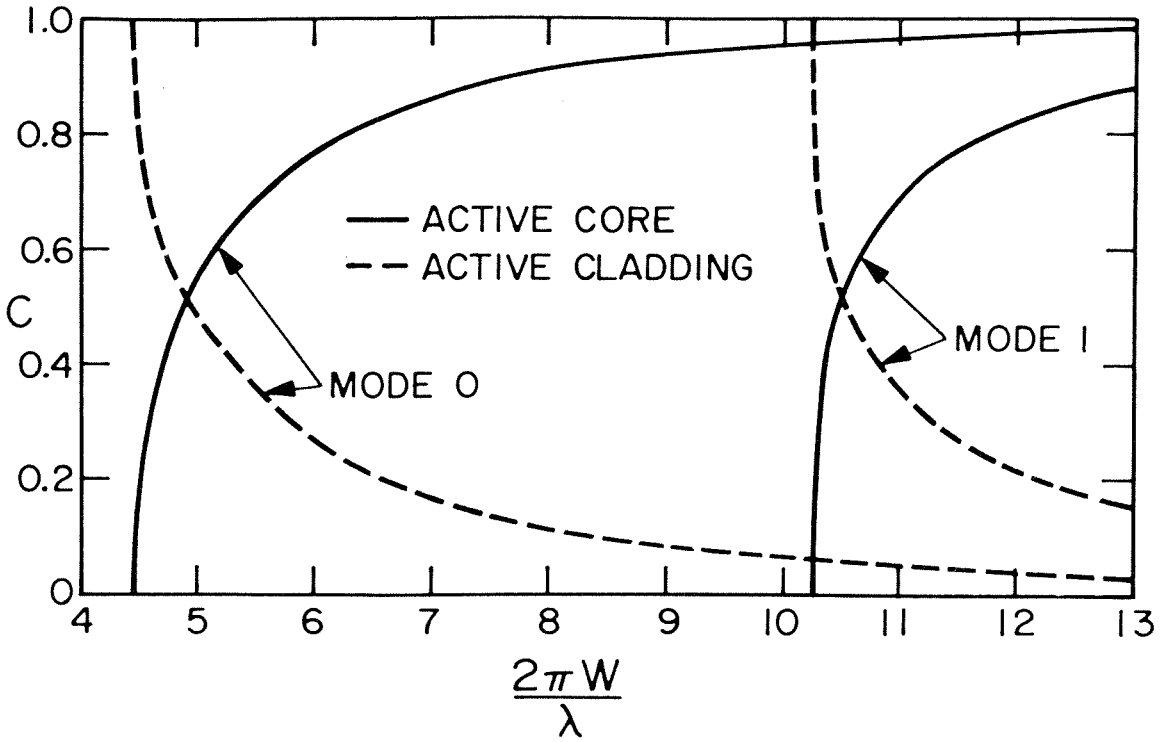

Fig. 3.4 Effective gain coefficients for the 0 and 1 TE modes of a fiber waveguide for the dielectric constants $\varepsilon_1 = (1.5)^2$ and $\varepsilon_2 = (1.4)^2$.

Chapter IV

Coupling Coefficients

In this chapter mode conversion in periodically disturbed dielectric waveguides is studied. In particular, we are interested in the contradirectional coupling of a p^{th} waveguide mode to a q^{th} waveguide mode. For the case of the thin film waveguide, we consider the three types of periodic structures shown in Fig. 2.1 of Chapter II: waveguides with a periodic inhomogeneity in the guiding region, waveguides with a periodic inhomogeneity in the substrate, and waveguides with periodic boundaries. For the case of diffusion and fiber waveguides, we limit our study to the case of waveguides with periodic boundaries. In all cases, the method of analysis is that developed by Elachi and Yeh[22] in their study of mode conversion in periodically and randomly disturbed thin film waveguides. The method is a perturbation analysis that considers a periodic disturbance (assumed small, i.e., $\eta \ll 1$ in (4.1a))to modify the transverse and longitudinal wave vectors of the unperturbed solutions.

A. Coupling Coefficient for a Periodically Inhomogeneous Thin Film Waveguide

We consider first the case of a periodically inhomogeneous guide imbedded in a homogeneous substrate, where

$$\varepsilon(z) = \begin{cases} \varepsilon_0\varepsilon_1(1+\eta \cos Kz) & |x| \leq w \qquad (4.1a) \\ \varepsilon_0\varepsilon_2 & |x| \geq w \qquad (4.1b) \end{cases}$$

and η is the amplitude of the relative permittivity change and K

is the wave vector of the perturbation as defined in Chapter II. We consider the interaction between a forward p mode and a backward q mode where the requirement for strong interaction was found in Chapter II to be

$$|\beta_p'| + |\beta_q'| = K \tag{4.2}$$

The condition (4.2) is referred to as longitudinal phase matching, and occurs at a frequency ω_{pq} as indicated in Fig. 2.7.

To formulate the coupling mechanism we consider the p^{th} waveguide mode of frequency $\omega = \omega_{pq} + \Delta\omega$ and write the corresponding electric field as

$$E_p(x,z) = d_p\, a_p'(x)\, \exp(i\beta_p' z) \tag{4.3}$$

The mode amplitude is d_p and the transverse behavior $a_p'(x)$ is given by (see Appendix A, (A.3))

$$a_p'(x) = \begin{cases} \dfrac{\cos(s_p' x)}{\cos(s_p' w)} & \text{even modes} \quad |x| \le w \qquad (4.4a) \\ \dfrac{\sin(s_p' x)}{\sin(s_p' w)} & \text{odd modes} \quad |x| \le w \qquad (4.4b) \\ \exp(\delta' w - \delta' |x|) & \text{even modes} \quad |x| \ge w \qquad (4.4c) \\ \text{sign}(x)\, \exp(\delta' w - \delta' |x|) & \text{odd modes} \quad |x| \ge w \qquad (4.4d) \end{cases}$$

The transverse wave vectors s_p' and δ_p' and the longitudinal wave vector β_p' are the wave vectors of the perturbed waveguide defined by

$$s_p' = s_p + \Delta s \tag{4.5a}$$

$$\delta_p' = \delta_p + \Delta\delta \tag{4.5b}$$

$$\beta_p' = \beta_p + \Delta\beta \tag{4.5c}$$

where s_p, δ_p, and β_p are the $(p+1)^{th}$ solution of the dispersion relations for the unperturbed waveguide. From Appendix A, the unperturbed dispersion relations are

$$s_p^2 = \varepsilon_1 k^2 - \beta_p^2 \tag{4.6}$$

$$\delta_p^2 = \varepsilon_2 k^2 + \beta_p^2 \tag{4.7}$$

$$\delta_p = s_p \begin{cases} \tan(s_p w) & \text{even modes} \\ -\cot(s_p w) & \text{odd modes} \end{cases} \tag{4.8}$$

The terms Δs, $\Delta\delta$, and $\Delta\beta$ are small perturbations (as $\eta << 1$ in (4.1a)) caused by the inhomogeneity.

Inserting the perturbed solution (4.3) into the wave equation (2.3) using (4.1a,b) gives

$$\left[\frac{\partial^2}{\partial x^2} + \frac{\partial^2}{\partial y^2} + \varepsilon_1 \frac{\omega^2}{c^2}\right] E_p(x,z) = -\eta \frac{\omega^2}{c^2} \varepsilon_1 E_p(x,z)\cos(Kz) \qquad |x| \leq w \tag{4.9a}$$

$$\left[\frac{\partial^2}{\partial x^2} + \frac{\partial^2}{\partial y^2} + \varepsilon_2 \frac{\omega^2}{c^2}\right] E_p(x,z) = 0 \qquad |x| \geq w \tag{4.9b}$$

We can identify the perturbation term on the left hand side of (4.9a) with a spatially periodic convection current J_c where

$$J_c = -i\omega\varepsilon_o\varepsilon_1 \eta E_p(x,z) \cos(Kz)\, h(x) \tag{4.10}$$

and

$$h(x) = \begin{cases} 1 & |x| < w \\ 0 & |x| > w \end{cases} \tag{4.11}$$

Writing $\cos(Kz)$ in exponential form and using (4.3)

$$J_c = -i\omega\eta \frac{\varepsilon_o\varepsilon_1}{2} d_p a_p'(x)\, h(x)[e^{i(\beta_p'+K)z} + e^{i(\beta_p'-K)z}] \tag{4.12}$$

Considering the case of contradirectional longitudinal phase matching (see (4.2)), we see that the current J_c has a term of phase $\exp(-i|\beta' q|z)$ and is therefore able to excite a backward q mode according to the wave equation

$$[\frac{\partial^2}{\partial x^2} + \frac{\partial^2}{\partial y^2} + \varepsilon_{1,2} \frac{\omega^2}{c^2}] Eq(x,z) = -\frac{\eta}{2} \frac{\omega^2}{c^2} \varepsilon_1 c_p a_p'(x) e^{-i|\beta_q'|z} h(x) \tag{4.13}$$

where, as in (2.43) of Chapter II,

$$\varepsilon_{1,2} = \varepsilon_1 h(x) + \varepsilon_2(1 - h(x)) \tag{4.14}$$

Using an expression similar to (4.3), we write the backward q mode as

$$Eq(x,z) = d_q a_q'(x)\, e^{i\beta_q' z} \tag{4.15}$$

To determine the effective excitation current for the new q^{th} mode, we must expand J_c as a function of the transverse modes.

Using

$$a'_p(x)\, h(x) = \sum_j \phi'^{g}_{pj}\, a'_j(x) \tag{4.16}$$

where

$$\phi'^{g}_{pj} = \frac{\int_{-\infty}^{\infty} a'_p(x)\, h(x) a'^{*}_j(x)\, dx}{\int_{-\infty}^{\infty} a'_j(x)\, a'^{*}_j(x)\, dx} = \frac{\int_{-w}^{w} a'_p(x)\, a'^{*}_j(x)\, dx}{\int_{-\infty}^{\infty} a'_j(x)\, a'^{*}_j(x)\, dx} \tag{4.17}$$

we write (4.13) as

$$\left[\frac{\partial^2}{\partial x^2} + \frac{\partial^2}{\partial z^2} + \varepsilon_{1,2}\frac{\omega^2}{c^2}\right] d_q a'_q(x) = -\frac{\eta}{2}\frac{\omega^2}{c^2}\varepsilon_1 d_p \sum_j \phi'^{g}_{pj}\, a'_j(x) \tag{4.18}$$

For $j = q$, (4.18) is independent of x and is said to be transversely phase matched[22]. For $j \neq q$, the driven term (left hand side) is not synchronized in space with the source term (right hand side). Thus the current terms corresponding to the $\phi'^{g}_{pj}\, a'_j(x)$'s $(j \neq q)$ are not effective in exciting the backward q mode. We can now write (4.18) as

$$\left[(s_q + \Delta s)^2 + (\beta_q + \Delta\beta)^2 - \varepsilon_1 \frac{(\omega_{pq} + \Delta\omega)}{c^2}\right] d_q = \frac{\eta}{2}\varepsilon_1 \frac{(\omega_{pq} + \Delta\omega)^2}{c^2} d_p\, \phi'^{g}_{pq} \tag{4.19a}$$

$$\left[-(\delta q + \Delta\delta)^2 + (\beta_q + \Delta\beta)^2 - \varepsilon_2 \frac{(\omega_{pq} + \Delta\omega)}{c^2}\right] d_q = \frac{\eta}{2}\varepsilon_1 \frac{(\omega_{pq} + \Delta\omega)^2}{c^2} d_p\, \phi'^{g}_{pq} \tag{4.19b}$$

Expanding (4.19a,b), neglecting second order terms, and using (4.6) and (4.7), we have

$$\left[s_q\,\Delta s + \beta_q \Delta\beta - \varepsilon_1 \frac{\omega_{pq}\Delta\omega}{c^2}\right]d_q = \frac{\eta\varepsilon_1}{4}\frac{\omega_{pq}^2}{c^2}\,d_p\,\phi_{pq}^g \tag{4.20a}$$

$$\left[-\delta_q\,\Delta\delta + \beta_q \Delta\beta - \frac{\varepsilon_2\omega_{pq}\Delta\omega}{c^2}\right]d_q = \frac{\eta\varepsilon_1}{4}\frac{\omega_{pq}^2}{c^2}\,d_p\,\phi_{pq}^g \tag{4.20b}$$

where

$$\phi_{pq}^g = \frac{\int_{-w}^{w} a_p(x)a_q^*(x)\,dx}{\int_{-\infty}^{\infty} a_q(x)a_q^*(x)\,dx} = \begin{cases} \dfrac{2\delta_q \cos^2(s_q w)}{(\delta_p+\delta_q)(1+\delta_q w)} & p \neq q;\ p \text{ even},\ q \text{ even} \quad (a) \\ \dfrac{\delta_p w + \sin^2(s_q w)}{(1+\delta_p w)} & p = q;\ p \text{ even},\ q \text{ even} \quad (b) \\ \dfrac{2\delta_q \sin^2(s_q w)}{(\delta_p+\delta_q)(1+\delta_q w)} & p \neq q;\ p \text{ odd},\ q \text{ odd} \quad (c) \\ \dfrac{\delta_p w + \sin^2(s_p w)}{(1+\delta_p w)} & p = q;\ p \text{ odd},\ q \text{ odd} \quad (d) \\ 0 & p \text{ odd},\ q \text{ even; or } q \text{ odd},\ p \text{ even} \quad (e) \end{cases} \tag{4.21}$$

In (4.20a,b) we have used a first order Taylor series expansion

$$f(x+\Delta x) = f(x) + \Delta x\, f'(x) \tag{4.22}$$

on the transverse functions $a_p'(x)$ to obtain the unperturbed transverse functions $a_p(x)$ given by (4.4a,b,c,d) with Δs, $\Delta\delta$, and $\Delta\beta$ equal to zero.

Equations (4.20a,b) require that

$$s_q \Delta s - \varepsilon_1 \frac{\omega_{pq} \Delta\omega}{c^2} = -\delta_q \Delta\delta - \varepsilon_2 \frac{\omega_{pq} \Delta\omega}{c^2} \tag{4.23}$$

Equation (4.23) relates the perturbed and unperturbed wave vectors in the perturbed waveguide. Due to the current J_c (see (4.10)), the unperturbed relations (4.6) and (4.7) do not hold for the perturbed wave vectors s_p', δ_p', and β_p'. However, the dispersion relation (4.8) results from the boundary condition at $x = \pm w$ (see Appendix A) and remains valid for the perturbed wave vectors. Hence we can use (4.22) and (4.8) to obtain

$$\Delta\delta = \Delta s \left[\begin{Bmatrix} \tan(s_q w) \\ -\cot(s_q w) \end{Bmatrix} + s_q w \begin{Bmatrix} \sec^2(s_q w) \\ \csc^2(s_q w) \end{Bmatrix} \right] \tag{4.24}$$

Combining (4.23) and (4.24) we write

$$\Delta s = \frac{(\varepsilon_1 - \varepsilon_2) \frac{\omega_{pq} \Delta\omega}{c^2}}{s_q + \delta_q \left[\begin{Bmatrix} \tan(s_q w) \\ -\cot(s_q w) \end{Bmatrix} + s_q w \begin{Bmatrix} \sec^2(s_q w) \\ \csc^2(s_q w) \end{Bmatrix} \right]} \tag{4.25}$$

We use (4.8) to write the product

$$s_q \Delta s = \frac{(\varepsilon_1 - \varepsilon_2)\omega_{pq} \Delta\omega \begin{Bmatrix} \cos^2(s_q w) \\ \sin^2(s_q w) \end{Bmatrix}}{1 + \delta_q w} \tag{4.26}$$

and (4.20a) becomes

$$\left[\beta_q \Delta\beta - \left(\frac{\varepsilon_1 \begin{cases} \sin^2(s_q w) \\ \cos^2(s_q w) \end{cases} + \varepsilon_1 \delta_q w}{1 + \delta_q w} + \frac{\varepsilon_2 \begin{cases} \cos^2(s_q w) \\ \sin^2(s_q w) \end{cases}}{1 + \delta_q w} \right) \frac{\omega_{pq} \Delta\omega}{c^2} \right] d_q$$

$$= \frac{\eta}{4} \varepsilon_1 \frac{\omega_{pq}^2}{c^2} d_p \phi_{pq}^g \qquad (4.27)$$

Multiplying (4.27) through by $(\beta_q K)^{-1}$ and rearranging, we have

$$\left[\frac{\Delta\beta}{K} - \left(\frac{\beta_q}{K}\right) B_q \frac{\Delta\omega}{\omega_{pq}}\right] d_q = \frac{\eta}{4} \varepsilon_1 \left(\frac{\omega_{pq}}{c}\right)^2 \frac{1}{\beta_q} \frac{1}{K} d_p \phi_{pq}^g \qquad (4.28)$$

where

$$B_q = \frac{\omega_{pq}^2}{c^2 \beta_q^2} \left(\frac{\varepsilon_1 \begin{cases} \sin^2(s_q w) \\ \cos^2(s_q w) \end{cases} + \varepsilon_1 \delta_q w}{1 + \delta_q w} + \frac{\varepsilon_2 \begin{cases} \cos^2(s_q w) \\ \sin^2(s_q w) \end{cases}}{1 + \delta_q w} \right) \qquad (4.29)$$

At the same time, as expected by symmetry considerations, a q^{th} mode generates a convection current which excites a p^{th} mode; therefore the coefficients d_q and d_p are also related by

$$\left[\frac{\Delta\beta}{K} - \left(\frac{\beta_p}{K}\right) B_p \frac{\Delta\omega}{\omega_{pq}}\right] d_p = \frac{\eta}{4} \varepsilon_1 \left(\frac{\omega_{pq}}{c}\right)^2 \frac{1}{\beta_p} \frac{1}{K} d_q \phi_{qp}^g \qquad (4.30)$$

where B_p and ϕ_{qp}^g are equivalent to B_q and ϕ_{pq}^g with p and q interchanged. As the q^{th} mode is travelling in the -z direction, $\beta_q = -|\beta_q|$. To satisfy both equations (4.35) and (4.37), we must have

$$\left[\frac{\Delta\beta}{K} + \frac{|\beta_q|}{K} B_q \frac{\Delta\omega}{\omega_{pq}}\right]\left[\frac{\Delta\beta}{K} - \frac{|\beta_p|}{K} B_p \frac{\Delta\omega}{\omega_{pq}}\right] = -\left(\frac{\eta\varepsilon_1}{4}\right)^2 \left(\frac{\omega_{pq}}{c}\right)^4 \frac{\phi^g_{qp}\ \phi^g_{pq}}{|\beta_p||\beta_q|K} \tag{4.31}$$

and therefore

$$\frac{\Delta\beta}{K} = (\theta_p - \theta_q)\frac{\Delta\omega}{\omega_{pq}} \pm \sqrt{(\theta_p + \theta_q)^2\left(\frac{\Delta\omega}{\omega_{pq}}\right)^2 - \eta^2(\xi^g_{pq})^2} \tag{4.32}$$

where

$$\theta_r = \frac{|\beta_r|}{2K}|B_r| \quad , \quad r = p,q \tag{4.33}$$

$$\xi^g_{pq} = \frac{\varepsilon_1}{4}\left(\frac{\omega_{pq}}{c}\right)^2 \frac{1}{K}\sqrt{\frac{\phi^g_{pq}\ \phi^g_{qp}}{|\beta_p||\beta_q|}} \tag{4.34}$$

Equation (4.32) gives the normalized change of the longitudinal wave vector for an operating frequency equal to $\omega_{pq} + \Delta\omega$ and a perturbation amplitude η . Equations (2.35) and (2.36) (see Chapter II, Section A) are the corresponding equations for a transversely unbounded medium. The choice of the + sign in (4.32) corresponds to $\Delta\beta_p/K$ as the p^{th} mode loses energy as it excites a q^{th} mode. Similarly, the choice of the - sign in (4.32) corresponds to $\Delta\beta_q/K$. Using (4.26) and (4.23) we can solve for Δs_p, Δs_q, $\Delta\delta_p$, $\Delta\delta_q$ and then use (4.3) and (4.4a,b,c,d) to completely express the transverse and longitudinal behavior of the guided modes.

As in the unbounded infinite case (Chapter II, Section A), the solution for the longitudinal wave vector is complex in a frequency band (called a stop band region) centered at ω_{pq} and of total width

$$\Omega = 2\eta\ \omega_{pq}\ \xi_{pq}/(\alpha_p+\alpha_q) \tag{4.35}$$

The corresponding Brillouin diagram is shown in Fig. 2.4 . For an interaction where $p = q$, $\Delta\beta$ is pure imaginary. Otherwise, for $\Delta\omega \neq 0$, $\Delta\beta$ has a real component as indicated in Fig. 2.6b.

The imaginary component of the longitudinal wave vector has a maximum value

$$\chi^g_{pq}(k) = \chi^g_{pq}\left(\frac{\omega_{pq}}{c}\right) = \eta\ \frac{\varepsilon_1}{4}\ \left(\frac{\omega_{pq}}{c}\right)^2 \sqrt{\frac{\phi^g_{pq}\ \phi^g_{qp}}{|\beta|\,|\beta|}} \tag{4.36}$$

Equation (4.36) is the required coupling coefficient analogous to $\varepsilon_1\eta\ h(x)k^2/(4\beta_{ro})$ in (2.49a,b) to be used in (2.53a,b) for the case of a periodic dielectric constant in the guiding region. The normalized coupling coefficient $\chi^g_{pq}(k)L$, where L is the length of the perturbation region, is plotted in Figs. 4-1 and 4-2. As we expect from physical reasoning, the value of $\chi^g_{pq}(k)L$ is small near cutoff as most of the mode energy is in the substrate where there is no perturbation. As the frequency increases, more optical energy is enclosed into the periodic guide leading to stronger coupling. This trend continues for coupling between $p = q$ modes (Fig. 4.1). However, for coupling between $p \neq q$ modes (Fig. 4.2), after a certain optimal frequency, $\chi^q_{pq}(k)L$ drops off as the overlap term ϕ^g_{pq} goes to zero.

The reciprocal of the group velocity for an unperturbed ($\eta = 0$) thin film waveguide can be obtained from (4.28) as

$$\psi_r = \frac{\Delta\beta}{\Delta\omega}\quad \frac{\beta_r B_r}{\omega_{pq}} \tag{4.37}$$

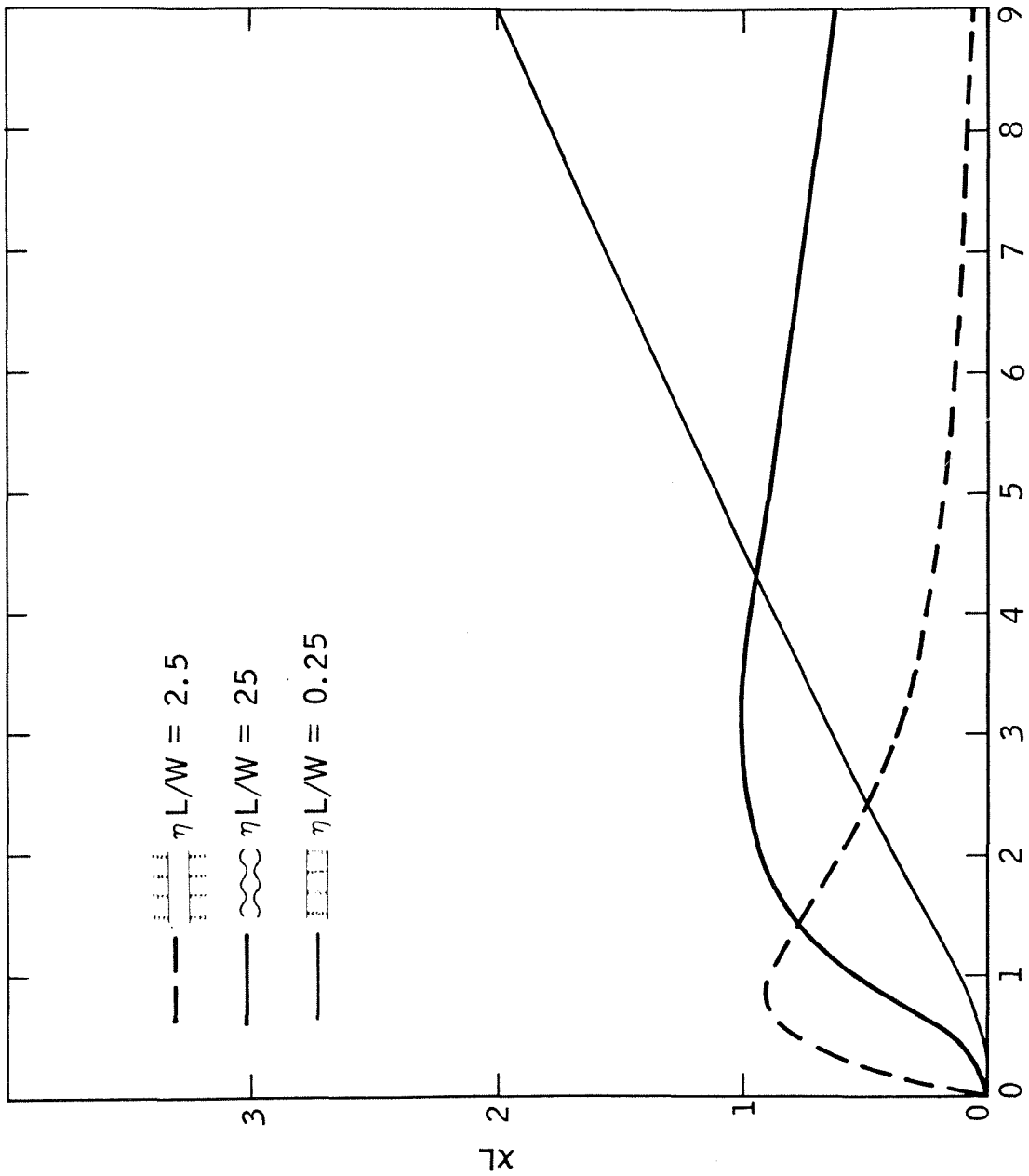

Fig. 4.1 Coupling between 0-0 modes of thin film waveguides for three types of periodic perturbations; $\varepsilon_1 = (3.6)^2$ and $\varepsilon_2 = (3.5)^2$.

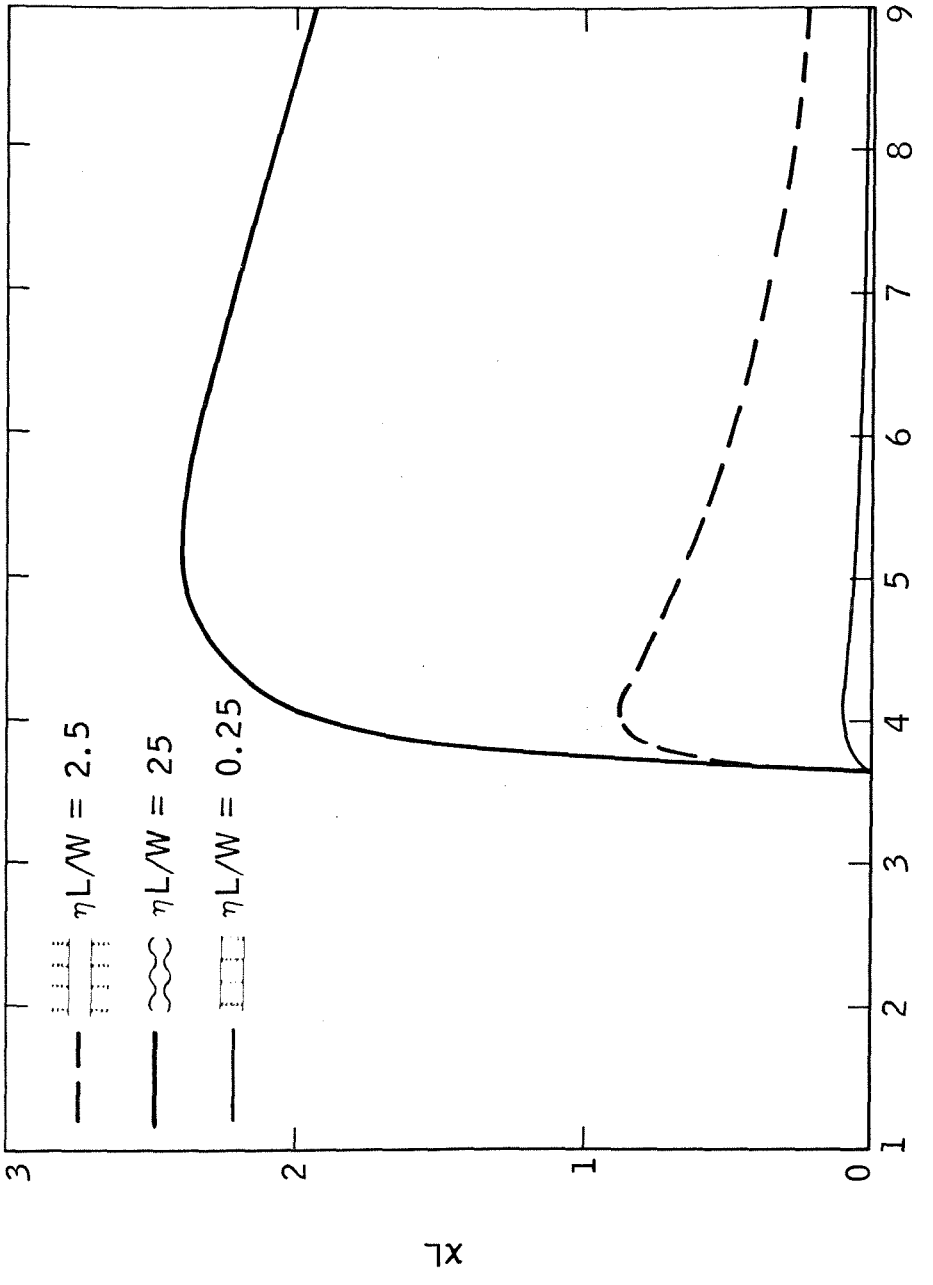

Fig. 4.2 Coupling between 0-1 modes of thin film waveguides for three types of periodic perturbations; $\varepsilon_1 = (3.6)^2$ and $\varepsilon_2 = (3.5)^2$.

B. Coupling Coefficients for a Homogeneous Thin Film Waveguide with a Periodic Substrate

The same method used in the previous section can be applied directly to the case where the waveguide is homogeneous and the substrate has a periodic dielectric constant. The analogous equation to (4.1a,b) is

$$\begin{cases} \varepsilon_o\varepsilon_1 & |x| < w \\ \varepsilon_o\varepsilon_2(1 + \eta \cos Kz) & |x| > w \end{cases} \tag{4.38}$$

In this case the source convection current is in the substrate, and equation (4.32) remains valid with ξ^g_{pq} replaced by

$$\xi^s_{pq} = \frac{\varepsilon_2}{4}\left(\frac{\omega_{pq}}{c}\right)^2 \frac{1}{K} \sqrt{\frac{\phi^s_{pq}\ \phi^s_{qp}}{|\beta_p||\beta_q|}}$$

where

$$\phi^s_{pq} = \frac{\int_{-\infty}^{w} a_p(x)\, a_q^*(x)\, dx + \int_{w}^{\infty} a_p(x)\, a_q^*(x)\, dx}{\int_{-\infty}^{\infty} a_q(x)\, a_q^*(x)\, dx}$$

$$= \begin{cases} \dfrac{2\delta_q \cos^2(s_q w)}{(\delta_p + \delta_q)(1 + \delta_q w)} & q \text{ even} \qquad (4.39a) \\ \dfrac{2\delta_q \sin^2(s_q w)}{(\delta_p + \delta_q)(1 + \delta_q w)} & q \text{ odd} \qquad (4.39b) \end{cases}$$

The coupling coefficient for the case of a periodic dielectric constant in the guiding region is thus given by

$$\chi^s_{pq}(k) = \eta \frac{\varepsilon_2}{4} \left(\frac{\omega_{pq}}{c}\right)^2 \sqrt{\frac{\phi^s_{pq}\,\phi^s_{qp}}{|\beta_p||\beta_q|}} \tag{4.40}$$

The normalized coupling coefficient $\chi^s_{pq}(k)L$ is plotted in Figs. 4.1 and 4.2. In this case, the coupling coefficient increases rapidly to a maximum close to the cutoff frequency of the waveguide, and then drops off with increasing frequency as the mode energy becomes confined to the unperturbed guide region and no longer "feels" the perturbation in the substrate region.

C. Coupling Coefficient for a Homogeneous Thin Film Waveguide with Periodic Boundaries

An approach similar to that used in sections A and B of this chapter can be used to study the case where the boundary between the waveguide and substrate is given by

$$x = \pm w(1 + \eta \cos Kz) \qquad (\eta << 1) \tag{4.41}$$

We will determine the coupling by using a surface current to represent the surface perturbation. We assume in this and the two following sections that $\eta w \lesssim \lambda/10$ so that the Rayleigh assumption for scattering from periodic surfaces is valid[74,75,76].

In Fig. 4.3a we have sketched a perturbed boundary of a waveguide and in Fig. 4.3b we have sketched an equivalent configuration consisting of an unperturbed waveguide boundary with a surface current $\underline{J}_s = J(z)\,\delta(x)\,\hat{e}_y$. The function $\delta(x)$ is the Dirac delta function.

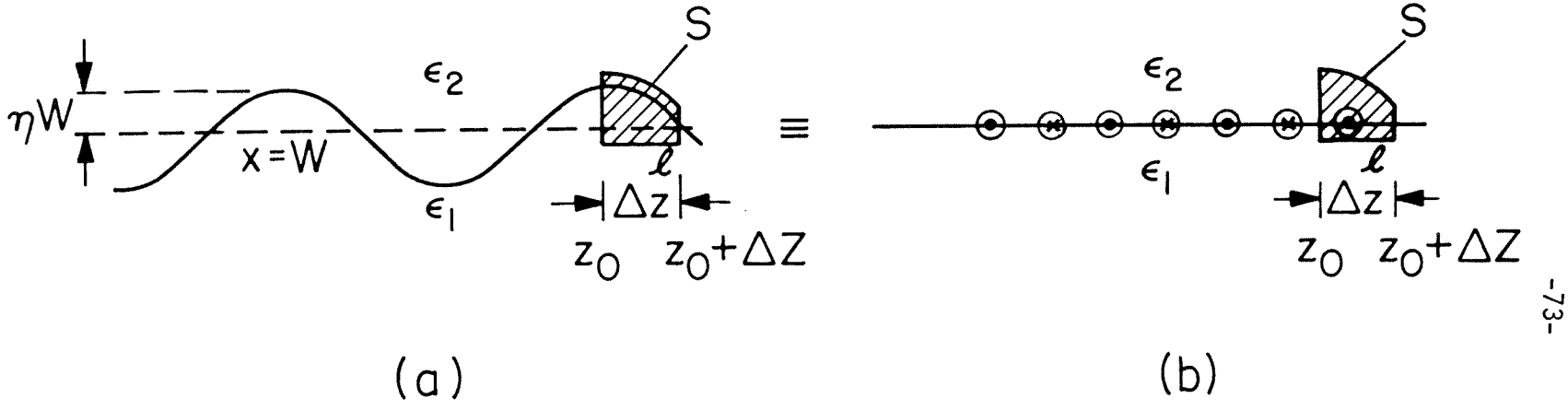

Fig. 4.3 A periodic boundary (a) can be represented by a surface current (b). The area S is bounded by ℓ composed of segments ℓ_1, ℓ_2, ℓ_3 and ℓ_4. ℓ_1 is described by $x = w^-$, z varies from z_0 to $z_0 + \Delta z$; ℓ_2 by $z = z_0 + \Delta z$, x varies from w^- to $\eta w \cos[K(z_0+\Delta z)]$; ℓ_3 by a varying from $z_0 + \Delta z$ to z_0 and $x = \eta w \cos(Kz)$; and ℓ_4 by $z = z_0$ and x varies from $\eta w \cos(Kz_0)$ to w^-.

Stokes's theorem states that

$$\oint_{\ell} \underline{F} \cdot d\underline{\ell} = \int_{S} (\nabla \times \underline{F}) \cdot d\underline{S} \tag{4.42}$$

where $\underline{F}$ is a vector field and $d\underline{\ell}$ is a line element of the closed curve bounding the open surface S. Using (2.1b),

$$\nabla \times \underline{H} = \frac{\partial}{\partial t} (\varepsilon_o \varepsilon_{rel} \underline{E}) + \underline{J} \tag{4.43}$$

we can use Stokes's theorem to write

$$\oint_{\ell} \underline{H} \cdot d\underline{\ell} = -i\omega\varepsilon_o\varepsilon_{rel} \int_{S} \underline{E} \cdot d\underline{S} + \int_{S} \underline{J} \cdot d\underline{S} \tag{4.44}$$

Applying (4.44) to Fig. 4.3a, we have

$$\oint_{\ell} \underline{H} \cdot d\underline{\ell} = -i\omega\varepsilon_o\varepsilon_1 \int_{S} \underline{E} \cdot d\underline{S} \tag{4.45}$$

Similarly, considering Fig. 4.3b, we find

$$\oint_{\ell} \underline{H} \cdot d\underline{\ell} = -i\omega\varepsilon_o\varepsilon_2 \int_{S} \underline{E} \cdot d\underline{S} + \int_{S} J(z)\ \delta(x)\hat{e}_y \cdot d\underline{S} \tag{4.46}$$

Thus

$$\int_{S} J(z)\ \delta(x)\ \hat{e}_y \cdot d\underline{S} = -i\varepsilon_o(\varepsilon_1-\varepsilon_2)\omega \int_{S} \underline{E} \cdot d\underline{S} \tag{4.47}$$

which yields

$$J(z)\ \Delta z = -i\varepsilon_o(\varepsilon_1 - \varepsilon_2)\omega\ \Delta x\ \Delta z\ E\Big|_{x=w}(x,z) \tag{4.48}$$

Using $\Delta x = \eta w \cos Kz$ and considering $E(x,z)$ to be the p^{th} waveguide mode of frequency $\omega = \omega_{pq} + \Delta\omega$ we can write

$$J(z) = -i\varepsilon_o \eta w(\varepsilon_1-\varepsilon_2)\omega \cos(Kz)\, d_p\, e^{i\beta'_p z} \tag{4.49}$$

This surface current can excite a backward q mode if the contradirectional phase matching condition (4.2) is satisfied. The boundary condition for this new q mode is

$$H_z\Big|_{x=w^+}(x,z) - H_z\Big|_{x=w^-}(x,z) = J_s(z) \tag{4.50}$$

where

$$J_s(z) = -i\varepsilon_o \eta\, w(\frac{\varepsilon_1-\varepsilon_2}{2})\omega\, d_p\, e^{-i|\beta'_q|z} \tag{4.51}$$

is the component of the surface current $J(z)$ in phase with the generated wave.

Using (2.1a) for TE modes we have

$$\frac{\partial E_y}{\partial x} = i\mu_o\omega H_z$$

and using (4.4a,b,c,d) we can write (4.50) as

$$\left[s'_q \begin{cases} \tan(s'_q w) \\ -\cot(s'_q w) \end{cases} - \delta'_q \right] d_q = (\frac{\omega}{c})^2 \eta w(\frac{\varepsilon_1-\varepsilon_2}{2})\, d_p \tag{4.52}$$

This relation for the perturbed wave vector is analogous to the dispersion relation (4.8) resulting from the boundary condition of the unperturbed waveguide, and couples the two modes p and q through

the perturbation of the boundary. From the wave equation (2.3), we see that the dispersion relations (4.6) and (4.7) remain valid for the perturbed wave vectors s_p', δ_p', and β_p'.

We now use (4.5a,b), (4.8), and (4.22) with (4.52) to obtain

$$\left\{ \Delta s \left[\begin{cases} \tan(s_q w) \\ -\cot(s_q w) \end{cases} + s_q w \begin{cases} \sec^2(s_q w) \\ \csc^2(s_q w) \end{cases} \right] - \Delta\delta \right\} d_q$$

$$= \left(\frac{\omega_{pq}}{c}\right)^2 \eta w \left(\frac{\varepsilon_1 - \varepsilon_2}{2}\right) d_p \tag{4.53}$$

As the dispersion relations (4.6) and (4.7) hold for the perturbed wave vectors, we can use (4.5a,b,c) to yield, neglecting second order terms,

$$\Delta s = \frac{1}{s_q}(\varepsilon_1 k \Delta k - \beta_q \Delta\beta) \tag{4.54}$$

$$\Delta\delta = \frac{1}{\delta_q}(\beta_q \Delta\beta - \varepsilon_2 k \Delta k) \tag{4.55}$$

With (4.54) and (4.55) we can write (4.53) as

$$\left[\left(\frac{\varepsilon_1 A_q}{s_q} + \frac{\varepsilon_2}{\delta_q}\right) k \Delta k - \left(\frac{A_q}{s_q} + \frac{1}{\delta_q}\right) \beta \Delta \beta \right] d_q$$

$$= \left(\frac{\omega_{pq}}{c}\right)^2 \eta\, w \left(\frac{\varepsilon_1 - \varepsilon_2}{2}\right) d_p \tag{4.56}$$

where

$$A_q = \begin{cases} \tan(s_q w) \\ -\cot(s_q w) \end{cases} + s_q w \begin{cases} \sec^2(s_q w) \\ \csc^2(s_q w) \end{cases} \tag{4.57}$$

By algebraic manipulation and use of (4.8)

$$\left(\frac{A_q}{s_q} + \frac{1}{\delta_q}\right) = \frac{1 + \delta_q w}{\delta_q \begin{cases} \cos^2(s_q w) \\ \sin^2(s_q w) \end{cases}} \tag{4.58}$$

and

$$\left(\frac{\varepsilon_1 A_q}{s_q} + \frac{\varepsilon_2}{\delta_q}\right)\left(\frac{A_q}{s_q} + \frac{1}{\delta_q}\right)^{-1} = \frac{\varepsilon_1 \begin{cases} \sin^2(s_q w) \\ \cos^2(s_q w) \end{cases} + \varepsilon_1 \delta_q w}{1 + \delta_q w} + \frac{\varepsilon_2 \begin{cases} \cos^2(s_q w) \\ \sin^2(s_q w) \end{cases}}{1 + \delta_q w} \tag{4.59}$$

Therefore, multiplying (4.56) through by $(\beta_q k)^{-1}(A_q/s_q + 1/\delta_q)^{-1}$ and rearranging, we have

$$\left[\frac{\Delta\beta}{k} - \left(\frac{\beta_q}{K}\right) B_q \frac{\Delta\omega}{\omega}\right] d_q = \left(\frac{\omega_{pq}}{c}\right)^2 \eta\left(\frac{\varepsilon_1 - \varepsilon_2}{2}\right) \phi^b_{pq}\, d_p \frac{1}{\beta_q K} \tag{4.60}$$

where

$$\phi^b_{pq} = w\left(\frac{A_q}{s_q} + \frac{1}{\delta_q}\right) = \frac{\delta_q w \begin{cases} \cos^2(s_q w) \\ \sin^2(s_q w) \end{cases}}{1 + \delta_q w} \tag{4.61}$$

and B_q, as in (4.29), is given by

$$B_q = \frac{\omega_{pq}^2}{c^2 \beta_q^2} \left(\frac{\varepsilon_1 \begin{cases} \sin^2(s_q w) \\ \cos^2(s_q w) \end{cases} + \varepsilon_1 \delta_q w}{1 + \delta_q w} + \frac{\varepsilon_2 \begin{cases} \cos^2(s_q w) \\ \sin^2(s_q w) \end{cases}}{1 + \delta_q w} \right) \tag{4.62}$$

By the same analysis that developed (4.60), a q^{th} mode will excite a p^{th} mode leading to the relation

$$[\frac{\Delta\beta}{K} - (\frac{\beta_p}{K})B_p \frac{\Delta\omega}{\omega}]d_p = (\frac{\omega_{pq}}{c})^2 \eta(\frac{\varepsilon_1-\varepsilon_2}{2})\phi^b_{qp} d_q \frac{1}{\beta_p K} \tag{4.63}$$

Multiplying (4.60) and (4.63) gives

$$[\frac{\Delta\beta}{K} + \frac{|\beta_q|}{K} B_q \frac{\Delta\omega}{\omega_{pq}}][\frac{\Delta\beta}{K} - \frac{|\beta_p|}{K} B_p \frac{\Delta\omega}{\omega_{pq}}] = -\eta^2(\frac{\varepsilon_1-\varepsilon_2}{2})^2(\frac{\omega_{pq}}{c})^4 \frac{1}{K^2} \frac{\phi^b_{qp}\phi^b_{pq}}{|\beta_p||\beta_q|} \tag{4.64}$$

Equation (4.64) is similar to (4.31) and the solution for $\Delta\beta/K$ has the same form:

$$\frac{\Delta\beta}{K} = (\theta_p - \theta_q)\frac{\Delta\omega}{\omega_{pq}} \pm \sqrt{(\theta_p+\theta_q)^2 (\frac{\Delta\omega}{\omega_{pq}})^2 - \eta^2(\xi^b_{pq})^2} \tag{4.65}$$

where

$$\theta_r = \frac{|\beta_r|}{2K}|B_r| \qquad r = p,q \tag{4.66}$$

$$\xi^b_{pq} = (\frac{\varepsilon_1-\varepsilon_2}{2})(\frac{\omega_{pq}}{c})^2 \frac{1}{K} \frac{\phi^b_{pq}\phi^b_{qp}}{|\beta_p||\beta_q|} \tag{4.67}$$

From (4.65) we obtain expressions for $\Delta\beta_p$ and $\Delta\beta_q$ and therefore, using (4.54) and (4.55), obtain Δs_p, Δs_q, $\Delta\delta_p$, and $\Delta\delta_q$. Thus with (4.3) and (4.4a,b,c,d) we can express the complete transverse and longitudinal behavior of the guided modes in a thin film waveguide with periodic boundaries.

The maximum value of the imaginary component of the longitudinal wave vector is

$$\chi^b_{pq}(k) = \eta(\frac{\varepsilon_1-\varepsilon_2}{2})(\frac{\omega^2_{pq}}{c}) \sqrt{\frac{\phi^b_{pq}\phi^b_{qp}}{|\beta_p||\beta_q|}} \tag{4.68}$$

The normalized coupling coefficient $\chi^{b}_{pq}(k)L$ is plotted in Figs. 4.1 and 4.2. We see that near cutoff, where most of the mode energy is in the substrate, the coupling is weak. At high frequency when the mode energy is inside the waveguide, the field at the boundary is small and the coupling is reduced. The strongest coupling occurs at an optimum frequency somewhere in between.

D. Coupling Coefficients for Diffusion Waveguides with Periodic Boundaries

In this section we derive the coupling coefficients for the two diffusion waveguides (shown in Fig. B.1a,b of Appendix B) for the case of periodic boundary perturbations.

The channel diffusion guide indicated in Fig. B.1a has perturbed boundaries given by

$$x = \pm w(1 + \eta \cos(Kz)) \tag{4.69a}$$

The half space diffusion guide (Fig. B.1b) has a perturbed boundary given by

$$x = \pm \eta' \cos(Kz) \tag{4.69b}$$

Both boundaries have the appearance sketched in Fig. 4.3a. For this reason, as explained in Section C, a forward p^{th} mode can excite a backward q^{th} mode through the boundary conditions (4.50)

$$H_z\Big|_{x=w^+}(x,z) - H_z\Big|_{x=w^-}(x,z) = J_s(z) \qquad \text{(channel guide)} \tag{4.70a}$$

$$H_z\Big|_{x=0^+}(x,z) - H_z\Big|_{x=0^-}(x,z) = J_s(z) \qquad \text{(half-space guide)} \tag{4.70b}$$

As in previous sections, we consider a p^{th} waveguide mode of frequency $\omega = \omega_{pq} + \Delta\omega$ with a corresponding electric field,

$$E_p(x,z) = d_p a_p'(x) \exp(i\beta_p' z) \tag{4.71}$$

The mode amplitude is d_p and the transverse behavior $a_p'(x)$ is given

by (see Appendix B)

$$a_p'(x) = \begin{cases} \dfrac{J_{\nu_p'}\left(2\sqrt{\alpha}\, kd_o e^{-\frac{|x|-w}{2d_o}}\right)}{J_{\nu_p'}(2\sqrt{\alpha}\, kd_o)} & \text{channel guide } |x| \geq w \quad \text{(a)} \\ \dfrac{\cosh(\delta_p' x)}{\cosh(\delta_p' w)} & \text{(even modes) channel guide } |x| \leq w \quad \text{(b)} \\ \dfrac{\sinh(\delta_p' x)}{\sinh(\delta_p' w)} & \text{(odd modes) channel guide } |x| \leq w \quad \text{(c)} \\ \dfrac{J_{\nu_p'}\left(2\sqrt{\alpha}\, kd_o e^{-\frac{|x|}{2d_o}}\right)}{J_{\nu_p'}(2\sqrt{\alpha}\, kd_o)} & \text{half-space guide } |x| > w \quad \text{(d)} \\ e^{-\delta_p'|x|} & \text{half-space guide } |x| < w \quad \text{(e)} \end{cases} \tag{4.72}$$

The transverse wave vectors $\nu_p'/(2d_o)$ and δ_p' and the longitudinal wave vector β_p' are the wave vectors of the perturbed waveguide defined by

$$\nu_p' = \nu_p + \Delta\nu \tag{4.73a}$$

$$\delta_p' = \delta_p + \Delta\delta \tag{4.73b}$$

$$\beta_p' = \beta_p + \Delta\beta \tag{4.73c}$$

where ν_p, δ_p, and β_p are the $(p+1)^{th}$ solution of the dispersion relations for the unperturbed diffusion waveguides. From Appendix B,

the unperturbed dispersion relations are

$$\frac{\nu_p^2}{(2d_o)^2} = \beta_p^2 - \varepsilon_o k^2 \tag{4.74}$$

$$\delta_p^2 = \beta_p^2 - \varepsilon_2 k^2 \tag{4.75}$$

for both geometries, and

$$\delta_p \begin{cases} \tanh(\delta_p w) \\ \coth(\delta_p w) \end{cases} = -\sqrt{\alpha}\, k\, \frac{J_\nu'(2\sqrt{\alpha}\, kd_o)}{J_\nu(2\sqrt{\alpha}\, kd_o)} \tag{4.76a}$$

for the channel diffusion waveguide, and

$$\delta_p = -\sqrt{\alpha}\, k\, \frac{J_\nu'(2\sqrt{\alpha}\, kd_o)}{J_\nu(2\sqrt{\alpha}\, kd_o)} \tag{4.76b}$$

for the half space diffusion waveguide. The primes in (4.76a,b) indicate differentiation with respect to the argument $2\sqrt{\alpha}\, kd_o$ of the Bessel function J_ν. In the above equations, d_o is the depth of diffusion. The terms $\Delta\nu$, $\Delta\delta$, and $\Delta\beta$ are small perturbations (as $\eta << 1$ in (4.69a), $\eta' << d$ in (4.69b)) caused by the boundary perturbation.

We can now use (4.48) and (4.51) to write (4.70a,b) in the form

$$[J'_{\nu_q}(2\sqrt{\alpha}\, kd_o)\sqrt{\alpha}\, k + \delta_q' \begin{cases} \tanh(\delta_q' w) \\ \coth(\delta_q' w) \end{cases} J_{\nu_q}(2\sqrt{\alpha}\, kd_o)]\, d_q$$

$$= \eta w\left(\frac{\omega}{c}\right)^2 \left(\frac{\varepsilon_1-\varepsilon_2}{2}\right) J_{\nu'_q}(2\sqrt{\alpha}\, kd_o)\, d_p \tag{4.77a}$$

$$\left[J'_{\nu'_q}(2\sqrt{\alpha}\, kd_o)\sqrt{\alpha}\, k + \delta'_q\, J_{\nu'_q}(2\sqrt{\alpha}\, kd_o)\right] d_q$$

$$= \eta'\left(\frac{\omega}{c}\right)^2 \left(\frac{\varepsilon_1-\varepsilon_2}{2}\right) J_{\nu'_q}(2\sqrt{\alpha}\, kd_o)\, d_p \tag{4.77b}$$

Equations (4.77a,b) for the perturbed wave vectors are analogous to the dispersion relations (4.76a,b) of the unperturbed waveguide, and couple the two modes p and q through the boundary perturbation. From the wave equation (2.3), the dispersion relations (4.74) and (4.75) are seen to remain valid for the perturbed wave vectors $\nu'_q/(2d_o)$, δ'_q, and β'_q.

We now use the first order Taylor series expansion

$$f(x+\Delta x, y+\Delta y) = f(x,y) + \frac{\partial f}{\partial x}\Delta x + \frac{\partial f}{\partial y}\Delta y \tag{4.78}$$

and (4.73a,b,c) along with $k = \frac{\omega_{pq} + \Delta\omega}{c} = k_{pq} + \Delta k$ to write (4.77a,b) neglecting second order terms, as

$$\left[\left(\sqrt{\alpha}\,\frac{\omega_{pq}}{c}\,\frac{\partial J'_{\nu_q}}{\partial \nu_q} + \begin{Bmatrix}\tanh(\delta_p w)\\ \coth(\delta_p w)\end{Bmatrix}\delta_p\,\frac{\partial J_{\nu_p}}{\partial \nu}\right)\Delta\nu\right.$$

$$+\left(J_{\nu_p}\,\delta_p w\begin{Bmatrix}\operatorname{sech}^2(\delta_p w)\\ -\operatorname{csch}^2(\delta_p w)\end{Bmatrix} + \begin{Bmatrix}\tanh(\delta_p w)\\ \coth(\delta_p w)\end{Bmatrix} J\nu_p\right)\Delta\delta_p$$

$$\left.+\left(\sqrt{\alpha}\,\frac{\omega_{pq}}{c}\,J''_{\nu_p}\,\frac{2\sqrt{\alpha}\,d_o}{c} + \frac{\sqrt{\alpha}}{c}\,J'_{\nu_p} + \begin{Bmatrix}\tanh(\delta_p w)\\ \coth(\delta_p w)\end{Bmatrix}\delta_p J'_{\nu}\,\frac{2\sqrt{\alpha}\,d_o}{c}\right)\Delta\omega\right] d_q$$

$$= \eta w \frac{(\varepsilon_1 - \varepsilon_2)}{2} \left(\frac{\omega_{pq}}{c}\right)^2 J_{\nu_q} d_p \qquad \text{(channel guide)} \qquad (4.79a)$$

$$\left(\sqrt{\alpha} \left(\frac{\omega_{pq}}{c}\right) \frac{\partial J'_\nu}{\partial \nu} + \delta_p \frac{\partial J_{\nu_p}}{\partial \nu} \right) \Delta\nu + J_{\nu_p} \Delta\delta$$

$$+ \left(\sqrt{\alpha} \left(\frac{\omega_{pq}}{c}\right) J''_{\nu_p} \frac{2\sqrt{\alpha}\, d_o}{c} + \frac{\sqrt{\alpha}}{c} J'_{\nu_p} + \delta_p J'_\nu \frac{2\sqrt{\alpha}\, d_o}{c} \right) \Delta\omega \Bigg] d_q$$

$$= \eta' \left(\frac{\varepsilon_1 - \varepsilon_2}{2}\right) \left(\frac{\omega_{pq}}{c}\right)^2 J_{\nu_q} d_p \quad \text{(half space guide)} \qquad (4.79b)$$

The suppressed argument of the Bessel function J_ν is understood to be $2\sqrt{\alpha}\, k_{pq} d_o$. In obtaining (4.79a,b) we have used the dispersion relations (4.76a,b) for the unperturbed wave vectors. As the dispersion relations (4.74) and (4.75) hold for the perturbed wave vectors, we can use (4.73a,b,c) to give, neglecting second order terms,

$$\Delta\nu = \frac{(2d_o)^2}{\nu_q} \left(\beta_q \Delta\beta - \frac{\varepsilon_1 \omega_{pq}}{c^2} \Delta\omega\right) \qquad (4.80)$$

and

$$\Delta\delta = \frac{1}{\delta_q} \left(\beta_q \Delta\beta - \frac{\varepsilon_2 \omega_{pq}}{c^2} \Delta\omega\right) \qquad (4.81)$$

With (4.80) and (4.81) we can write (4.79a,b) as

$$\left(\beta_q D^q_\beta \Delta\beta + D^q_\omega \Delta\omega\right) d_q = \eta'' \left(\frac{\varepsilon_1 - \varepsilon_2}{2}\right) \left(\frac{\omega_{pq}}{c}\right)^2 J_{\nu_q} d_p \qquad (4.82)$$

where

$$D_\beta^q = \frac{(2d)^2}{\nu_q}\left[\frac{\sqrt{\alpha}\ \omega_{pq}}{c}\frac{\partial J_{\nu_q}}{\partial \nu_q} + \delta_q \begin{Bmatrix} \tanh(\delta_q w) \\ \coth(\delta_q w) \end{Bmatrix} \frac{\partial J_{\nu_q}}{\partial \nu_q}\right]$$

$$+ \frac{1}{\delta_q}\left[\delta_q w\, J_{\nu_q} \begin{Bmatrix} \operatorname{sech}^2(\delta_q w) \\ -\operatorname{csch}^2(\delta_q w) \end{Bmatrix} + J_{\nu_q} \begin{Bmatrix} \tanh(\delta_q w) \\ \coth(\delta_q w) \end{Bmatrix}\right] \qquad (4.83a)$$

(channel guide)

$$D_\beta^q = \frac{(2d_o)^2}{\nu_q}\left[\frac{\sqrt{\alpha}\ \omega_{pq}}{c}\ \frac{\partial J'_{\nu_q}}{\partial \nu_q} + \delta_q \frac{\partial J_{\nu_q}}{\partial \nu_q}\right] + J_{\nu_q}/\delta_q \qquad (4.83b)$$

(half space guide)

$$D_\omega^q = -\frac{\varepsilon_2 \omega_{pq}}{\delta_q c^2}\left[\delta_q w\, J_{\nu_q} \begin{Bmatrix} \operatorname{sech}^2(\delta_q w) \\ -\operatorname{csch}^2(\delta_q w) \end{Bmatrix} + J_{\nu_q} \begin{Bmatrix} \tanh(\delta_q w) \\ \coth(\delta_q w) \end{Bmatrix} \frac{\partial J_{\nu_q}}{\partial \nu_q}\right]$$

$$+ \frac{2d_o \alpha \omega_{pq}}{c^2} J''_{\nu_q} + \frac{\sqrt{\alpha}}{c} J'_{\nu_q} + \begin{Bmatrix} \tanh(\delta_q w) \\ \coth(\delta_q w) \end{Bmatrix} \frac{2\sqrt{\alpha}\ \delta_q d}{c} J'_{\nu_q} \qquad (4.84a)$$

(channel guide)

$$D_\omega^q = -\frac{\varepsilon_2 \omega_{pq}}{\delta_q c^2} J_{\nu_q} \frac{\partial J_{\nu_q}}{\partial \nu_q} + \frac{2d_o \alpha \omega_{pq}}{c^2} J''_{\nu_q} + \frac{\sqrt{\alpha}}{c} J'_{\nu_q} + \frac{2\sqrt{\alpha}\ \delta d_o}{c} J'_{\nu_q}$$

(half space guide)

(4.84b)

and

$$\eta'' = \begin{cases} \eta w & \text{(channel guide)} \qquad (4.85a) \\ \eta' & \text{(half space guide)} \qquad (4.85b) \end{cases}$$

Multiplying (4.82) through by $(\beta K)^{-1}(D_\beta^q)^{-1}$, we have

$$\left[\frac{\Delta\beta}{K} + \left(\frac{\omega_{pq}}{K\beta_q}\right)\frac{D_\omega^q}{D_\beta^q}\frac{\Delta\omega}{\omega_{pq}}\right] d_q = \eta''\left(\frac{\varepsilon_1-\varepsilon_2}{2}\right)\left(\frac{\omega_{pq}}{c}\right)^2 \frac{J_{\nu_q}}{K\,\beta_q D_\beta^q}\, d_p \tag{4.86}$$

By the same analysis that we used to derive (4.86), a q^{th} mode will excite a p^{th} mode resulting in the relation

$$\left[\frac{\Delta\beta}{K} + \left(\frac{\omega_{pq}}{K\beta_p}\right)\frac{D_\omega^p}{D_\beta^p}\frac{\Delta\omega}{\omega_{pq}}\right] d_p = \eta''\left(\frac{\varepsilon_1-\varepsilon_2}{2}\right)\left(\frac{\omega_{pq}}{c}\right)^2 \frac{J_{\nu_p}}{K\beta_p D_\beta^p}\, d_q \tag{4.87}$$

Multiplying (4.86) and (4.87) gives

$$\left[\frac{\Delta\beta}{K} - \left(\frac{\omega_{pq}}{K|\beta_q|}\right)\frac{D_\omega^q}{D_\beta^q}\frac{\Delta\omega}{\omega_{pq}}\right]\left[\frac{\Delta\beta}{K} + \left(\frac{\omega_{pq}}{K|\beta_p|}\right)\frac{D_\omega^p}{D_\beta^p}\frac{\Delta\omega}{\omega_{pq}}\right]$$

$$= -(\eta'')^2\left(\frac{\varepsilon_1-\varepsilon_2}{2}\right)\left(\frac{\omega_{pq}}{c}\right)^4 \frac{J_{\nu_q} J_{\nu_p}}{K^2|\beta_p||\beta_q|\, D_\beta^q D_\beta^p} \tag{4.88}$$

Equation (4.88) is similar to (4.31) and the solution for $\Delta\beta/K$ has the same form:

$$\frac{\Delta\beta}{K} = (\theta_p-\theta_q)\frac{\Delta\omega}{\omega_{pq}} \pm \sqrt{(\alpha_p+\alpha_q)^2\left(\frac{\Delta\omega}{\omega_{pq}}\right)^2 - (\eta'')^2\,(\xi_{pq}^D)^2} \tag{4.89}$$

where

$$\theta_r = \left(\frac{\omega_{pq}}{K|\beta_r|}\right)\frac{D_\omega^r}{D_\beta^r} \qquad r = p,q \tag{4.90}$$

$$\xi_{pq} = \left(\frac{\varepsilon_1-\varepsilon_2}{2}\right)\left(\frac{\omega_{pq}}{c}\right)^2 \frac{1}{K} \sqrt{\frac{J_{\nu_p} J_{\nu_q}}{|\beta_p||\beta_q| D_\beta^q D_\beta^p}} \tag{4.91}$$

The maximum imaginary value of $\Delta\beta$ is given by

$$\chi_{pq}^D(k) = \eta''\left(\frac{\varepsilon_1-\varepsilon_2}{2}\right)\left(\frac{\omega_{pq}}{c}\right)^2 \sqrt{\frac{J_{\nu_p} J_{\nu_q}}{|\beta_p||\beta_q| D_\beta^p D_\beta^q}} \tag{4.92}$$

The normalized coupling coefficient $\chi_{pq}^D(k)L$ is plotted in Fig. 5.1 abcd. As shown in Figs. B.4ab, the electric field at the boundary of a diffusion waveguide increases as the waveguide frequency is increased above cutoff, explaining the monotonic increase of $\chi_{pq}^D(k)L$ with frequency.

The reciprocal of the group velocity for the unperturbed diffusion waveguides ($\eta'' = 0$) can be obtained from (4.82) as

$$\psi_r = \frac{\Delta\beta}{\Delta\omega} = \frac{D_\omega^r}{\beta_r D_\beta^r} \qquad r = p,q \tag{4.93}$$

The expressions for $\Delta\beta_p$, $\Delta\beta_q$ obtained from (4.89) can be used with (4.80) and (4.81) to obtain $\Delta\nu_p$, $\Delta\nu_q$, Δs_p, and Δs_q. Thus, using (4.71) and (4.72a,b,c,d,e) we can express the complete transverse and longitudinal behavior of the guided modes in diffusion waveguides with periodic boundaries.

E. Coupling Coefficient for a Fiber Waveguide with Periodic Boundaries

In this section we derive the coupling coefficients for TE modes of a fiber waveguide with a boundary (Fig. 4.4) between the core and cladding described by a periodic radius $\rho_B(z)$ where

$$\rho_B(z) = W(1 + \eta \cos(Kz)) \quad , \qquad \eta << 1 \tag{4.94}$$

A fiber waveguide with a periodic boundary can be considered equivalent to an unperturbed waveguide with a periodic surface current as indicated in Fig. 4.3a,b and discussed in Section C of this chapter. For this reason, a forward p^{th} mode can excite a backward q^{th} mode through the boundary condition (4.50):

$$H_z\Big|_{\rho=w^+}(\rho,z) \; - \; H_z\Big|_{\rho=w^-}(\rho,z) \; = \; J_s(z) \tag{4.95}$$

As in previous sections, we consider a p^{th} waveguide mode of frequency $\omega = \omega_{pq} + \Delta\omega$ with a corresponding electric field

$$E_p(\rho,z) = d_p a_p'(\rho)\, e^{i\beta_p' z} \tag{4.96}$$

The mode amplitude is d_p and the transverse behavior $a_p'(\rho)$ is given by (see Appendix C)

$$a_p'(\rho) = \begin{cases} -\dfrac{i}{s_p'}\, \mu_o\, J_o'(s_p'\rho) & \rho < w \qquad (4.97a) \\[2ex] \dfrac{-i\omega\mu}{s_p'}\, K_o'(\delta_p'\rho) \quad \dfrac{J_1(\delta_p'w)}{K_1(s_p'w)} & \rho > w \qquad (4.97b) \end{cases}$$

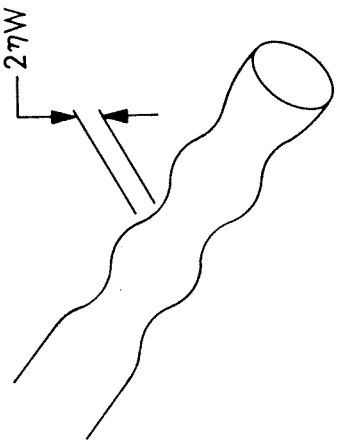

Fig. 4.4 Fiber waveguide with periodic boundary.

where

$$\rho = \sqrt{x^2 + y^2} \tag{4.98}$$

The z component of the magnetic field intensity vector is, from Appendix C,

$$H_z(\rho,z) = \begin{cases} J_o(s_p'\rho)\, e^{i\beta_p' z} & \rho < w \quad (4.99a) \\ -\dfrac{\delta_p'}{s_p'} \dfrac{J_1(sw)}{K_1(\delta w)} K_o(\delta_p'\rho) & \rho > w \quad (4.99b) \end{cases}$$

Primes, as in (4.97b), are used to indicate differentiation with respect to the arguments $s_p'\rho$ and $\delta_p'\rho$ of the Bessel functions J and K. The transverse wave vectors s_p', δ_p', and the longitudinal wave vector β_p' are the wave vectors of the perturbed waveguide defined, as in previous sections, by

$$s_p' = s_p + \Delta s \tag{4.100a}$$

$$\delta_p' = \delta_p + \Delta\delta \tag{4.100b}$$

$$\beta_p' = \beta_p + \Delta\beta \tag{4.100c}$$

where s_p, δ_p, and β_p are the $(p+1)^{th}$ solution of the dispersion relations for the unperturbed fiber waveguide given in Appendix C:

$$s_p^2 = \varepsilon_1 k^2 - \beta_p^2 \tag{4.101}$$

$$\delta_p^2 = \beta_p^2 - \varepsilon_2 k^2 \tag{4.102}$$

$$s_p w \frac{J_o(s_p w)}{J_1(s_p w)} + \delta_p w \frac{K_o(\delta_p w)}{K_1(\delta_p w)} = 0 \tag{4.103}$$

The terms Δs, $\Delta\delta$, and $\Delta\beta$ are small perturbations (as $\eta << 1$ in (4.94)) caused by the boundary perturbation.

We now use (4.48) with (4.99a,b) to write (4.95) as

$$\left[\frac{\delta_q'}{s_q'}\frac{J_1(s_q'w)}{K_1(\delta_q'w)}K_o(\delta_q'w) + J_o(s_q'w)\right]d_q = -\frac{\eta w}{2}(\varepsilon_1-\varepsilon_2)\frac{k^2}{s_p'}J_o'(s_p'w)d_p \quad (4.104)$$

Multiplying (4.104) through by $K_1(\delta_q'w)s_q'$ and using $J_o'(x) = -J_1(x)$, we have

$$\left[\delta_q' J_o(s_q'w)\, K_o(\delta_q'w) + s_q'K_1(\delta_q'w)\, J_o(s_q'w)\right] d_q$$

$$= \eta w \frac{s_q}{s_p}\left(\frac{\varepsilon_1-\varepsilon_2}{2}\right)k^2 J_1(s_p'w)\, K_1(\delta_q'w)d_p \quad (4.105)$$

Equation (4.104) or (4.105) for the perturbed wave vectors is analogous to the dispersion relation (4.103) of the unperturbed waveguide, and couples the two modes p and q through the boundary perturbation. From the wave equation (2.3), the dispersion relations (4.101) and (4.102) are seen to remain valid for the perturbed wave vectors s_q', δ_q' and β_q'.

We now use (4.22), (4.100a,b,c) and (4.103) to write (4.105), neglecting second order terms, as

$$\left[\Delta s(\delta_q J_1'(s_qw)K_o(\delta_qw) + K_1(\delta_qw)J_o(s_qw) - s_qK_1(\delta_qw)J_1(s_qw)\right.$$

$$\left. + \Delta\delta(s_qK_1'(\delta_qw)J_o(s_qw) + J_1(s_qw)K_o(\delta_qw) - \delta_qJ_1(s_qw)K_1(\delta_qw)\right]d_q$$

$$= \eta w \frac{s_q}{s_p}\left(\frac{\varepsilon_1-\varepsilon_2}{2}\right)k_{pq}^2 J_1(s_pw)K_1(\delta_qw)d_p \quad (4.106)$$

As (4.101) and (4.102) hold for the perturbed wave vectors, we can use (4.100a,b,c) to write, neglecting second order terms,

$$\Delta s = \frac{1}{s_q} (\varepsilon_1 k \Delta k - \beta_q \Delta\beta) \tag{4.107}$$

and

$$= \frac{1}{\delta_q} (\beta_q \Delta\beta - \varepsilon_2 k \Delta k) \tag{4.108}$$

With (4.107) and (4.108), (4.106) becomes

$$\{\beta_q \Delta\beta \, F_\beta^q + \Delta\omega \, F_\omega^q\} \, d_q = \eta w \frac{s_q}{s_p} \left(\frac{\varepsilon_1 - \varepsilon_2}{2}\right)\left(\frac{\omega_{pq}}{c}\right)^2 J_1(s_p w) \, K_1(\delta_q w) d_p \tag{4.109}$$

where

$$F_\beta^q = \frac{1}{\delta_q} [s_q w K_1'(\delta_q w) J_o(s_q w) + J_1(s_q w) K_o(\delta_q w) - \delta_q w \, J_1(s_q w) K_1(\delta_q w)]$$

$$- \frac{1}{s_q} [\delta_q w \, J_1'(s_q w) K_o(\delta_q w) + K_1(\delta_q w) J_o(s_q w) - s_q w \, K_1(\delta_q w) J_1(s_q w)] \tag{4.110}$$

$$F_\omega^q = \frac{\varepsilon_1 k}{c s_q} [\delta_q w \, J_1'(s_q w) K_o(\delta_q w) + K_1(\delta_q w) J_o(s_q w) - s_q w \, K_1(\delta_q w) J_1(s_q w)]$$

$$- \frac{\varepsilon_2 k}{c \delta_q} [s_q w \, K_1'(\delta_q w) J_o(s_q w) + J_1(s_q w) K_o(\delta_q w) - \delta_q w \, J_1(s_q w) K_1(\delta_q w)] \tag{4.111}$$

Multiplying (4.109) through by $(\beta K)^{-1}(F_\beta^q)^{-1}$, we have

$$\left[\frac{\Delta\beta}{K} + \left(\frac{\omega_{pq}}{K\beta_q}\right) \frac{F_\omega^q}{F_\beta^q} \frac{\Delta\omega}{\omega_{pq}}\right] d_q = \eta w \frac{s_q}{s_p} \left(\frac{\varepsilon_1 - \varepsilon_2}{2}\right)\left(\frac{\omega_{pq}}{c}\right)^2 \frac{J_1(s_p w) \, K_1(\delta_q w)}{K \beta_q F_\beta^q} d_p \tag{4.112}$$

By the same analysis that resulted in (4.112), a q^{th} mode will excite a p^{th} mode described by the relation

$$\left[\frac{\Delta\beta}{K} + \left(\frac{\omega_{pq}}{K\beta_p}\right)\frac{F_\omega^p}{F_\beta^p}\frac{\Delta\omega}{\omega_{pq}}\right]d_p = \eta w \frac{s_p}{s_q}\left(\frac{\varepsilon_1-\varepsilon_2}{2}\right)\left(\frac{\omega_{pq}}{c}\right)^2 \frac{J_1(s_q w)K_1(\delta_p w)}{K\,\beta_p\,F_\beta^p}\,dq \tag{4.113}$$

Multiplying (4.12) and (4.113) gives

$$\left[\frac{\Delta\beta}{K} - \left(\frac{\omega_{pq}}{K|\beta_q|}\right)\frac{F_\omega^q}{F_\beta^q}\frac{\Delta\omega}{\omega_{pq}}\right]\left[\frac{\Delta\beta}{K} + \left(\frac{\omega_{pq}}{K|\beta_p|}\right)\frac{F_\omega^p}{F_\beta^p}\frac{\Delta\omega}{\omega_{pq}}\right]$$

$$= (\eta w)^2 \left(\frac{\varepsilon_1-\varepsilon_2}{2}\right)^2 \left(\frac{\omega_{pq}}{c}\right)^4 \frac{J_1(s_p w)J_1(s_q w)K_1(\delta_p w)K_1(\delta_q w)}{K^2|\beta_p||\beta_q|\,F_\beta^p\,F_\beta^q} \tag{4.114}$$

Equation (4.114) is similar to (4.31) and the solution for $\Delta\beta/K$ has the same form:

$$\frac{\Delta\beta}{K} = (\theta_p - \theta_q)\frac{\Delta\omega}{\omega_{pq}} \pm \sqrt{(\theta_p + \theta_q)^2\left(\frac{\Delta\omega}{\omega_{pq}}\right)^2 - \eta^2(\xi_{pq}^F)^2} \tag{4.115}$$

where

$$\theta_r = \left(\frac{\omega_{pq}}{K|\beta_r|}\right)\frac{F_\omega^r}{F_\beta^r} \qquad r = p,q \tag{4.116}$$

$$\xi_{pq}^F = \left(\frac{\varepsilon_1-\varepsilon_2}{2}\right)\left(\frac{\omega_{pq}}{c}\right)^2 \frac{1}{K}\sqrt{\frac{J_1(s_p w)J_1(s_q w)K_1(\delta_q w)K_1(\delta_p w)}{|\beta_p||\beta_q|\,F_\beta^p\,F_\beta^q}} \tag{4.117}$$

The maximum imaginary value of $\Delta\beta$ is given by

$$\chi^F_{pq}(k) = w\left(\frac{\varepsilon_1-\varepsilon_2}{2}\right)\left(\frac{\omega_{pq}}{c}\right)^2 \sqrt{\frac{J_1(s_p w)J_1(s_q w)K_1(\delta_p w)K_1(\delta_q w)}{|\beta_p||\beta_q|\ F^p_\beta\ F^q_\beta}} \qquad (4.118)$$

The normalized coupling coefficient $\chi^F_{pq}(k)L$ is plotted in Fig. 4.5. The physical behavior is similar to that of the thin film waveguide with a periodic boundary. Near cutoff, the field strength is small as the mode energy is spread over the cladding region. With increasing frequency, the mode energy becomes localized around the waveguide core and the increased field strength at the core-cladding boundary results in increased coupling. At very high frequencies (with respect to cutoff), the mode energy becomes confined well inside the core region, and the negligible field strength at the perturbed boundary results in negligible coupling.

The reciprocal of the group velocity for the unperturbed ($\eta = 0$) fiber waveguides can be obtained from (4.109) as

$$\psi_r = \frac{\Delta\beta}{\Delta\omega} = \frac{F^r_\omega}{\beta_r\ F^r_\beta} \qquad r = p,q \qquad (4.119)$$

The expressions for $\Delta\beta_p$, $\Delta\beta_q$ obtained from (4.115) can be used with (4.107) and (4.108) to obtain Δs_p, Δs_q, $\Delta\delta_p$, and $\Delta\delta_q$. Thus, using (4.96), we can express the complete transverse and longitudinal behavior of the TE guided modes in a fiber waveguide with periodic boundaries.

F. Comments

The use of the boundary condition (4.50) for the thin film waveguide with periodic boundaries (Section C) and the channel diffusion

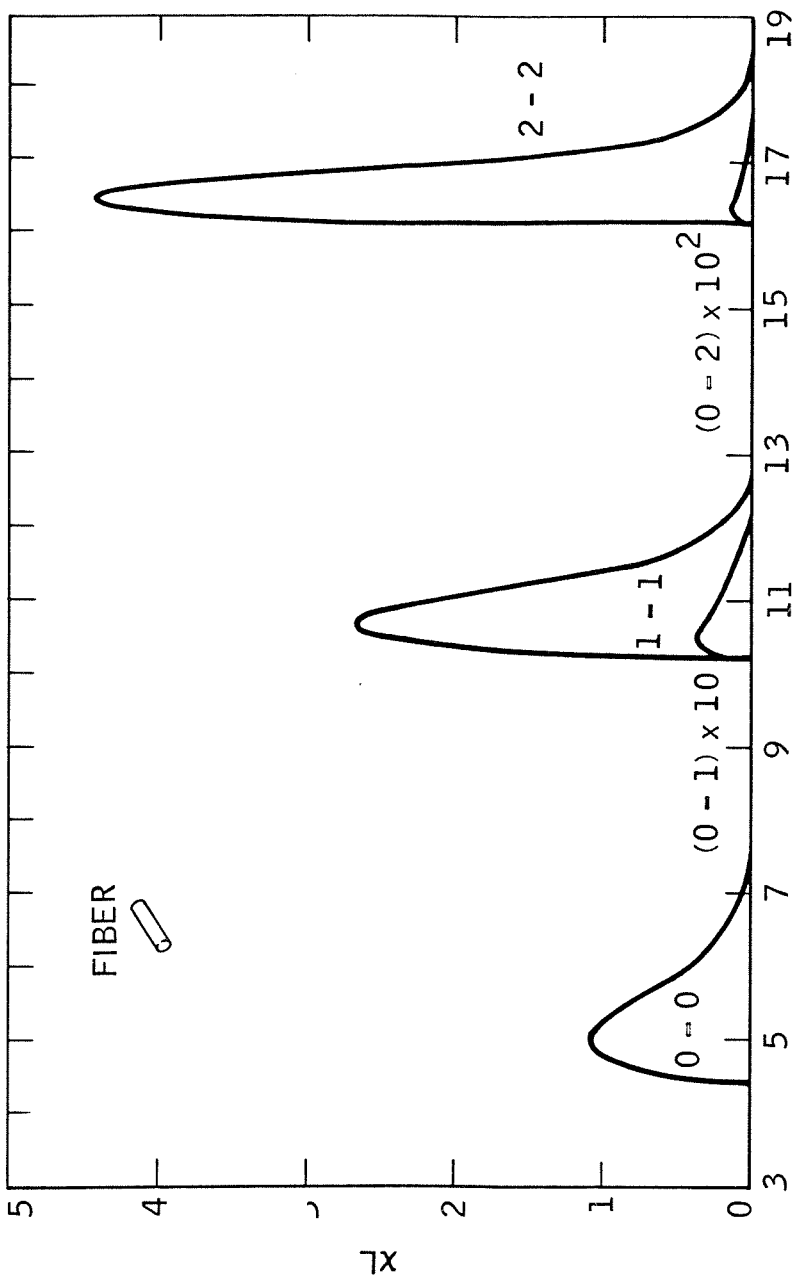

Fig. 4.5 Coupling between modes of a fiber waveguide with a periodic boundary. $\varepsilon_1 = (1.5)^2$ and $\varepsilon_2 = (1.4)^2$. $\eta L/w = 5$.

waveguide (Section D) assumes that both waveguide boundaries are symmetrically perturbed as given by (4.41) and (4.69a). By symmetry considerations[62], such a waveguide only couples even-even and odd-odd mode pairs. The physical reason for this is that the mode coupling is proportional to the field strength of the two modes at the boundary multiplied by the equivalent surface current at each boundary. For a symmetric guide with an even-odd mode pair, the excitation is proportional to $|d_p||a_p||d_q||a_q|J_s$ at one boundary and $-|d_p||a_p||d_q||a_q|J_s$ at the other, which cancels each other. By the same considerations, an antisymmetric waveguide (see Fig. 4.6b) only couples even-odd mode pairs. If only one boundary is perturbed, all types of coupling are possible. In this case, the boundary condition (4.50) remains the same at $x = w$, but the unperturbed boundary condition holds at $x = -w$. This has the effect of halving the effective excitation current, and all results hold with η replaced by $\eta/2$.

Similarly, if only one of the substrate regions (see Fig. 2.1) is periodically perturbed, η in (4.40) should be replaced by $\eta/2$.

Finally, it should be mentioned that for the case $p=q$, the results of Sections A, B, and C are identical to the ones derived by Elachi and Yeh[20] using the exact space harmonics method to solve the wave equation.

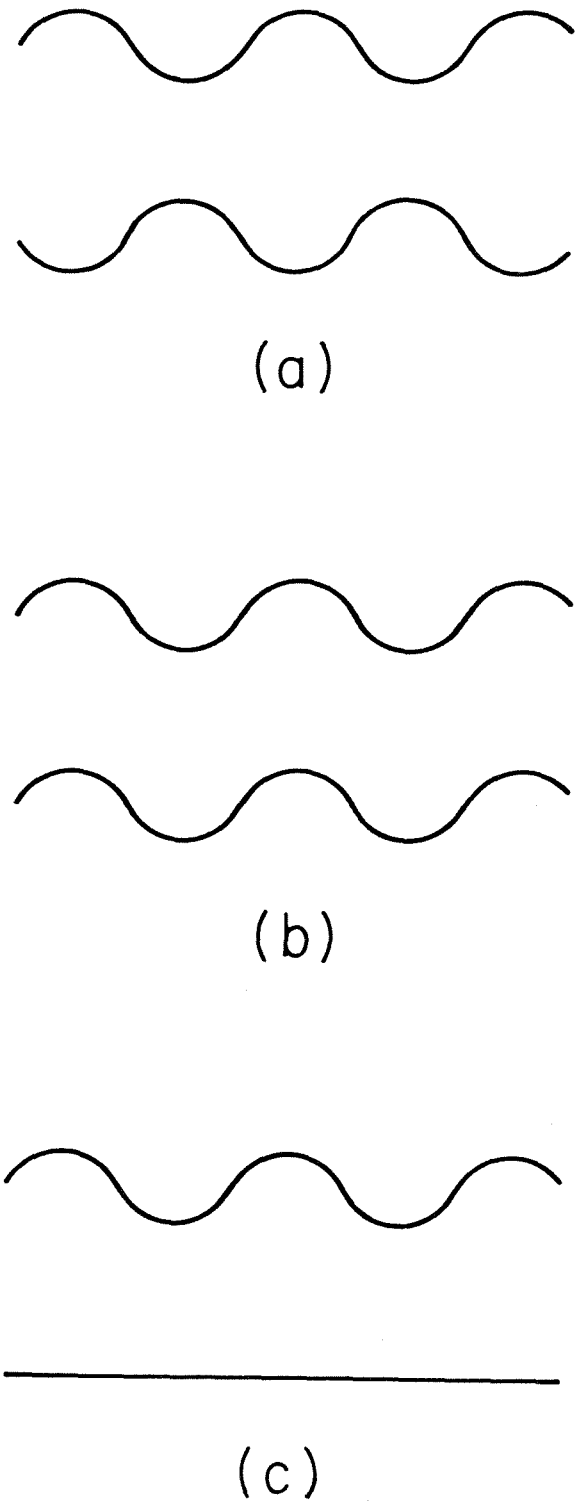

Fig. 4.6 Possible periodic boundary perturbations of a thin film waveguide. (a) couples only even-even and odd-odd modes; (b) couples only even-odd modes; and (c) can couple all combinations of modes. The corrugations are highly exaggerated for clarity.

Chapter V

Theoretical Results

In this chapter, we use the equations derived in Chapters II, III, and IV to study distributed feedback lasers in dielectric waveguides.

The required threshold gain for laser oscillation is given by (2.66a):

$$G = \frac{2}{c_p(k) + c_q(k)} \mathrm{Re}\{Y_{pq}\} \tag{5.1}$$

and the corresponding phase mismatch by (2.66b):

$$\Delta k = \frac{2}{c(\psi_p(k) + \psi_q(k))} \mathrm{Im}\{Y_{pq}\} \tag{5.2}$$

where

$$Y_{pq} = \left(\frac{c_p(k) + c_q(k)}{2}\right) G + i\, c \left(\frac{\psi_p(k) + \psi_q(k)}{2}\right) \Delta k \tag{5.3}$$

is a solution of

$$Y_{pq} = \sqrt{\chi_{pq}^2(k) + Y_{pq}^2(k)}\, \coth \sqrt{\chi_{pq}^2(k) + Y_{pq}^2(k)}\, L \tag{5.4}$$

and L is the length of the laser.

A. Thin Film Distributed Feedback Lasers

In this section a detailed study of thin film DFB lasers is made. The effects of geometry and use of different waveguide modes to provide feedback is investigated. The gain region is considered to be either in the guide or in the substrate.

The coupling coefficient $\chi_{pq}^g(k)$ in (5.4) is derived in

Chapter IV for a thin film waveguide with a periodic permittivity variation in the guide region as

$$\chi^{g}_{pq}(k) = \eta \frac{\varepsilon_1}{4} \left(\frac{\omega_{pq}}{c}\right)^2 \sqrt{\frac{\phi^{g}_{pq}\ \phi^{g}_{qp}}{|\beta_p|\ |\beta_q|}} \tag{5.5}$$

for a periodic substrate as

$$\chi^{s}_{pq}(k) = \eta \frac{\varepsilon_2}{4} \left(\frac{\omega_{pq}}{c}\right)^2 \sqrt{\frac{\phi^{s}_{pq}\ \phi^{s}_{qp}}{|\beta_p|\ |\beta_q|}} \tag{5.6}$$

and for a periodic boundary as

$$\chi^{b}_{pq}(k) = \eta \left(\frac{\varepsilon_1 - \varepsilon_2}{2}\right) \left(\frac{\omega_{pq}}{c}\right)^2 \sqrt{\frac{\phi^{b}_{pq}\ \phi^{b}_{qp}}{|\beta_p|\ |\beta_q|}} \tag{5.7}$$

where the longitudinal wave vectors of the p and q waveguide modes satisfy the phase matching condition $|\beta_p| + |\beta_q| = K$. The coefficients $\phi^{g}_{pq}, \phi^{s}_{pq}$, and ϕ^{b}_{pq} are given by equations (4.21a,b,c,d,e), (4.39a,b), and (4.61). The reciprocal of the group velocity $\psi_r(k)$ in (5.3) is given by (4.37) and (4.29) as

$$\psi_r(k) = \frac{\omega_{pq}}{c^2 \beta_r} \left(\varepsilon_1 \frac{\begin{cases} \sin^2(s_r w) \\ \cos^2(s_r w) \end{cases} + \varepsilon_1 \delta_r w}{1 + \delta_r w} + \varepsilon_2 \frac{\begin{cases} \cos^2(s_r w) \\ \sin^2(s_r w) \end{cases}}{1 + \delta_r w} \right) \tag{5.8}$$

The gain efficiency coefficient $c_r(k)$ in (5.3) is given by (3.20) and (3.21) as

$$c_r(k) = \sqrt{\varepsilon_1}\, \frac{k}{\beta_r} \frac{\alpha_{t.f.}}{1 + \alpha_{t.f.}} \tag{5.9}$$

for an active guide, and as

$$c_r(k) = \sqrt{\varepsilon_2}\, \frac{k}{\beta_r} \frac{1}{1 + \alpha_{t.f.}} \tag{5.10}$$

where $\alpha_{t.f.}$ is given by (3.14).

Using (5.5), (5.6), or (5.7), we can solve (5.4) for the Y_{pq} that correspond to various perturbed thin film waveguides. The Y_{pq} are complex and multi-valued, with different values corresponding to the different branches of the complex hyperbolic cotangent function. The unperturbed thin film waveguide wave vectors s, δ, and β used in (5.5) through (5.10) are solutions of the dispersion relations (A.6) and (A.7) of Appendix A. A generalized Newton's method[63] approach was used to numerically solve (A.6) and (A.7) and also (5.4) on a computer.

In Figs. 5.1 through 5.10 the normalized threshold gain GL required for oscillation and the wave vector mismatch is plotted as a function of the normalized free space wave vector for a number of cases and for different longitudinal modes. Some of these curves show that there are optimum regions where the gain is at a minimum. These regions correspond to an optimum design. To illustrate let us consider the case of a surface corrugated thin film DFB laser with gain in the guide and 0-0 mode coupling (Fig. 5.8). The minimum threshold gain occurs at $2\pi w/\lambda = 3.2$. The laser oscillation frequency $\omega_o = 2\pi c/\lambda_o$ is fixed by the choice of the gain medium. Thus the optimum waveguide width is fixed at $w \simeq 3.2\lambda/(2\pi)$. The ratio of parameters $\eta L/w = 25$ requires the product $\eta L \geq 25\ (3.2\ \lambda_o)/2\pi$ to obtain a threshold gain $GL \leq 1.9$.

If we arbitrarily consider $\lambda = 0.9\mu$, $2w = 1.2\mu$, $L = 1$ mm and $\eta = 1.5 \times 10^{-2}$, the threshold gain required for the first three longitudinal modes with 0-0 mode coupling is, from Fig. 5.8,

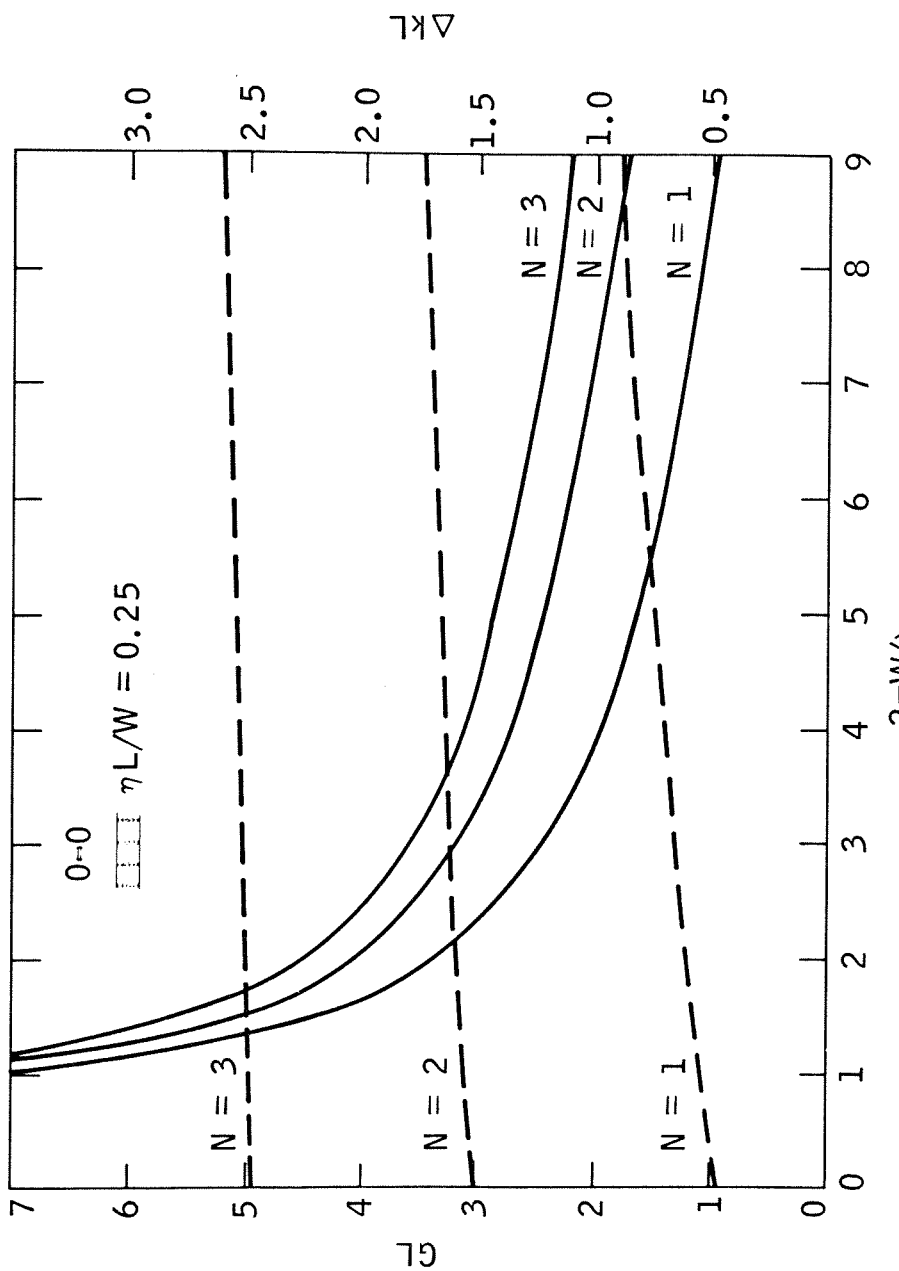

Fig. 5.1 Threshold gain curves for a thin film waveguide with periodicity in the guiding region. The first three longitudinal modes arising from coupling of the 0-0 waveguide modes are plotted. $\varepsilon_1 = (3.6)^2$ and $\varepsilon_2 = (3.5)^2$.

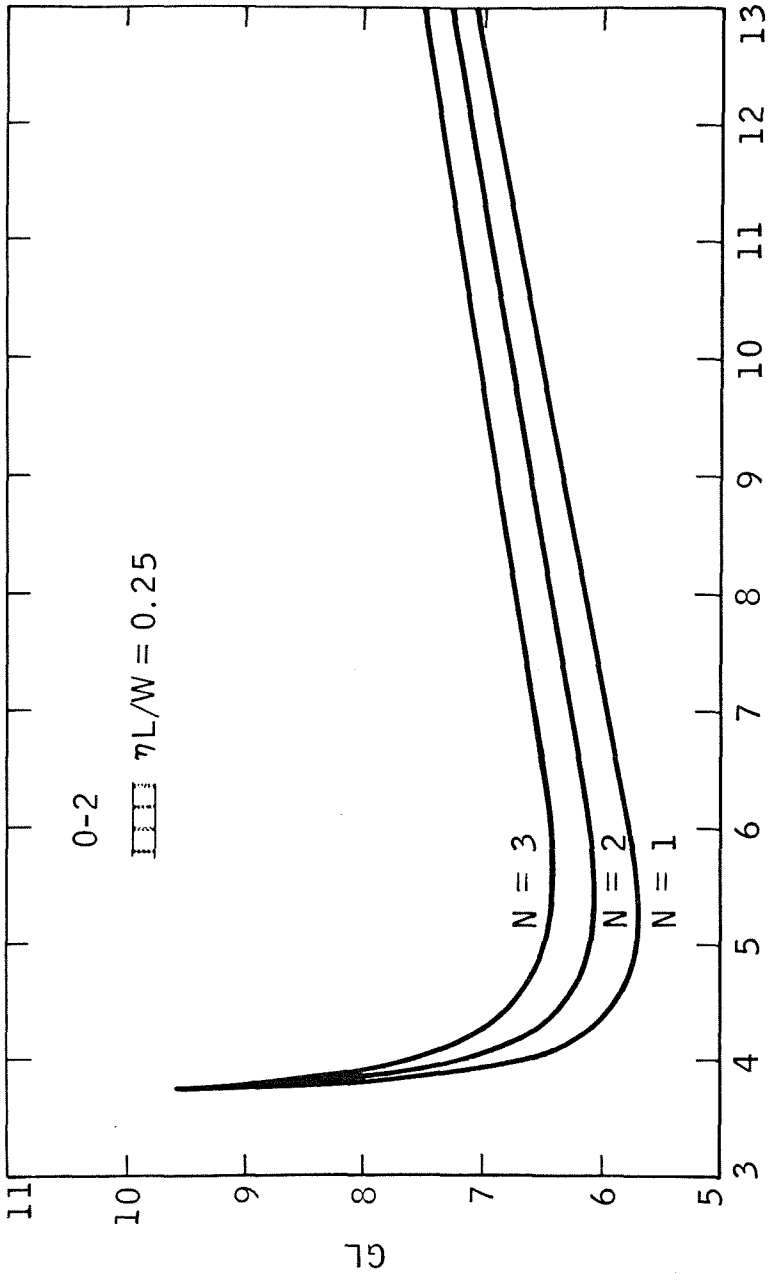

Fig. 5.2 Threshold gain curves for a thin film waveguide with periodicity in the guiding region. The first three longitudinal modes arising from coupling of the 0-2 waveguide modes are plotted. $\varepsilon_1 = (3.6)^2$ and $\varepsilon_2 = (3.5)^2$.

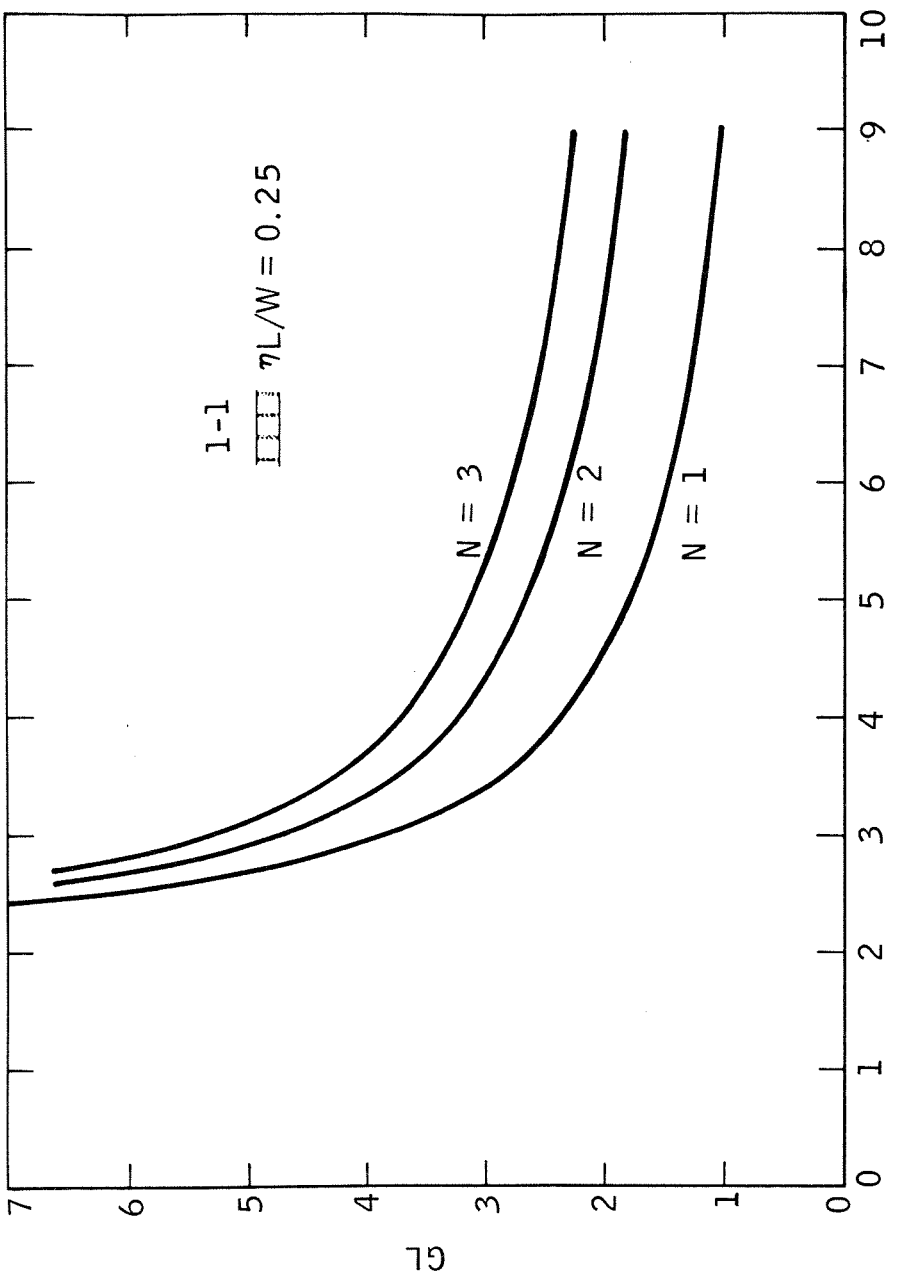

Fig. 5.3 Threshold gain curves for a thin film waveguide with periodicity in the guiding region. The first three longitudinal modes arising from coupling of the 1-1 waveguide modes are plotted. $\varepsilon_1 = (3.6)^2$ and $\varepsilon_2 = (3.5)^2$.

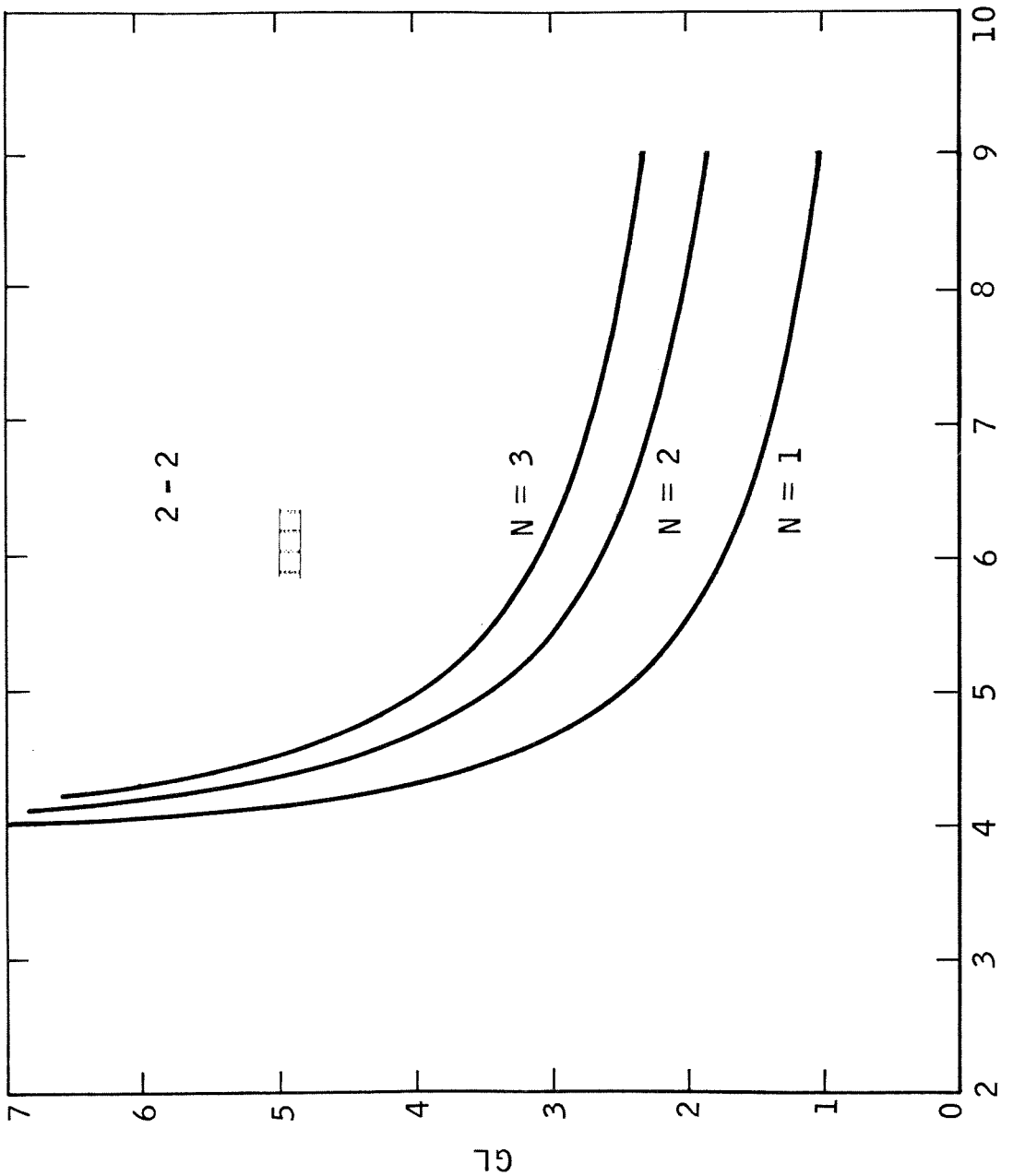

Fig. 5.4 Threshold gain curves for a thin film waveguide with periodicity in the guiding region. The first three longitudinal modes arising from coupling of the 2-2 waveguide modes are plotted. $\varepsilon_1 = (3.6)^2$ and $\varepsilon_2 = (3.5)^2$.

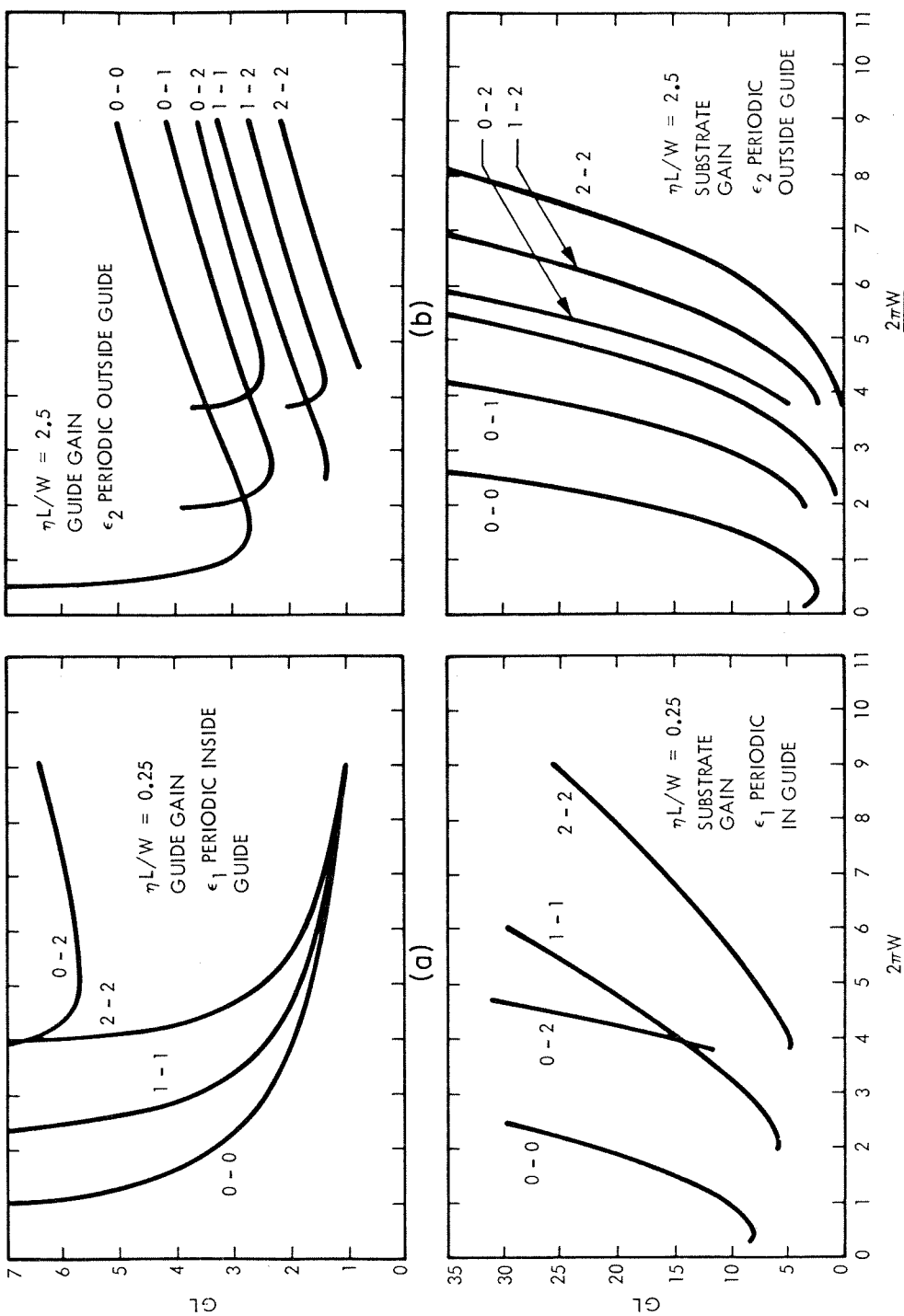

Fig. 5.5 Threshold gain curves for coupling between various waveguide modes in thin film waveguides. (a) periodic guide, active guide; (b) periodic substrate, active guide; (c) periodic guide, active substrate; and (d) periodic substrate, active substrate. $\varepsilon_1 = (3.6)^2$ and $\varepsilon_2 = (3.5)^2$.

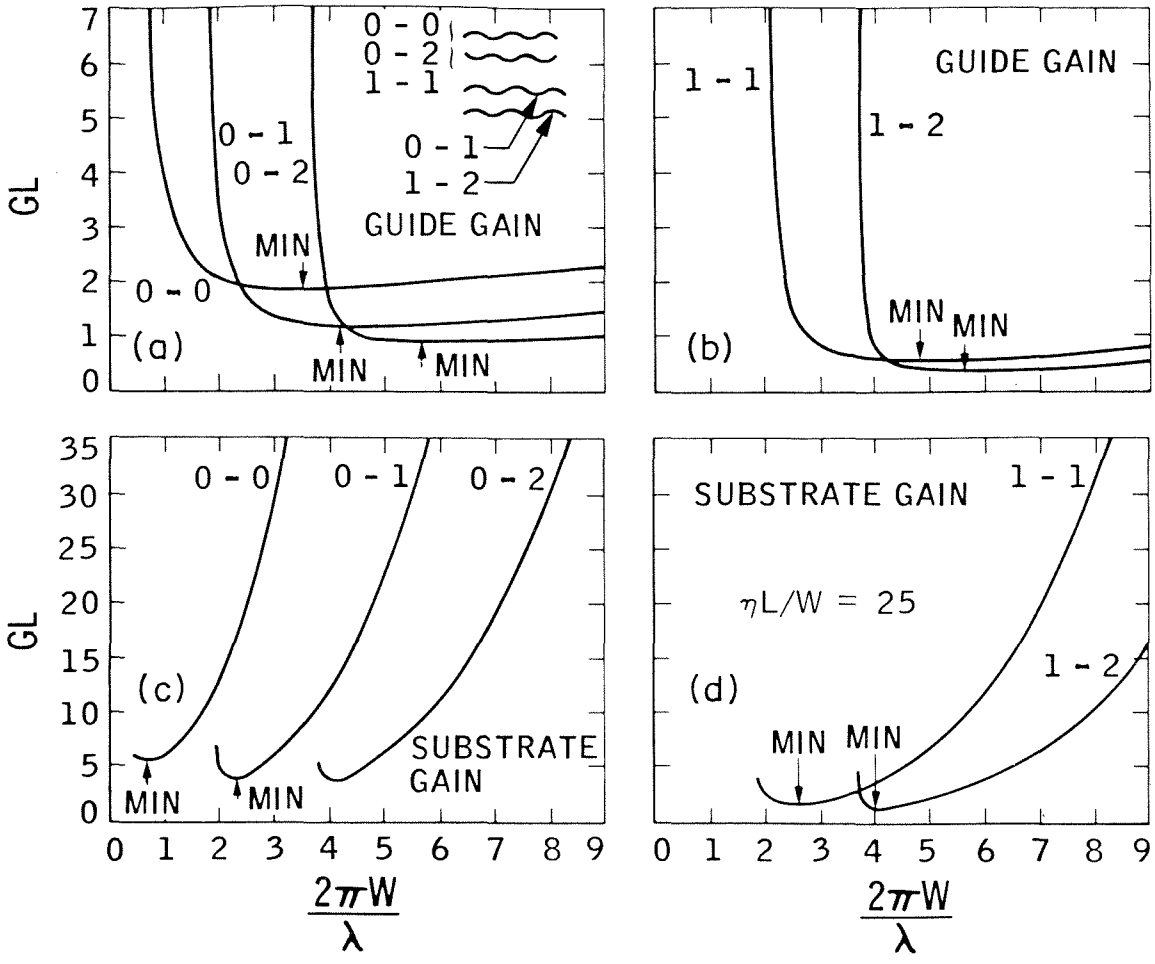

Fig. 5.6 Threshold gain curves for coupling between various waveguide modes of a thin film waveguide with periodic boundaries. (a) and (b), active guide; (c) and (d), active substrate. $\eta L/W = 25$, $\varepsilon_1 = (3.6)^2$, and $\varepsilon_2 = (3.5)^2$.

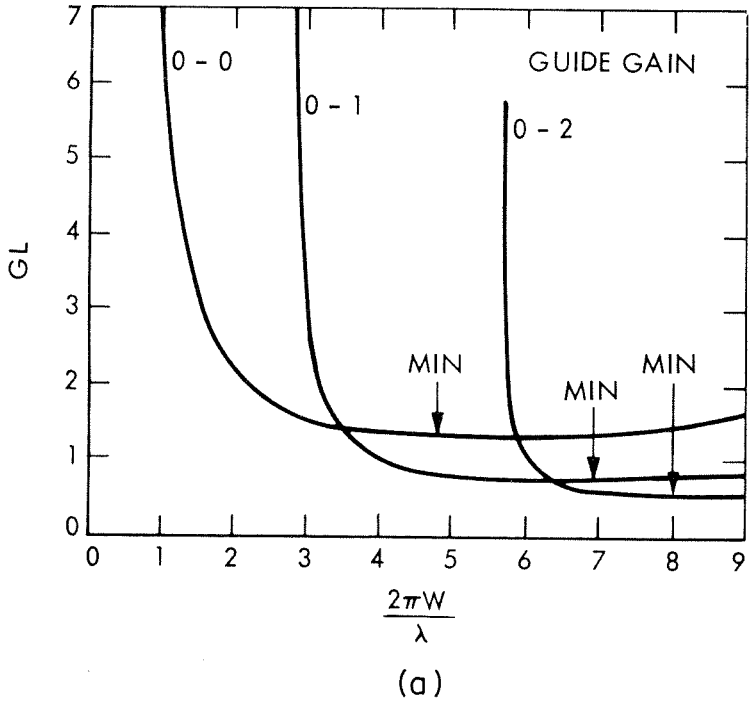

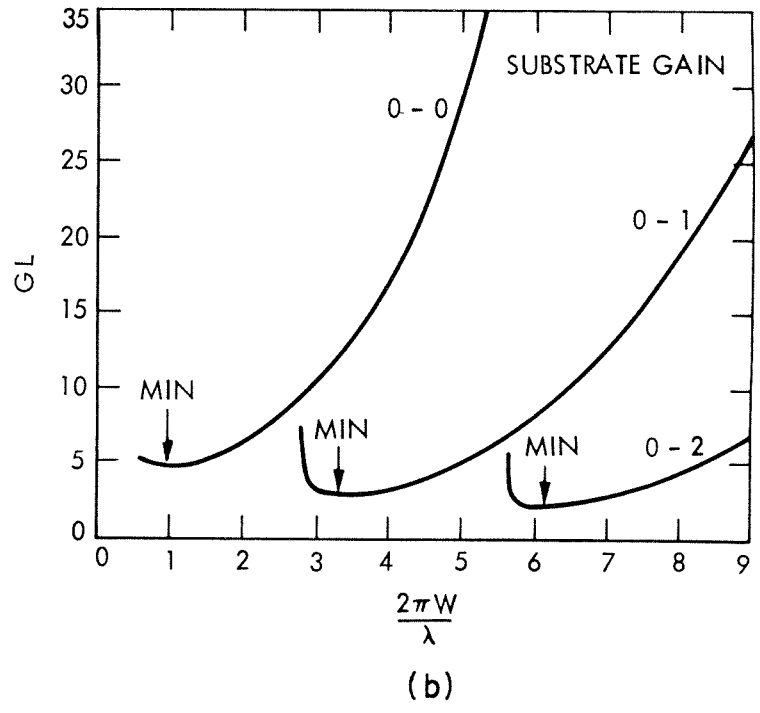

Fig. 5.7 Threshold gain curves for coupling between various waveguide modes of a thin film waveguide with periodic boundaries. (a) active guide; (b) active substrate $\eta L/W = 25$, $\varepsilon_1 = (1.6)^2$ and $\varepsilon_2 = (1.5)^2$.

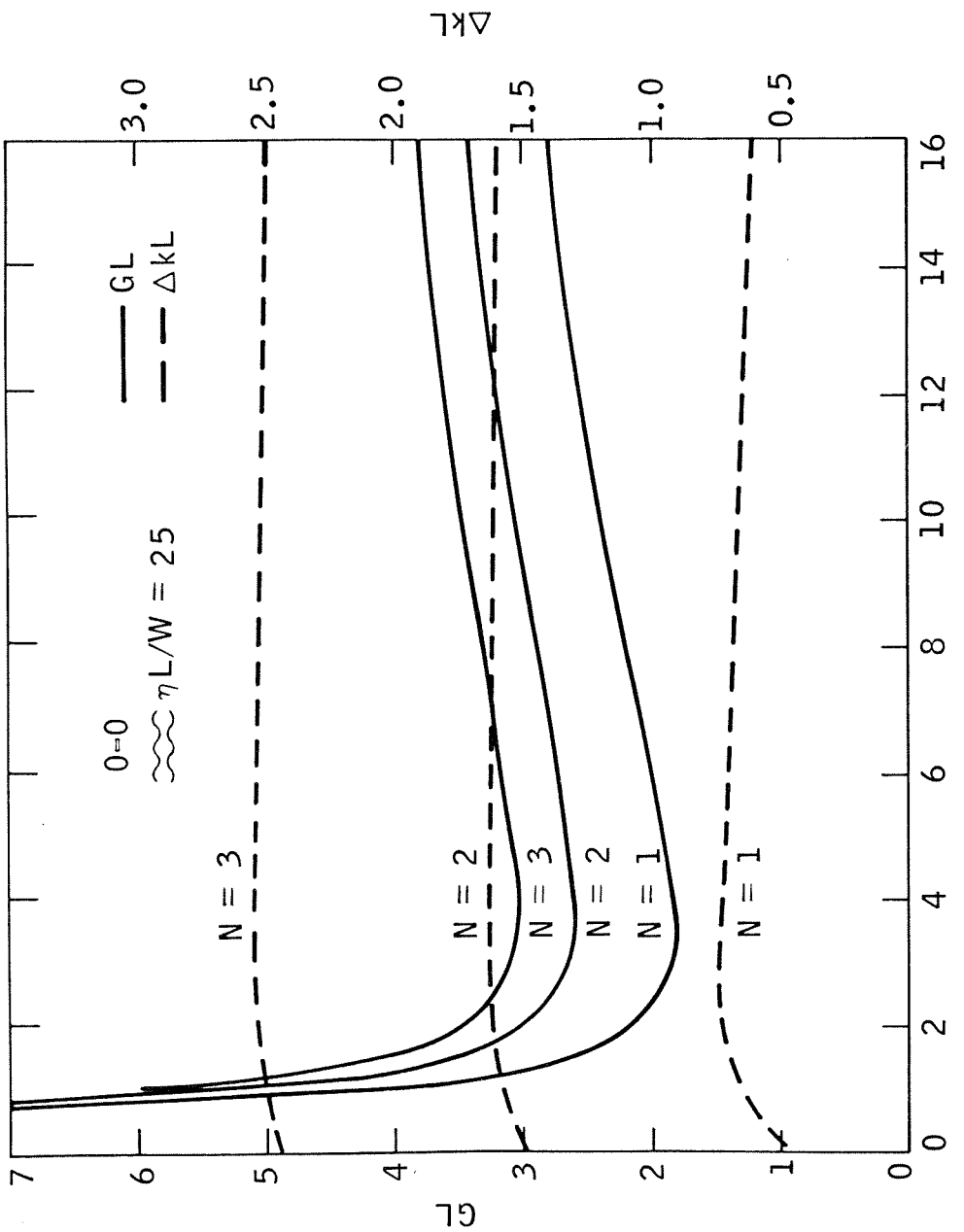

Fig. 5.8 Threshold gain curves for a thin film waveguide (active guide) with periodic boundaries. The first three longitudinal modes arising from coupling of the 0-0 waveguide modes are plotted. $\varepsilon_1 = (3.6)^2$ and $\varepsilon_2 = (3.5)^2$.

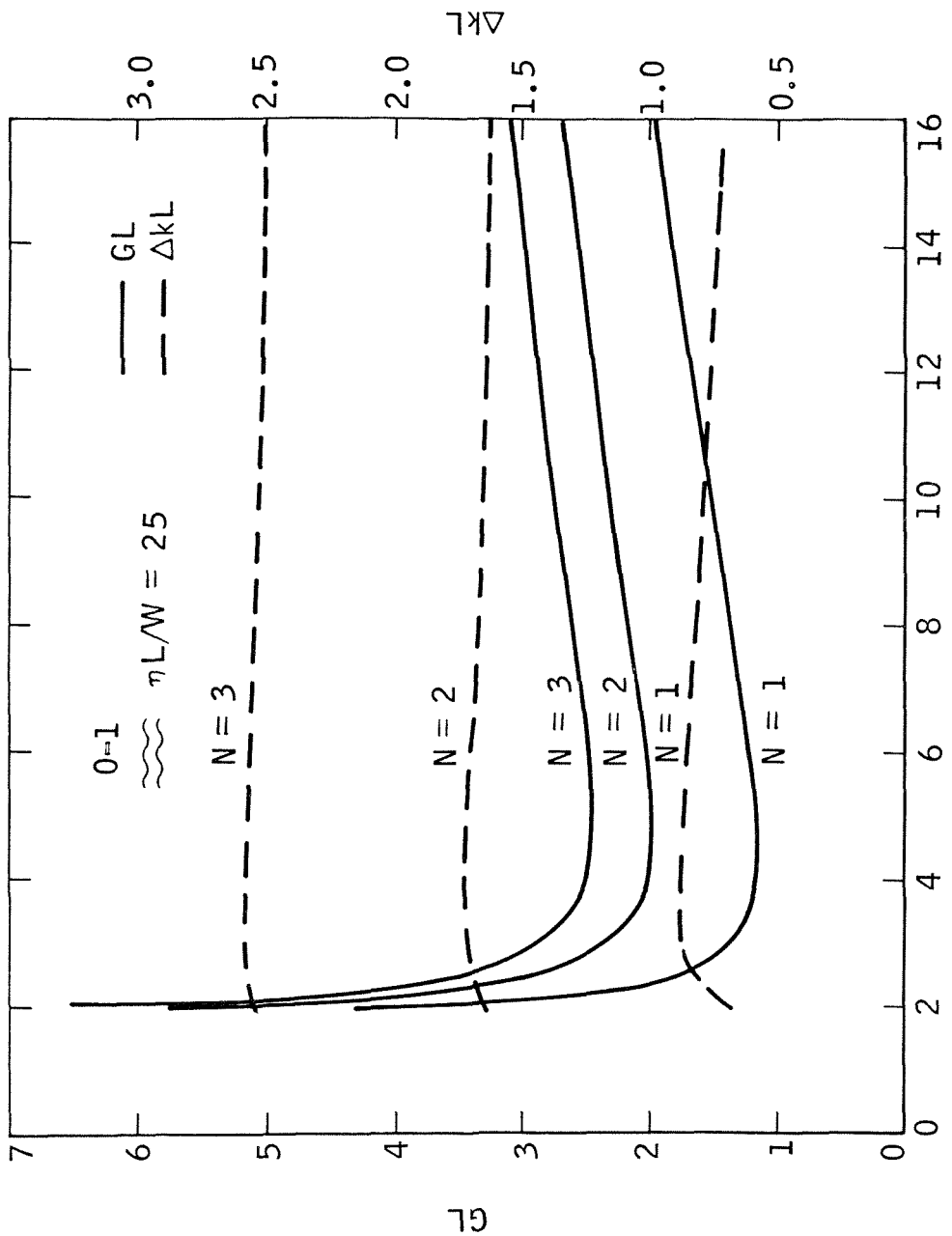

Fig. 5.9 Threshold gain curves for a thin film waveguide (active guide) with periodic boundaries. The first three longitudinal modes arising from coupling of the 0-1 waveguide modes are plotted. $\varepsilon_1 = (3.6)^2$ and $\varepsilon_2 = (3.5)^2$.

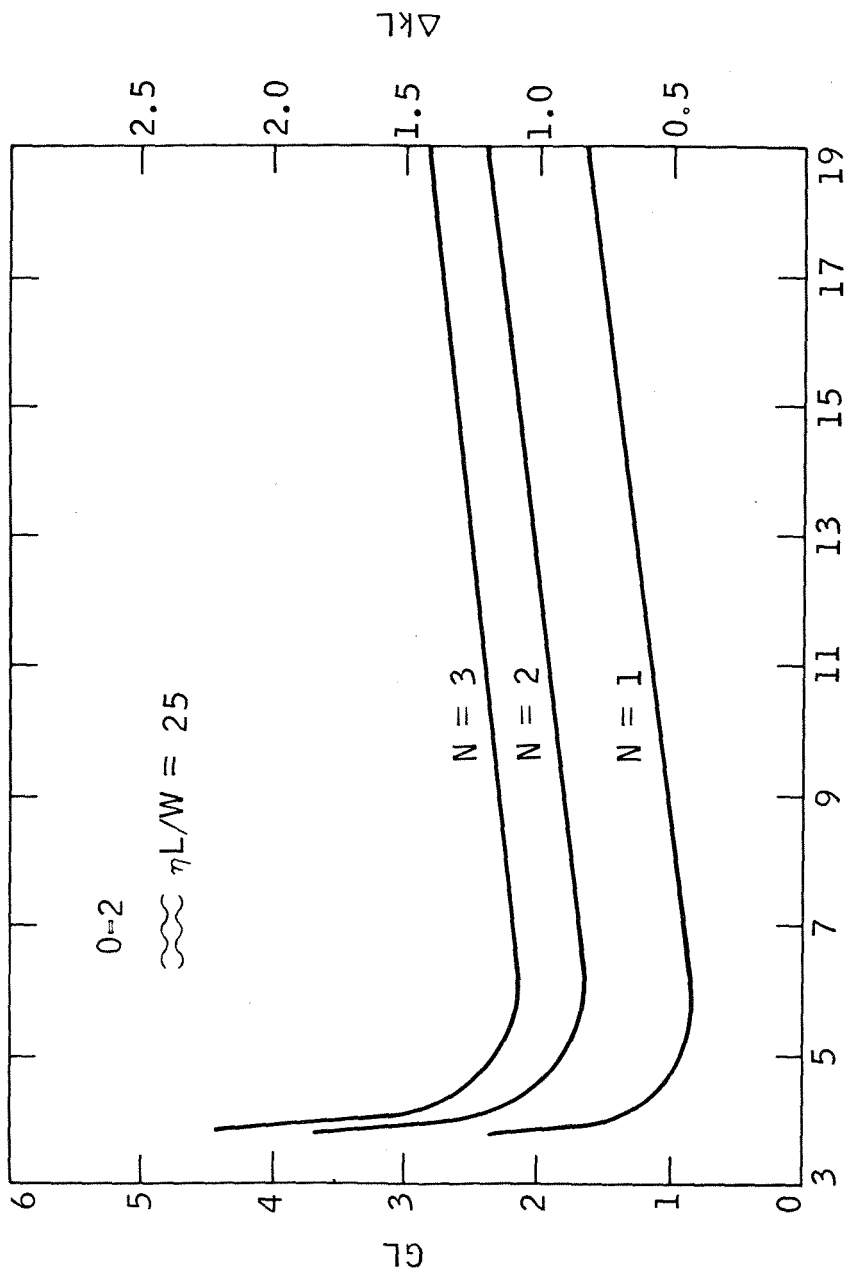

Fig. 5.10 Threshold gain curves for a thin film waveguide (active guide) with periodic boundaries. The first three longitudinal modes arising from coupling of the 0-2 waveguide modes are plotted. $\varepsilon_1 = (3.6)^2$ and $\varepsilon_2 = (3.5)^2$.

$$G_1 = 20 \text{ cm}^{-1}$$

$$G_2 = 27 \text{ cm}^{-1}$$

$$G_3 = 30 \text{ cm}^{-1}$$

If the period of the surface perturbation is chosen to couple 0-1 modes, the threshold gain required is (Fig. 5.9);

$$G_1 = 12 \text{ cm}^{-1}$$

$$G_2 = 20 \text{ cm}^{-1}$$

$$G_3 = 25 \text{ cm}^{-1}$$

For coupling between the 0-2 modes, the threshold gain required is even lower (Fig. 5.10).

The threshold gain curves can be explained by the behavior of the gain efficiency coefficients (see Chapter III) and the coupling coefficients (see Chapter IV). In Figs. 5.1, 5.3, 5.4, and 5.5a, the threshold gain is plotted versus the normalized free space wave vector for coupling between 0-0, 1-1, and 2-2 modes in a waveguide where the electric permittivity varies periodically in the guide region. In this case, the effective gain and coupling coefficient are near zero around cutoff resulting in a very large threshold gain. As the transverse wave vector increases above cutoff, the effective gain increases approaching one. The coupling coefficient similarly increases because the mode energy becomes more and more confined to the perturbation region. Thus, the threshold gain monotonically decreases with increasing transverse wave vector

(or frequency). This is not true for coupling between 0-2 modes of a similar structure (Fig. 5.2, 5.5a). If the coupled modes are not identical, the coupling coefficient reaches a maximum and then goes to zero because the overlap integral ϕ^{g}_{pq} in (5.5) vanishes at high frequency (i.e., the mode distributions inside the guide become orthogonal). For this reason, the threshold gain has a minimum value, increasing as the coupling coefficient decreases. If the gain medium is in the substrate region and the periodic permittivity is in the guide region, there is always a minimum value of threshold gain because the effective gain coefficient is one near cutoff and decreases to zero at frequencies well above cutoff. In Fig. 5.5c, the threshold gain for the 0-2 configuration is increasing more rapidly than that of the 0-0, 1-1, 2-2 configurations because the coupling coefficient and the effective gain coefficient are both decreasing.

Fig. 5.5b,d is a plot of threshold gain versus the normalized free space wave vector for a thin film structure with a periodic electric permittivity in the substrate. For coupling between different modes, $\phi^{s}_{pq} = \phi^{b}_{pq}$ (see 4.21 a,c and 4.39 a,b) and therefore

$$\chi^{s}_{pq}(k) = \frac{\varepsilon_2}{\varepsilon_1}\,\chi^{g}_{pq}(k) \qquad (p\neq q) \tag{5.11}$$

Thus the threshold gain curves have the same form indicated by the 0-2 mode coupling in Fig. 5.5a,c. Physically, the threshold gain increases in Fig. 5.5b at high frequencies (with respect to the cutoff frequency of the waveguide) because the mode energy becomes confined

to the homogeneous guide region and no longer feels the periodicity in the substrate. In Fig. 5.5d, the threshold gain increases at high frequencies because both the coupling coefficient and the gain efficiency are falling off.

Figures 5.6 through 5.10 are plots of threshold gain and wave vector mismatch for thin film waveguides with boundary perturbations. The resulting coupling coefficients have a maximum value at intermediate frequencies because near cutoff the energy is spread mostly in the substrate region and the mode amplitude at the boundary is very small. With increasing frequency the mode energy becomes confined to the guide region and the mode amplitude at the boundary increases. At very high frequencies, the mode energy becomes well confined inside the guide region and the small mode amplitude at the boundary perturbation results in reduced coupling. For thin film DFB lasers with boundary perturbations and gain in the guide region, the threshold gain is high near cutoff because both the gain efficiency and coupling coefficient are small. As the gain efficiency and coupling coefficient increase with increasing frequency, the threshold gain decreases. Eventually, the effective gain coefficient approaches one, the coupling coefficient starts decreasing, and the threshold gain begins increasing. If the gain is in the substrate region of a thin film waveguide with boundary perturbations, the different effective gain (Eq. 5.10) moves the threshold gain minimum in the direction of the cutoff frequency because the effective gain is about unity near cutoff. At frequencies moderately above cutoff, the threshold gain begins to rise rapidly due to the decrease in both

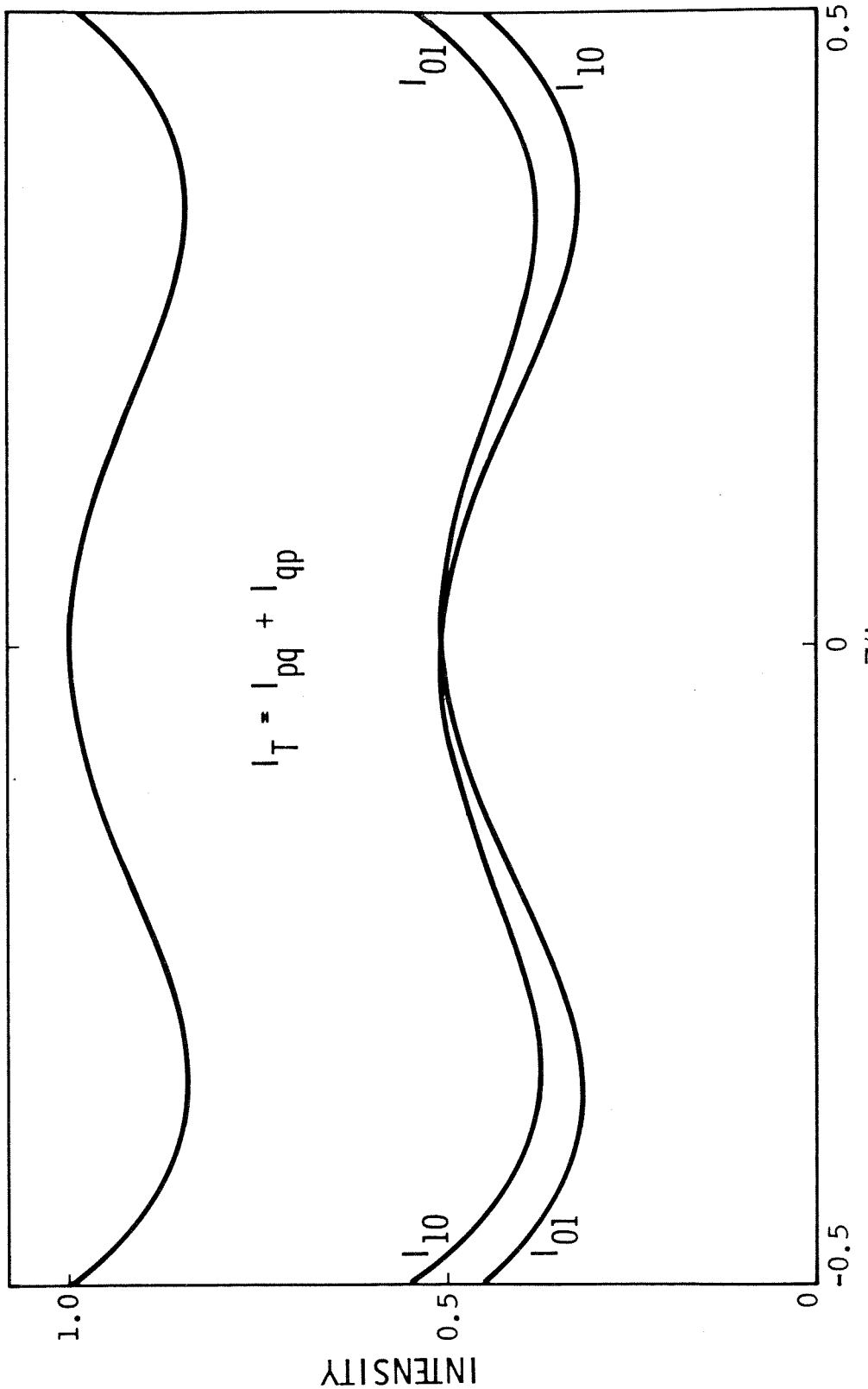

Fig. 5.11 The complete longitudinal intensity distribution is the sum of two independent mode patterns.

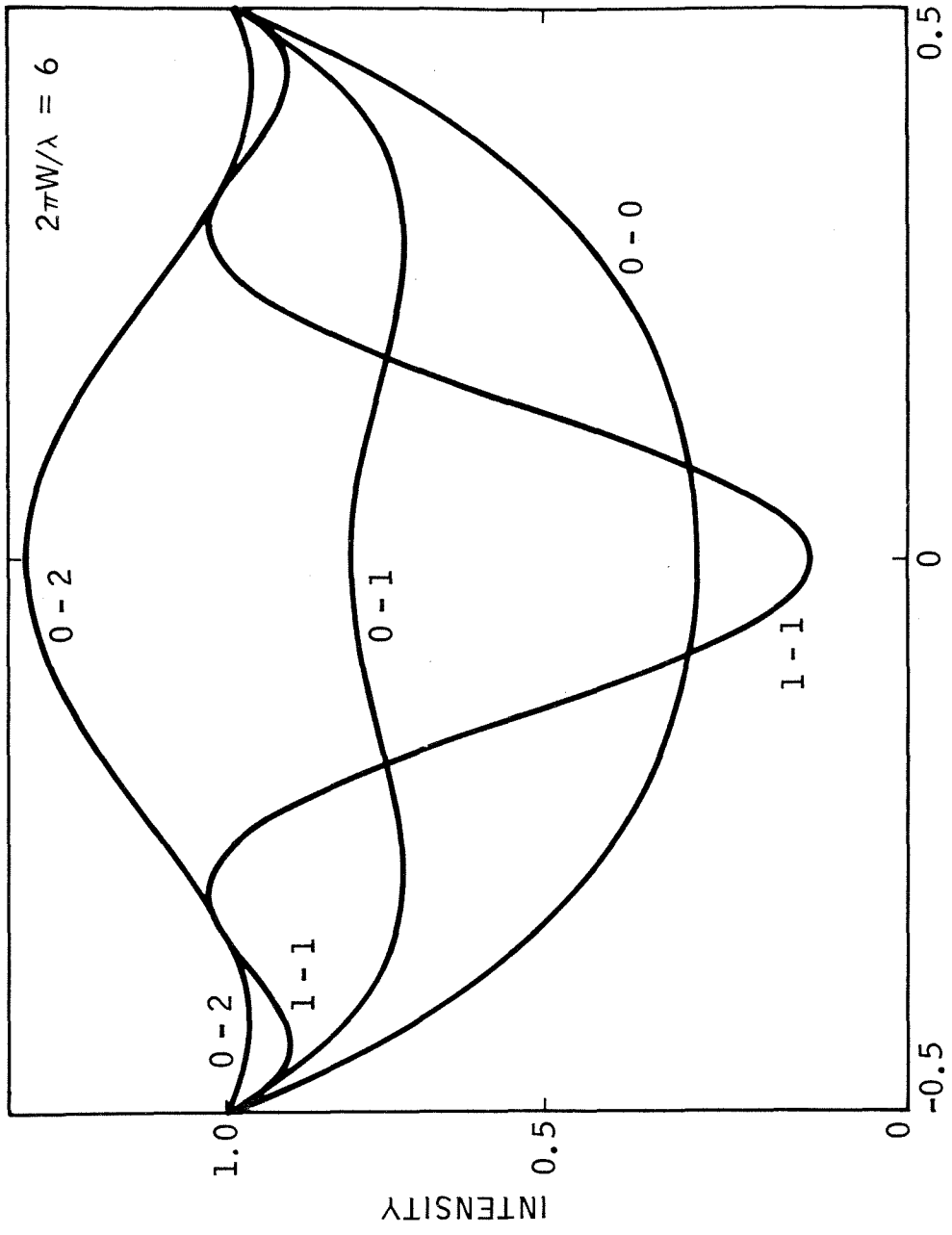

Fig. 5.12 Longitudinal intensity distributions for coupling between various modes of a thin film waveguide (active guide) with periodic boundaries. $2\pi W/\lambda_2 = 6$, $\eta L/W = 25$, $\varepsilon_1 = (3.6)^2$, and $\varepsilon_2 = (3.5)^2$.

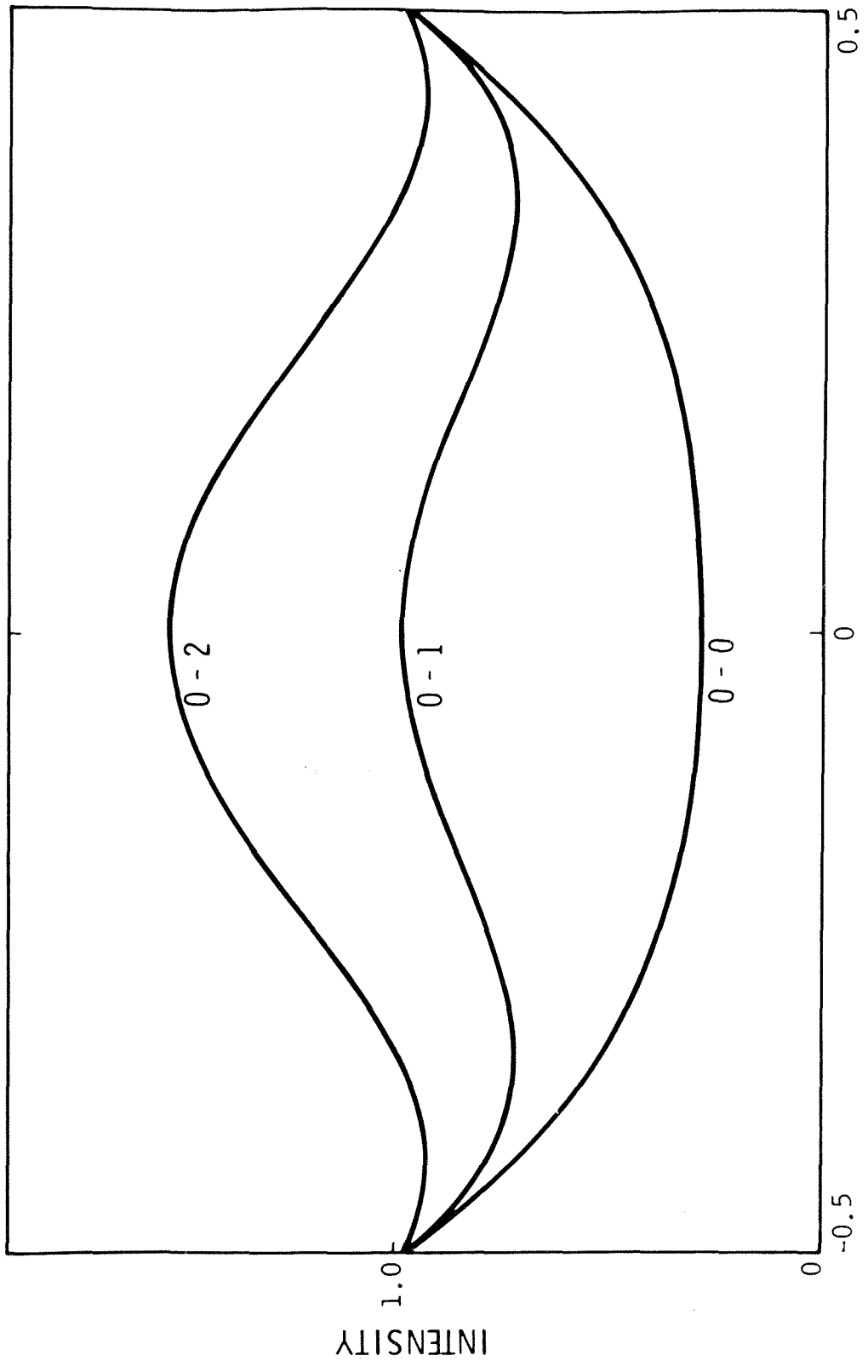

Fig. 5.13 Longitudinal intensity distributions at the minimum threshold gain points indicated in Fig. 5.6a.

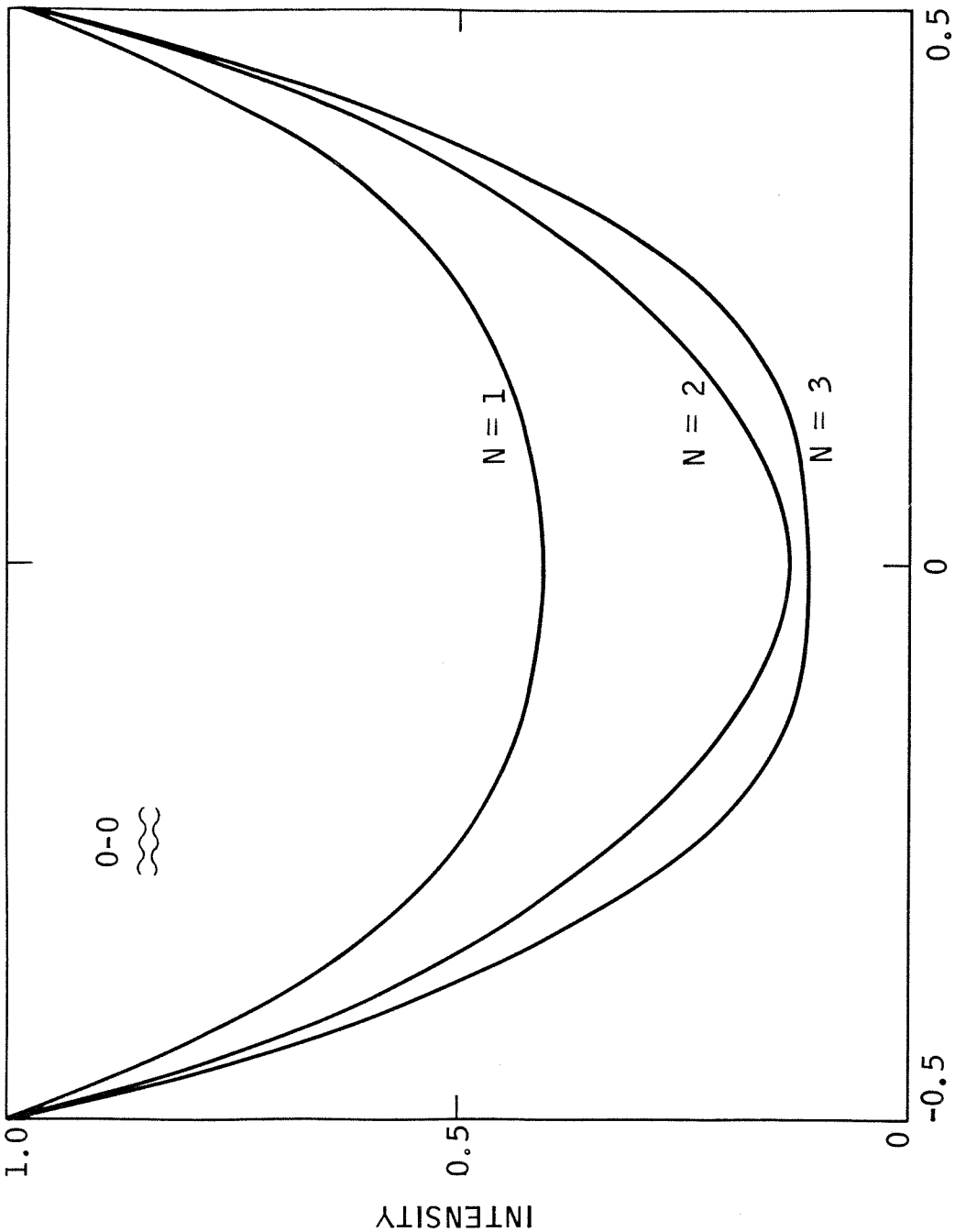

Fig. 5.14 Longitudinal intensity distributions for the first three longitudinal modes due to coupling between 0-0 modes in a thin film waveguide (active guide) with periodic boundaries. $\eta L/W = 25$, $2\pi W/\lambda = 3.5$, $\varepsilon_1 = (3.6)^2$ and $\varepsilon_2 = (3.5)^2$.

the gain efficiency and the coupling coefficient.

Equation (2.67) describes the electric field distribution which represents an oscillating mode of the DFB structure. The relative intensity distribution $F_p(w,z)F_p^*(w,z) + B_q(w,z)B_q^*(w,z)$ represents the longitudinal intensity envelope (or "mode pattern") of the modal standing wave pattern at the waveguide boundary. By symmetry, the structure also supports an independent solution giving rise to the relative intensity distribution $F_q(w,z)F_q^*(w,z) + B_p(w,z)B_p^*(w,z)$. The complete mode pattern at the waveguide boundary is therefore the sum

$$I(z) = F_pF_p^* + B_qB_q^* + F_qF_q^* + B_pB_p^*$$
$$\propto \cosh[(c_p-c_q)Gz]\{|\sinh(b_{pq}[z+L/2])|^2 + |\sinh(b_{pq}[z-L/2])|^2\} \quad (5.12)$$

Intensity distributions are plotted in Figs. 5.11-5.14 for various waveguide modes and longitudinal modes of thin film DFB lasers. For some configurations, the intensity varies appreciably as a function of z suggesting that for operation above threshold, where saturation plays a role, the field distribution has to be accounted for in the original coupled equations leading to a nonlinear system of equations.

B. Diffusion Waveguide Distributed Feedback Lasers

In this section we study the application of optical waveguides formed by diffusion for distributed feedback lasers. This type of waveguide is of considerable interest because it is simple to

fabricate. Two configurations are considered: a planar half-space diffusion guide which is of importance in integrated optics and a channel guide with an inhomogeneous substrate. The channel diffusion guide (Fig. B.1a) provides a simplified model of a cylindrical diffused structure (Fig. 5.15) which can be applied to capillary gas lasers. The inhomogeneity will mainly play the role of guiding the wave and therefore eliminate the losses encountered in hollow capillary guides due to transmission at the boundary[2].

The coupling coefficient $\chi_{pq}(k)$ in (5.4) is derived in Chapter IV for diffusion waveguides with periodic boundaries as

$$\chi_{pq}(k) = \eta'' \left(\frac{\varepsilon_1-\varepsilon_2}{2}\right)\left(\frac{\omega_{pq}}{c}\right)^2 \sqrt{\frac{J_{\nu_p} J_{\nu_q}}{|\beta_p|\ |\beta_q| D_\beta^p D_\beta^q}} \tag{5.13}$$

where the longitudinal wave vectors of the p and q waveguide modes satisfy the phase matching condition $|\beta_p|+|\beta_q|= K$ and η'' and D_β^r are given by (4.85a,b) and (4.83a,b). The reciprocal of the group velocity $\psi_r(k)$ in (5.3) for a diffusion waveguide is given by

$$\psi_r(k) = \frac{D_\omega^r}{\beta_r D_\beta^r} \tag{5.14}$$

where D_ω^r is given by (4.84a,b). The gain efficiency coefficient $C_r(k)$ in (5.3) for a diffusion waveguide is given by (3.37) and (3.38) as

$$c_r(k) = \sqrt{\varepsilon_1}\,\frac{k}{\beta_r}\,\frac{\alpha_D}{1+\alpha_D} \tag{5.15}$$

for gain in the diffused region, and as

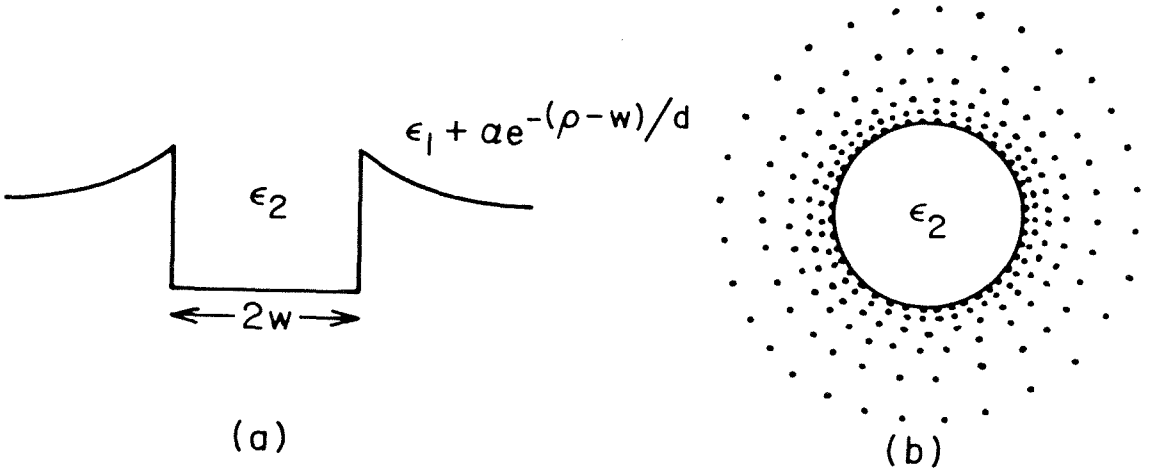

Fig. 5.15 Diffused capillary waveguide. (a) electric permittivity profile across the waveguide; (b) cylindrical gas filled region is surrounded by an exponentially inhomogeneous cladding.

$$c_r(k) = \sqrt{\varepsilon_2}\,\frac{k}{\beta_r}\,\frac{1}{1+\alpha_D} \tag{5.16}$$

for gain in the half space or channel region. The coefficient α_D is given by (3.36).

Using (5.13), we can solve (5.4) for the Y_{pq} that correspond to diffusion waveguides with periodic boundaries. The unperturbed diffusion waveguide wave vectors δ, $\nu/(2d_0)$, and β used in (5.13) through (5.16) are solutions of the dispersion relations (B.11) and (B.10) (channel guide), or (B.11) and (B.14) (half space guide) and are obtained numerically using a generalized Newton's method approach on a computer. To evaluate the partial derivative of the Bessel function with respect to order (used in (5.13) through (5.16)), a special subroutine was written using[30]

$$\frac{\partial J_\nu(z)}{\partial \nu} = J_\nu(z)\,\ell n\left(\tfrac{1}{2}z\right) - \left(\tfrac{1}{2}z\right)^\nu \sum_{k=0}^{\infty} (-)^k \frac{\psi(\nu+k+1)\left(\tfrac{1}{4}z^2\right)^k}{\Gamma(\nu+k+1)\;\;k!} \tag{5.17}$$

where $\psi(z)$ is the logarithmic derivative of the gamma function and $\Gamma(z)$ is the gamma function[30,64]. The subroutine to compute $\partial J_\nu/\partial\nu$ reproduced tabulated values[65,66].

The threshold gain is computed using (5.1) and is plotted in Fig. 5.16 for channel diffusion guides with $\alpha = 0.1$ and $\alpha = 0.025$. In Fig. 5.17 the coupling coefficient, gain efficiency, and threshold gain is plotted versus normalized transverse wave vector for half space and channel diffusion guides. Because the mode energy becomes localized at the perturbed diffusion boundary, the coupling

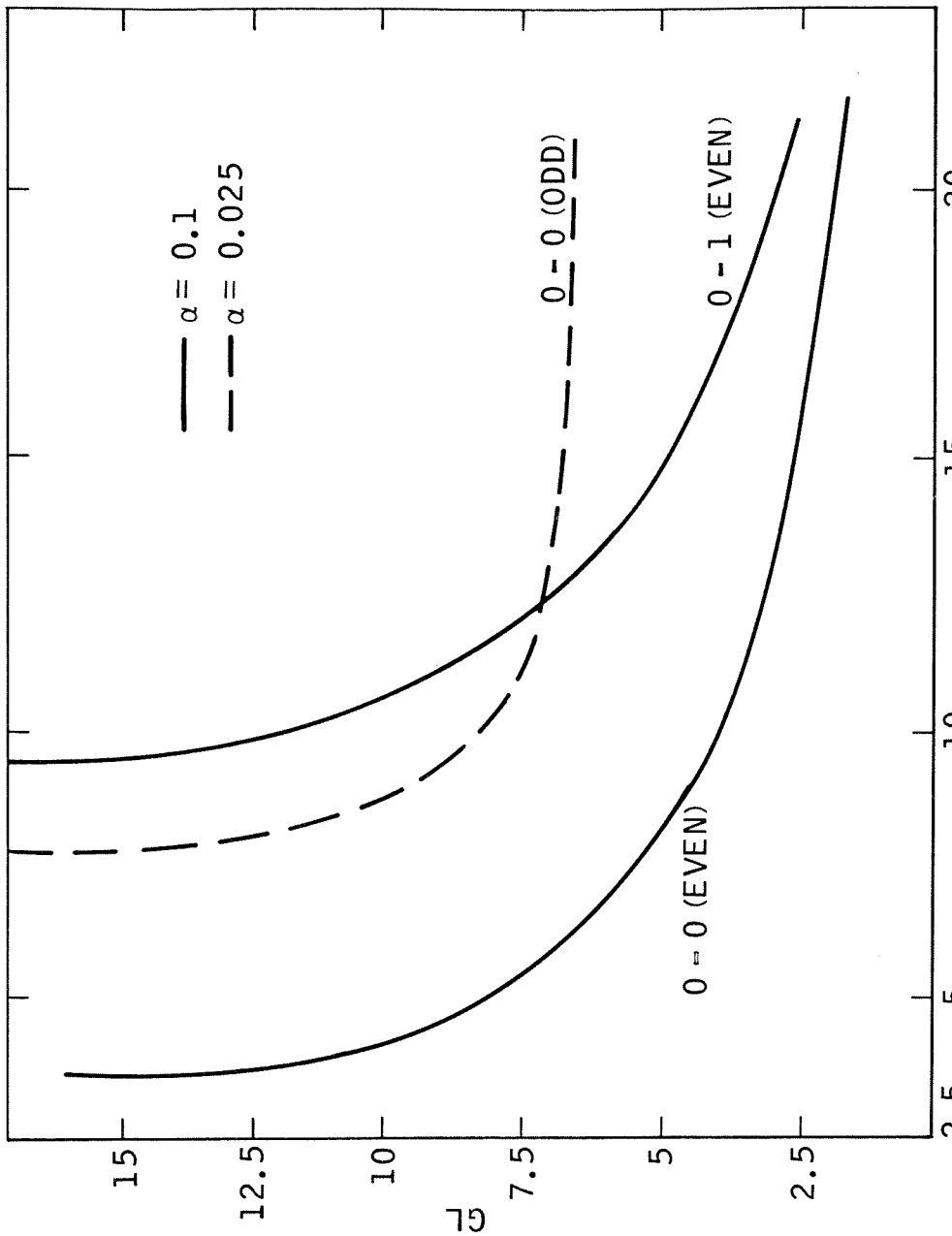

Fig. 5.16 Threshold gain curves for coupling of 0-0 and 0-1 modes of a channel diffusion waveguide with periodic boundaries. $w/d = 0.3$, $\eta L/wd = 250$, $\varepsilon_1 = (1.5)^2$, and $\varepsilon_2 = 1$. The active medium is in the channel.

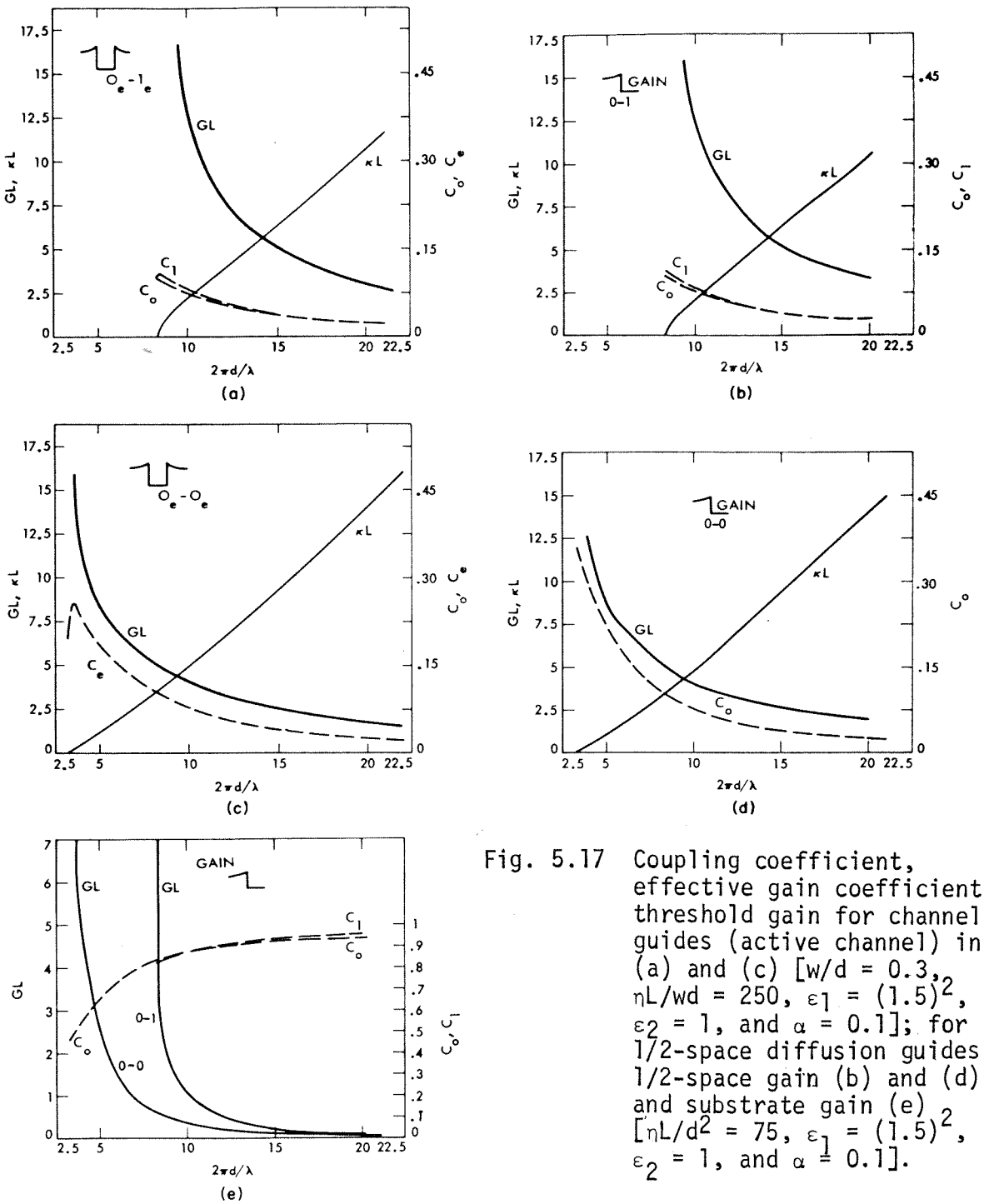

Fig. 5.17 Coupling coefficient, effective gain coefficient, and threshold gain for channel guides (active channel) in (a) and (c) [$w/d = 0.3$, $\eta L/wd = 250$, $\varepsilon_1 = (1.5)^2$, $\varepsilon_2 = 1$, and $\alpha = 0.1$]; for 1/2-space diffusion guides for 1/2-space gain (b) and (d), and substrate gain (e) [$\eta L/d^2 = 75$, $\varepsilon_1 = (1.5)^2$, $\varepsilon_2 = 1$, and $\alpha = 0.1$].

coefficient increases with frequency. When the gain is in the inhomogeneous region (Fig. 5.17e), very low threshold gain results at high frequencies because the effective gain approaches unity. To illustrate, let us consider $\lambda = .63\mu$, $d_o = 1\mu$, $\eta = .015\mu$, and $L = 0.5$ cm. The threshold gain coefficient required for the active inhomogeneous case is:

$$G = 0.8 \text{ cm}^{-1}$$

for the 0-0 mode coupling, and

$$G = 3 \text{ cm}^{-1}$$

for the 0-1 mode coupling. These gains are well below the limits of many active materials such as organic dyes or semiconductors.

From Fig. 5.17c we can estimate the threshold gain of a diffused capillary gas laser. Let us take $\lambda = 10\mu$, $d_o = 33\mu$, $2w = 20\mu$, and $\eta = 0.5\mu$. The threshold gain required is

$$GL \cong 1.8$$

Such a gain can be achieved in capillary structures where the high pressure results in a high gain.

The longitudinal mode pattern of a channel diffusion DFB laser is compared to the longitudinal mode patterns of fiber and thin film DFB lasers in Fig. 5.23.

C. Fiber Waveguide Distributed Feedback Lasers

Large scale optical communications networks using optical fibers are expected to be a reality before the end of this decade[67].

Presently, the light energy is coupled to the fiber from an outside source by directing it to the end of the fiber. However, this scheme leads to coupling losses and a desirable alternative would be direct generation of light in the fiber. In this section, we study the possibility of developing a fiber distributed feedback laser which could be incorporated in a section of an optical fiber communication channel.

The coupling coefficient $\chi_{pq}(k)$ in (5.4) is derived in Chapter IV for a fiber waveguide with a periodic boundary as

$$\chi_{pq}(k) = \eta w\left(\frac{\varepsilon_1-\varepsilon_2}{2}\right)\left(\frac{\omega_{pq}}{c}\right)^2 \sqrt{\frac{J_1(s_p w)J_1(s_q w)K_1(\delta_p w)K_1(\delta_q w)}{|\beta_p|\ |\beta_q|\ F_\beta^p F_\beta^q}} \tag{5.18}$$

where the longitudinal wave vectors of the p and q waveguide modes satisfy the phase matching condition $|\beta_p|+|\beta_q| = K$ and F_β^r is given by (4.110). The reciprocal of the group velocity $\psi_r(k)$ in (5.3) for a fiber waveguide is given by

$$\psi_r(k) = \frac{F_\omega^r}{\beta_r F_\beta^r} \tag{5.19}$$

where F_ω^r is given by (4.111). The gain efficiency coefficient $c_r(k)$ for the fiber waveguide in (5.3) is given by (3.50) and (3.51) as

$$c_r(k) = \sqrt{\varepsilon_1}\left(\frac{k}{\beta_r}\right)\frac{\alpha_F}{1+\alpha_F} \tag{5.20}$$

for gain in the fiber, and as

$$c_r(k) = \sqrt{\varepsilon_2}\,\frac{k}{\beta_r}\,\frac{1}{1+\alpha_F} \tag{5.21}$$

for gain in the cladding. Equation (3.49) gives the expression

for α_F.

Using (5.18) we can solve (5.4) for the Y_{pq} that correspond to fiber waveguides with periodic boundaries. The unperturbed fiber waveguide wave vectors s, δ, and β used in (5.18) through (5.21) are solutions of the dispersion relations (C.25) and (C.26) and are obtained using a generalized Newton's method[63] approach on a computer.

The threshold gain for fiber waveguide DFB lasers is computed using (5.1) and (5.4) and is plotted in Figs. 5.18, 5.19 and 5.20 for various waveguide modes and longitudinal modes. The physical explanation of the threshold gain curves for boundary perturbation fiber waveguide DFB lasers is the same as for boundary perturbation thin film waveguide DFB lasers. The main distinction is that the coupling coefficients (see Figs. 4.1, 4.2, and 4.5) for the fiber waveguide fall off more rapidly with frequency than those of the similarly perturbed thin film waveguide. Thus the minimum threshold gain region for fiber DFB lasers is more pronounced than for thin film DFB lasers with boundary perturbations.

To obtain an idea of the physical dimensions involved, let us consider $\lambda = 1\mu$. Operation near the minimum threshold gain occurs at approximately $\lambda/w \tilde{=} 1.2$ for both an active core and an active cladding (Fig. 5.18a,b). Thus if $w = 0.83\mu$, we can choose $\lambda = 4.15 \times 10^{-3}$ and $L = 1$ cm. The corresponding threshold gain coefficient is

$$G = 3 \text{ cm}^{-1}$$

for an active fiber, and

$$G = 4.2 \text{ cm}^{-1}$$

for an active cladding. These gains could be achieved with many active materials.

Longitudinal mode patterns for fiber DFB lasers are plotted in Figs. 5.21, 5.22, and 5.23.

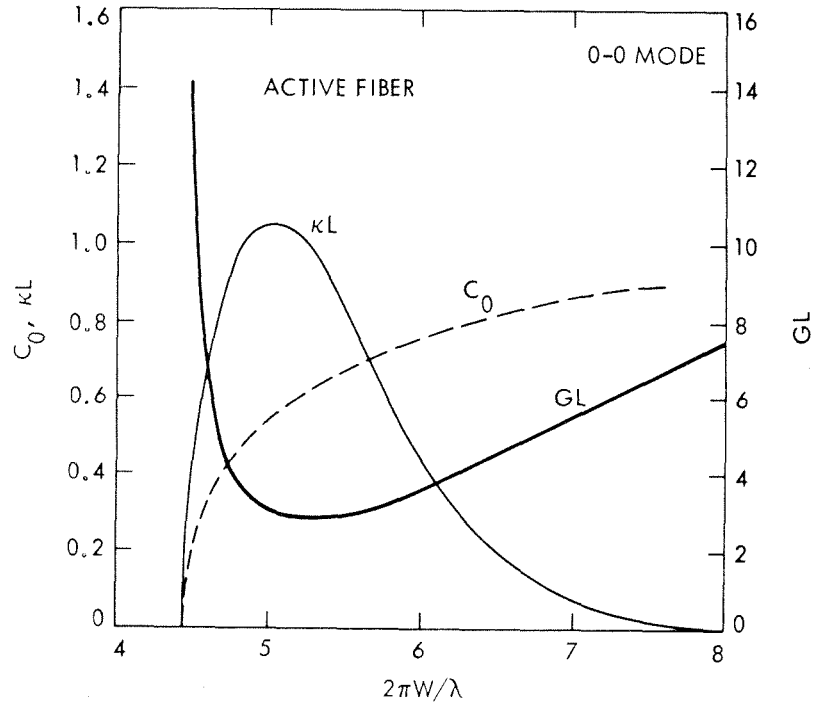

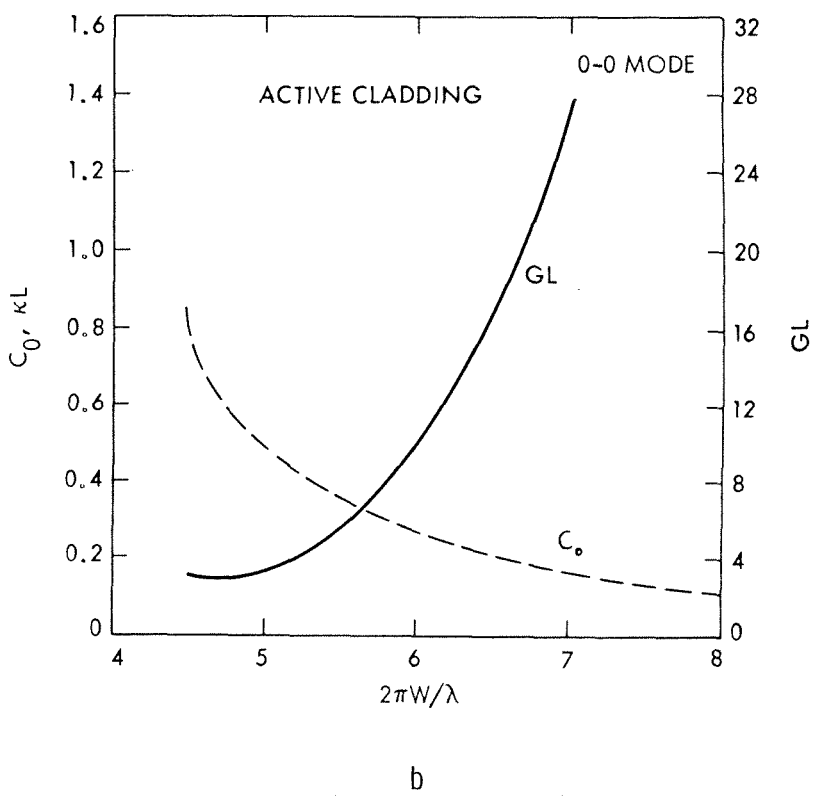

Fig. 5.18 Coupling coefficient, effective gain coefficients and threshold gain for 0-0 mode coupling of a fiber waveguide with periodic boundaries. (a) active fiber, (b) active cladding. $\varepsilon_1 = (1.5)^2$, $\varepsilon_2 = (1.4)^2$, and $\eta L/w = 5$.

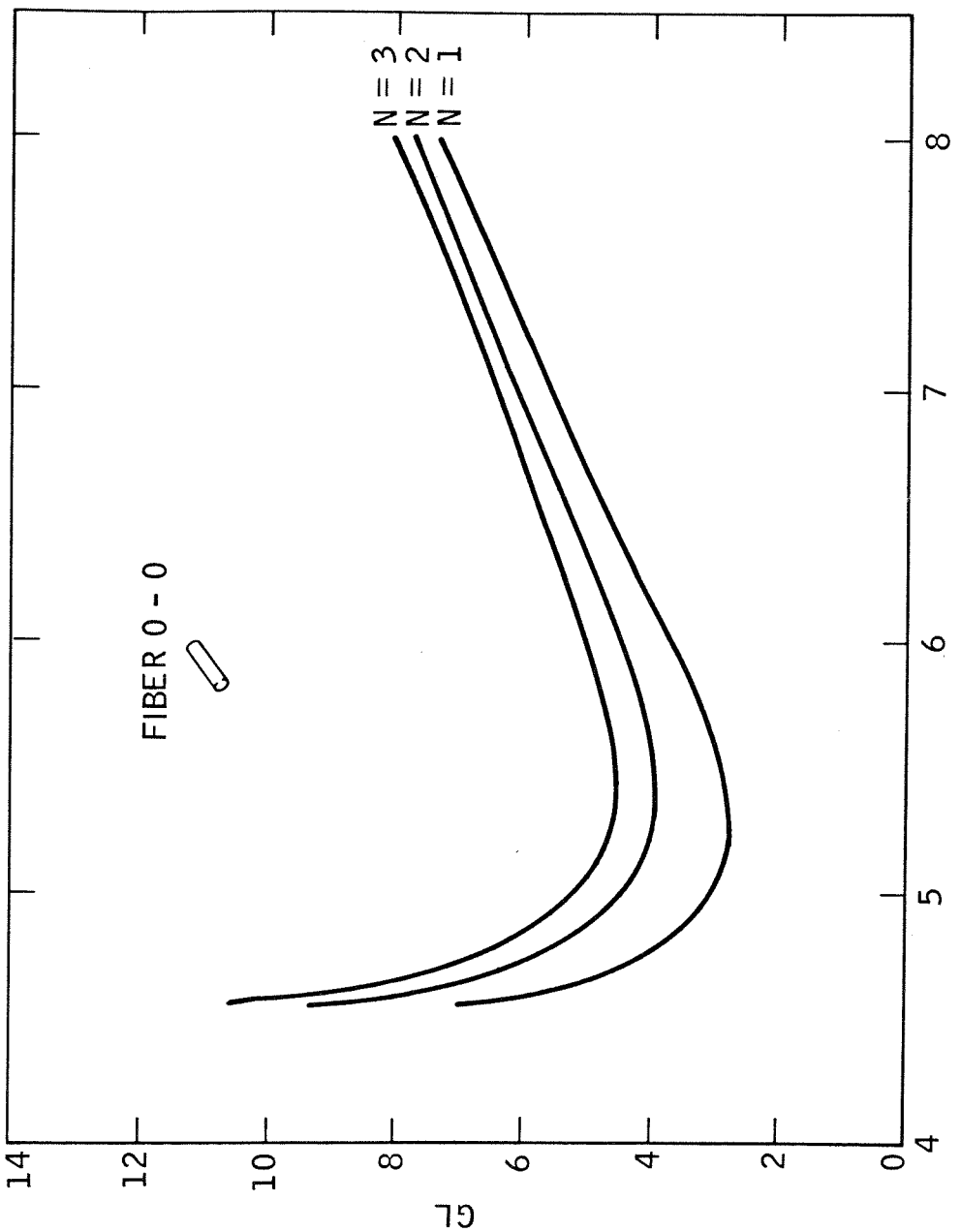

Fig. 5.19 Threshold gain curves for a fiber waveguide (active fiber) with periodic boundaries. The first three longitudinal modes arising from coupling of the 0-0 waveguide modes are plotted. $\eta L/w = 5$, $\varepsilon_1 = (1.5)^2$, and $\varepsilon_2 = (1.4)^2$.

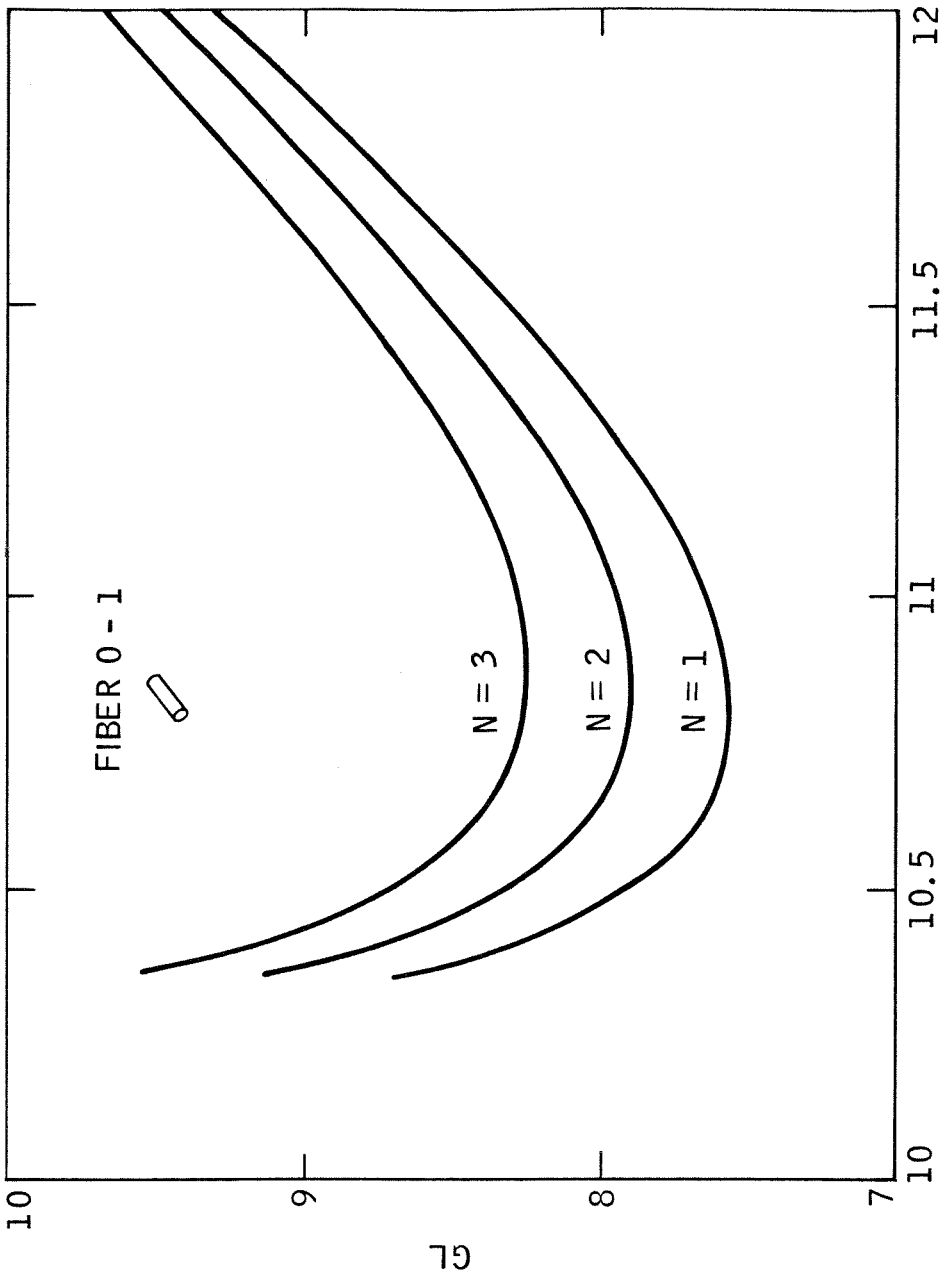

Fig. 5.20 Threshold gain curves for a fiber waveguide (active fiber) with periodic boundaries. The first three longitudinal modes arising from coupling of the 0-1 waveguide modes are plotted. $\eta L/W = 5$, $\varepsilon_1 = (1.5)^2$, and $\varepsilon_2 = (1.4)^2$.

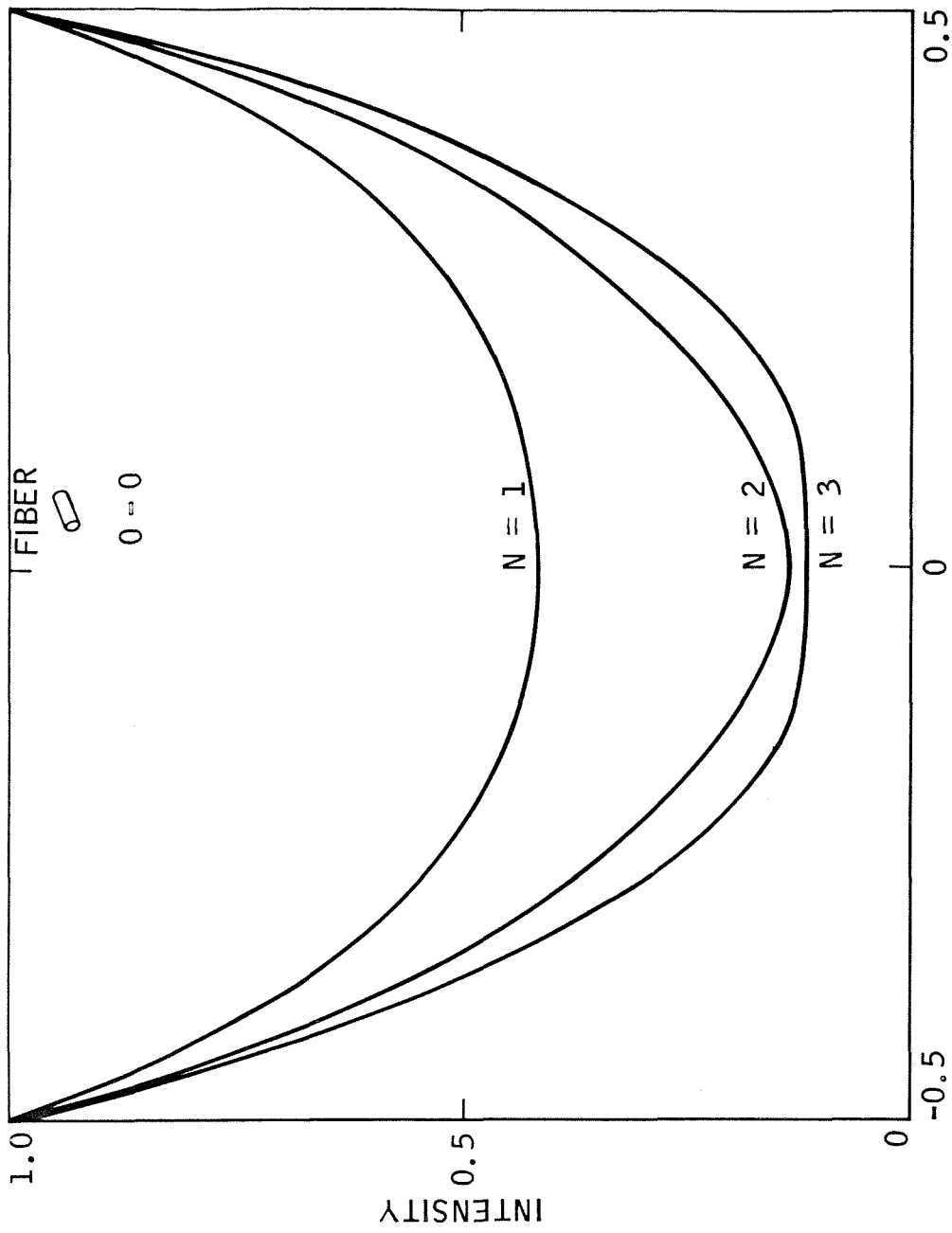

Fig. 5.21 Longitudinal intensity distributions for the first three longitudinal modes due to coupling between 0-0 modes in a fiber waveguide (active fiber) with a periodic boundary. $\eta L/W = 5$, $2\pi W/\lambda = 5.25$, $\varepsilon_1 = (1.5)^2$, and $\varepsilon_2 = (1.4)^2$.

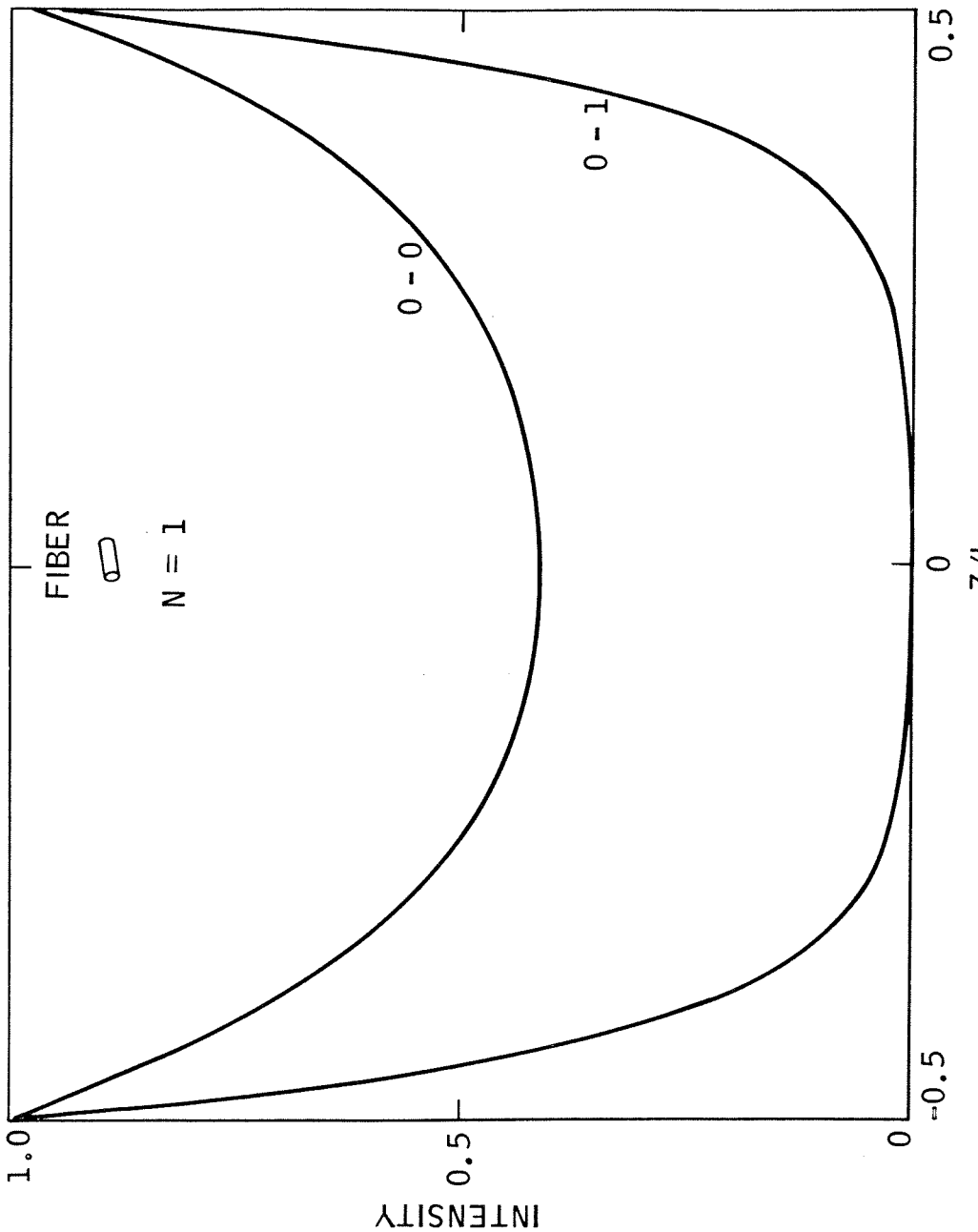

Fig. 5.22 Longitudinal intensity distributions for 0-0 coupling (@ $2\pi w/\lambda = 5.25$ in Fig. 5.19) and 0-1 coupling (@ $2\pi w/\lambda = 10.95$ in Fig. 5.20).

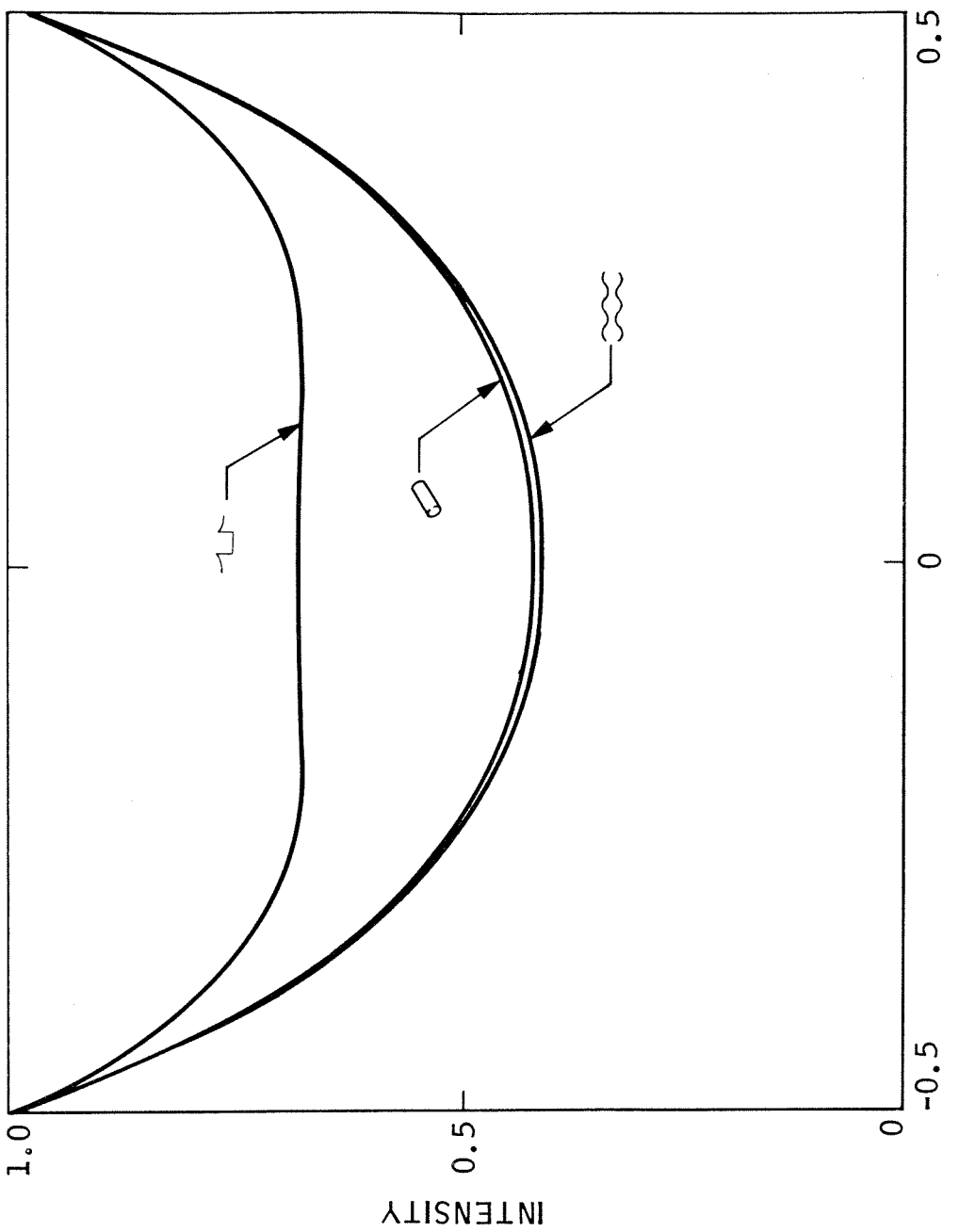

Fig. 5.23 Longitudinal intensity distributions of the first longitudinal mode due to 0-0 coupling in a channel diffusion guide (@ $2\pi d/\lambda = 8$ in Fig. 5.17c), a fiber guide (@ $2\pi w/\lambda = 5.25$ in Fig. 5.19), and a thin film guide (@ $2\pi w/\lambda = 3.5$ in Fig. 5.8).

Chapter VI

Conclusion

To study distributed feedback lasers, we have investigated electromagnetic wave propagation in active, periodic waveguides. The waveguide structures considered were thin film waveguides, half-space diffusion waveguides, channel diffusion waveguides, and fiber waveguides. The periodicity of the waveguide structure was considered to be a sinusoidal perturbation of either the electric permittivity or the waveguide boundary.

The basic properties of periodic media were obtained for an infinite medium using the Floquet theorem in conjunction with the principle of superposition to solve the wave equation. Coupled mode theory was used to derive equations for the threshold gain, longitudinal mode structure, and electromagnetic field distribution for transversely bounded distributed feedback lasers.

The amplification of a waveguide mode that extends transversely over regions with and without gain was calculated.

Analytical expressions were derived for coupling between modes in periodically perturbed dielectric waveguides.

Theoretical results indicated that an optimum design of distributed feedback lasers could be achieved by an appropriate choice of geometrical parameters. Regions of optimum design were illustrated for eleven distributed feedback laser configurations in numerous plots of normalized threshold gain versus normalized laser frequency.

Appendix A

THIN FILM WAVEGUIDES

This appendix derives the dispersion relations, field distributions, and power distribution for the TE guided modes of the thin film (dielectric slab) waveguide of width 2W illustrated in Fig. A.1. We assume that there is no variation of either the waveguide geometry or the field in the y direction. Assuming $\varepsilon_2 < \varepsilon_1$ and considering

$$E_y(x,z) = df(x)e^{i(\beta z-\omega t)} \quad , \qquad (A.1)$$

Eq. (2.3) Chapter II becomes

$$\frac{d^2f(x)}{dx^2} + (\varepsilon_1 k^2-\beta^2)\, f(x) = 0 \qquad |x| < W \quad , \qquad (A.2a)$$

$$\frac{d^2f(x)}{dx^2} + (\varepsilon_2 k^2-\beta^2)\, f(x) = 0 \qquad |x| > W \quad . \qquad (A.2b)$$

Requiring even and odd oscillating solutions inside the guide, an exponentially decaying behavior outside the guide, and continuity of the E field at the boundary,

$$f(x) = \begin{cases} \dfrac{\cos(sx)}{\cos(sw)} & \text{even modes,} \quad |x| \leq W \quad , \qquad (A.3a) \\ \dfrac{\sin(sx)}{\sin(sw)} & \text{odd modes,} \quad |x| \leq W \quad , \qquad (A.3b) \\ \exp(\delta W-\delta|x|) & \text{even modes,} \quad |x| \geq W \quad , \qquad (A.3c) \\ \text{sign } (x)\, \exp(\delta W-\delta|x|) & \text{odd modes,} \quad |x| \geq W \quad , \qquad (A.3d) \end{cases}$$

where

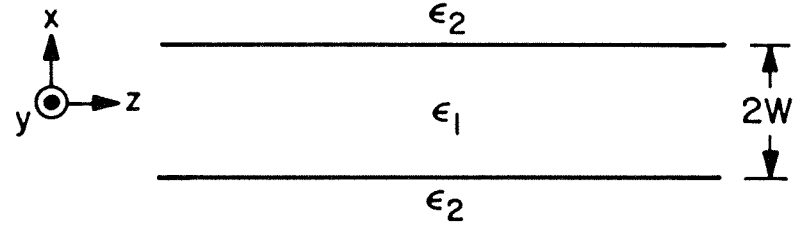

Fig. A.1 Thin film waveguide geometry.

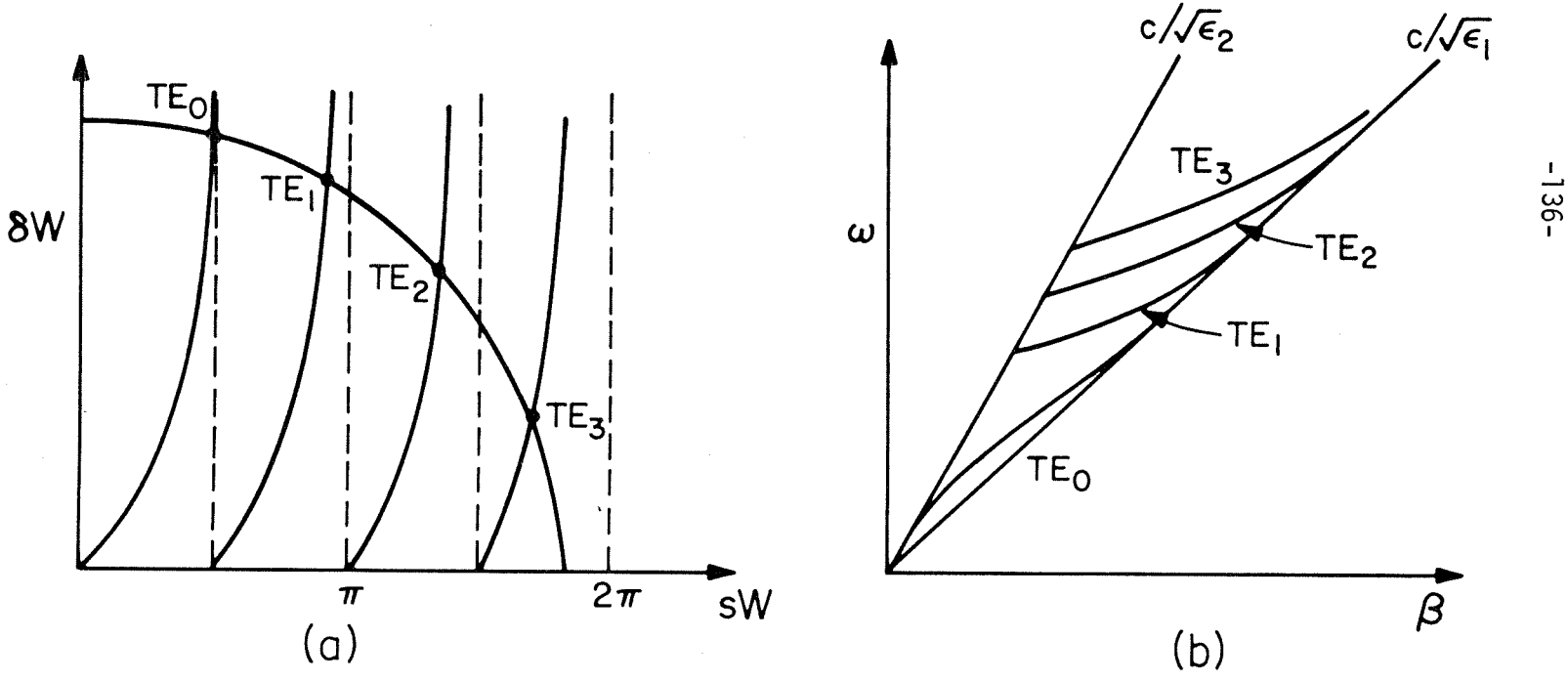

Fig. A.2 (a) graphical solution of equations (A.6) and (A.7);
(b) ω-β diagram for TE modes of a thin film waveguide.

$$s^2 = \varepsilon_1 k^2 - \beta^2 \quad , \qquad (A.4)$$

$$\delta^2 = -\varepsilon_2 k^2 + \beta^2 \quad . \qquad (A.5)$$

The field amplitude at the boundary is d, the waveguide thickness is 2W, β is the longitudinal component of the wavevectors, s and δ are respectively the transverse component of the wavevector inside and outside the waveguide, and $k = \omega/c$ where c is the speed of light in vacuum.

Requiring the H field ($H_z = -i/(\omega\mu)\,\frac{\partial E_y}{\partial x}$) to be continuous at the boundary,

$$\delta = s \begin{cases} \tan(sW) & \text{even modes} \\ -\cot an(sW) & \text{odd modes} \end{cases} \quad . \qquad (A.6)$$

Combining (A.4) and (A.5),

$$s^2 + \delta^2 = (\varepsilon_1 - \varepsilon_2)k^2 \quad . \qquad (A.7)$$

The different solutions of (A.6) and (A.7) correspond to the different modes which can be supported by the dielectric waveguide. A graphical solution to Eqs. (A.6) and (A.7) is illustrated in Fig. A.2a and the resulting Brillouin diagram in Fig. A.2b.

The normalized power inside the waveguide is given by

$$P_{in} = \int_{-W}^{W} \frac{\cos^2(sx)dx}{\cos^2(sw)} \qquad \text{(even modes)} \quad , \qquad (A.8a)$$

$$P_{in} = \int_{-W}^{W} \frac{\sin^2(sx)dx}{\sin^2(sw)} \qquad \text{(odd modes)} \quad , \qquad (A.8b)$$

and the normalized power outside the waveguide is given by

$$P_{out} = 2 \int_{W}^{\infty} e^{-2\delta x} e^{-2\delta w} dx \qquad \text{(all modes)} \quad , \qquad \text{(A.9)}$$

Integrating (A.8 a,b) and (A.9), we find

$$P_{in} = \frac{1}{s} \left[\frac{sw + \sin(sw)\cos(sw)}{\cos^2(sw)} \right] \qquad \text{(even modes)} \quad , \qquad \text{(A.10a)}$$

$$P_{in} = \frac{1}{s} \left[\frac{sw - \sin(sw)\cos(sw)}{\sin^2(sw)} \right] \qquad \text{(odd modes)} \quad , \qquad \text{(A.10b)}$$

and

$$P_{out} = \delta^{-1} \quad . \qquad \text{(A.11)}$$

The ratio of the power inside the guide to the total power can be written

$$\frac{P_{in}}{P_{in} + P_{out}} = \frac{\alpha}{1 + \alpha} \quad , \qquad \text{(A.12)}$$

where

$$\alpha = \frac{\delta}{s} \left[\frac{sw + \sin(sw)\cos(sw)}{\cos^2(sw)} \right] \qquad \text{(even modes)} \quad , \qquad \text{(A.13a)}$$

$$\alpha = \frac{\delta}{s} \left[\frac{sw - \sin(sw)\cos(sw)}{\cos^2(sw)} \right] \qquad \text{(odd modes)} \quad . \qquad \text{(A.13b)}$$

Using the trigonometric identities

$$\cos^2 x = \frac{1}{2} (\cos 2x + 1) \quad , \qquad \text{(A.14a)}$$

$$\tan x = \frac{\sin 2x}{1 + \cos 2x} \quad , \qquad \text{(A.14b)}$$

$$\sin^2 x = \frac{1}{2}(-\cos 2x + 1) \quad , \qquad \text{(A.14c)}$$

$$\text{cotan } x = \frac{\sin 2x}{1 - \cos 2x} \quad , \qquad \text{(A.14d)}$$

and Eq. (A.6),

$$\alpha = \tan^2(sw)\left[1 + \frac{2\,sw}{\sin(2\,sw)}\right] \quad \text{(even modes)} \quad , \qquad \text{(A.15a)}$$

$$\alpha = -\text{cotan}^2(sw)\left[1 - \frac{2\,sw}{\sin(2\,sw)}\right] \quad \text{(odd modes)} \quad . \qquad \text{(A.15b)}$$

Detailed treatments of thin film waveguides appear in several texts, including those authored by Marcuse[28] and Collin[29]. Applications of thin film waveguides to integrated data processors are discussed by Shubert and Harris.[44]

Appendix B

DIFFUSION WAVEGUIDES

This appendix derives the dispersion relations and field distributions for TE guided modes of diffusion waveguides. We consider two separate diffusion waveguide geometries, a dielectric channel embedded in exponentially inhomogeneous substrates (see Fig. B.1a), and a half space diffusion guide (see Fig. B.1b).

A. Channel Diffusion Guide

We consider the channel diffusion guide characterized by the relative dielectric constant

$$\begin{aligned} \varepsilon_2 &= \text{constant} && |x| < W \\ \varepsilon_1(x) &= \varepsilon_1 + \alpha \exp\left(\frac{-|x| + W}{d_o}\right) && |x| > W \end{aligned} \quad , \qquad (B.1)$$

where d_o is the diffusion depth, $2W$ is the channel width, $\varepsilon_1 > \varepsilon_2$, and α is usually small relative to ε_1.

Assuming no y variation of the waveguide geometry, and considering

$$E_y(x,z,t) = df(x)e^{i(\beta z-\omega t)} \quad , \qquad (B.2)$$

where d is the field amplitude at the boundary, Eq. (2.3) Chapter II becomes

$$\frac{d^2f(x)}{dx^2} + (\varepsilon_2 k^2 - \beta^2)f(x) = 0 \qquad |x| \leq W \quad , \qquad (B.3a)$$

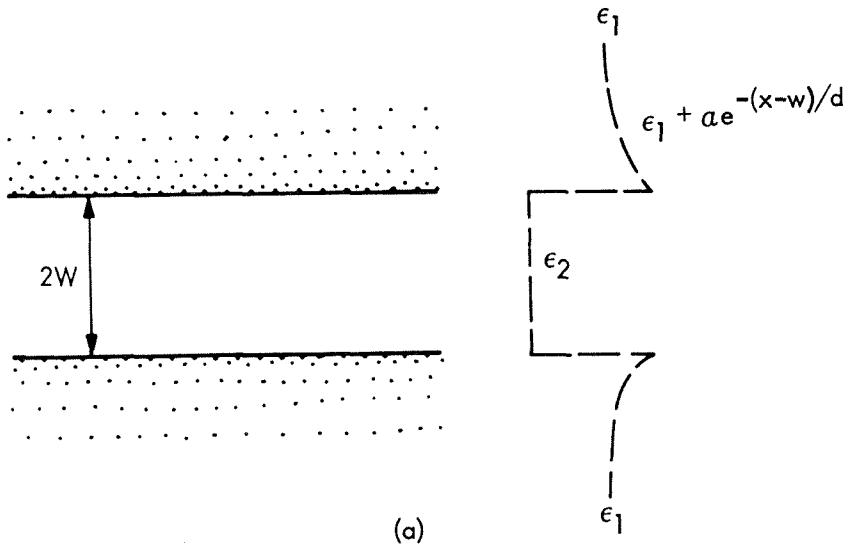

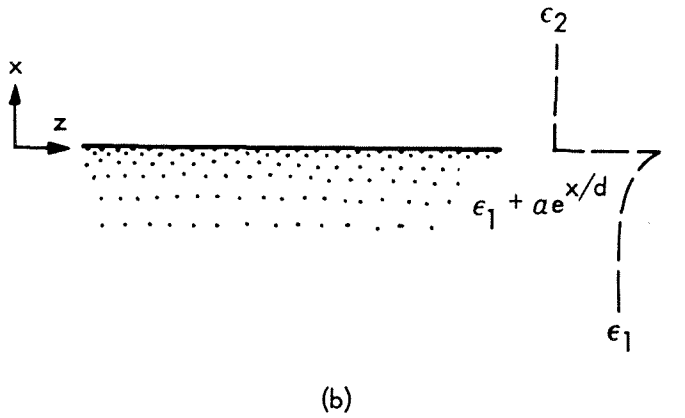

Fig. B.1 (a) a homogeneous channel between transversely inhomogeneous substrates; (b) a transversely inhomogeneous diffusion waveguide. α is $<< \varepsilon_1$ and $\varepsilon_2 < \varepsilon_1$.

$$\frac{d^2f(x)}{dx^2} + (\varepsilon_1 k^2 - \beta^2)f(x) + \alpha k^2 e^{-\frac{|x| - W}{d_o}} f(x) = 0 \quad |x| \geq W \quad . \tag{B.3b}$$

Substituting

$$\xi = e^{-\frac{|x| - W}{2d_o}} 2\sqrt{\alpha}\, kd_o \quad , \tag{B.4}$$

(B.3b) transforms to the well known differential equation for Bessel functions[30]:

$$\xi^2 \frac{d^2f}{d\xi^2} + \xi \frac{df}{d\xi} + (\xi^2 - \nu^2)f = 0 \quad , \tag{B.5}$$

where

$$\nu^2 = (\beta^2 - \varepsilon_1 k^2)(2d_o)^2 \quad . \tag{B.6}$$

We can write, after requiring E field continuity at the boundary,

$$f(x) = J_\nu \left(2\sqrt{\alpha}\ kd_o\, e^{-\frac{|x|-W}{2d_o}} \right) / J_\nu(2\sqrt{\alpha}\, kd_o) \quad |x| \geq W \quad , \tag{B.7}$$

and

$$f(x) = \begin{cases} \cosh(\delta x) / \cosh(\delta w) & \text{(even modes)} \\ \sinh(\delta x) / \sinh(\delta w) & \text{(odd modes)} \end{cases} \quad |x| \leq W \quad , \tag{B.8}$$

where

$$\delta^2 = \beta^2 - \varepsilon_2 k^2 \quad , \tag{B.9}$$

and J_ν is the Bessel function of first order..

The H field continuity condition gives the relation

$$-2\sqrt{\alpha}kd_o \frac{J_\nu'(2\sqrt{\alpha}\, kd_o)}{J_\nu(2\sqrt{\alpha}\, kd_o)} = 2\,\delta d_o \begin{cases} \tanh(\delta w) \\ \text{cotanh}(\delta w) \end{cases} , \qquad (B.10)$$

where the prime in (B.10) indicates differentiation with respect to the argument $2\sqrt{\alpha}\, kd_o$ of the Bessel function. Combining (B.6) and (B.9),

$$\delta^2 - (\nu/2d_o)^2 = (\varepsilon_1 - \varepsilon_2)\, k^2 . \qquad (B.11)$$

Equations (B.10) and (B.11) have multiple solutions which correspond to the different guided modes.

The cut-off frequencies correspond to the limit $\nu \to 0$, and in this limit,

$$\beta = k\sqrt{\varepsilon_1}$$

$$\delta = k\sqrt{\varepsilon_1 - \varepsilon_2} , \qquad (B.12)$$

$$2\sqrt{\alpha}\, kd_o \left(\frac{J_1(2\sqrt{\alpha}\, kd_o)}{J_0(2\sqrt{\alpha}\, kd_o)}\right) - 2\,\delta d_o \begin{cases} \tanh(\delta w) \\ \text{cotanh}(\delta w) \end{cases} .$$

We can write (B.12) as

$$\frac{J_1(2\sqrt{\alpha}\, kd_o)}{J_0(2\sqrt{\alpha}\, kd_o)} = a \begin{cases} \tanh(ar_o 2\sqrt{\alpha}\, kd_o) \\ \text{cotanh}(ar_o 2\sqrt{\alpha}\, kd_o) \end{cases} , \qquad (B.13)$$

where $a = \sqrt{(\varepsilon_1 - \varepsilon_2)/\alpha}$ and $r_o = w/2d_o$. The cut-off frequencies are thus determined from the intersection of the two curves $Y = J_1(2\sqrt{\alpha}\, kd_o)/J_0(2\sqrt{\alpha}\, kd_o)$ and $Y = a \tanh (ar_o 2\sqrt{\alpha}\, kd_o)$ for the even modes, or $Y = a$ cotanh$(a\, r_o 2\sqrt{\alpha}\, kd_o)$ for the odd modes. From Fig. B.2a it is clear that there are always cut-off frequencies for odd modes for all values of a and r_o. This is true for all even modes except the first one. As "ar_o" decreases, the cut-off frequency of the first even mode decreases, reaching zero at "ar_o" = $\frac{1}{2}$, and for "ar_o" less than $\frac{1}{2}$, the first even mode disappears.

In summary, the main properties of the channel diffusion guide are:

1) For $w/d_o < \alpha/(\varepsilon_1-\varepsilon_2)$, the first mode is an odd mode.
2) For $w/d_o = \alpha/(\varepsilon_1-\varepsilon_2)$, an even mode appears with a cut-off frequency equal to zero.
3) For $w/d_o > \alpha/(\varepsilon_1-\varepsilon_2)$, the first even mode will also have a cut-off frequency.
4) All odd modes and higher even modes ($p \geq 2$) always have cut-off frequencies.
5) The higher modes ($p \geq 2$) always appear in even-odd pairs with cut-off frequencies given by

$$\Omega < 2\sqrt{\alpha}\, k_p d_o(\text{even}) < 2\sqrt{\alpha}\, k_p d_o(\text{odd}) < \Omega'$$

where Ω is the $(p-1)^{st}$ root of J_1 and Ω' is the p^{th} root of J_0.

6) For high order modes, $k_p(\text{even}) \to k_p(\text{odd}) \to k_p$ where

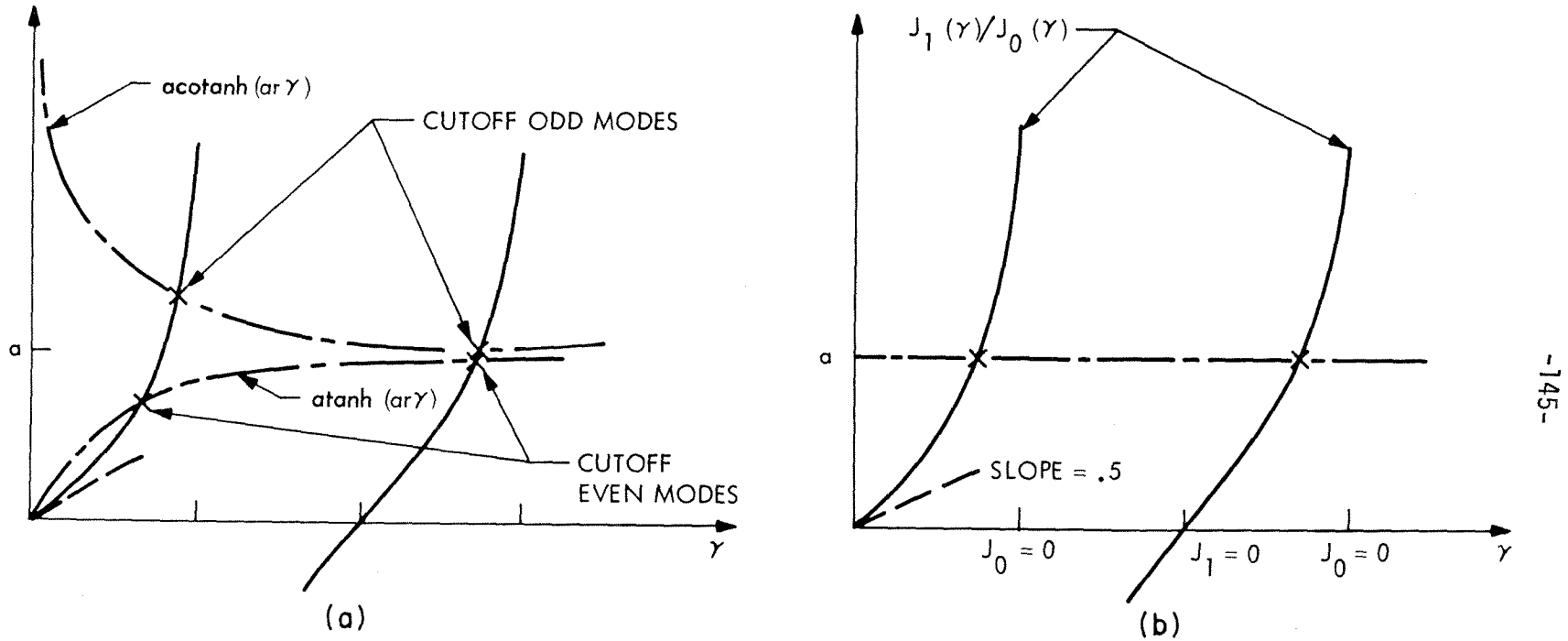

Fig. B.2 Graphical solution for the cutoff frequencies. (a) corresponds to the channel waveguide where even and odd modes can be guided; (b) corresponds to the 1/2 space waveguide.

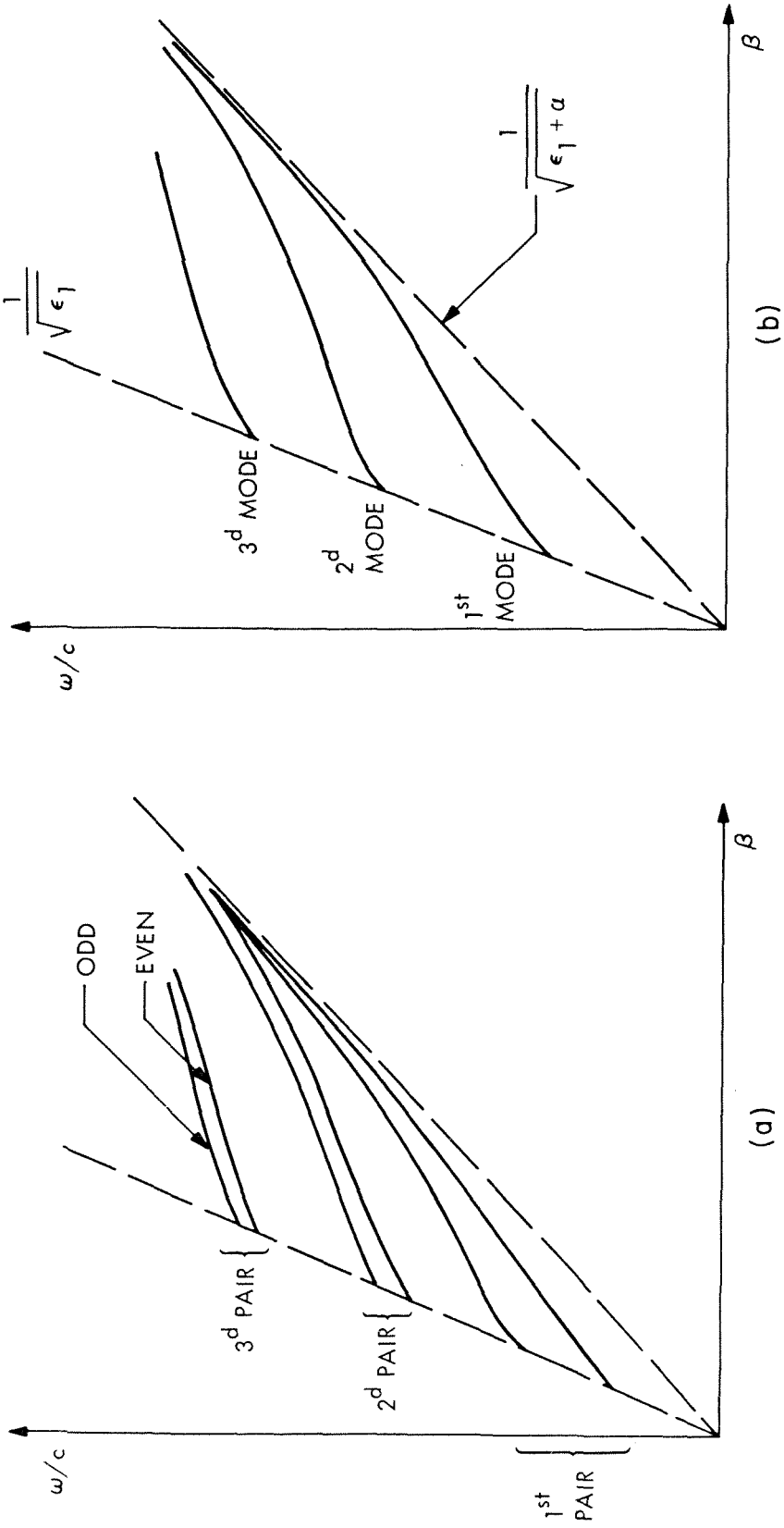

Fig. B.3 Sketches of the ω-β diagram for the channel waveguide (a), and the 1/2 space waveguide (b).

$$\frac{J_1(2\sqrt{\alpha}k_p d_o)}{J_0(2\sqrt{\alpha}k_p d_o)} = \left(\frac{\varepsilon_1 - \varepsilon_2}{\alpha}\right)^{1/2}$$

A sketch of a typical Brillouin diagram is shown in Fig. B.3a. Transverse field distributions for the channel guide are shown in Figs. B.4, B.5, and B.6.

B. Half Space Diffusion Guide

The above results can be easily changed for the case of a $\frac{1}{2}$ space diffusion guide (Fig. B.1b). In this case, the field in the inhomogeneous medium is given by Eq. (B.7) with W = 0. However, in the homogeneous half space, the field is equal to $de^{-\delta|x|}$. The resulting dispersion relation is

$$-2\sqrt{\alpha}\, kd_o \frac{J_\nu'(2\sqrt{\alpha}\, kd_o)}{J_\nu(2\sqrt{\alpha}\, kd_o)} = 2\,\delta d_o \quad , \qquad \text{(B.14)}$$

and the cut-off frequencies are given by

$$\frac{J_1(2\sqrt{\alpha}\, kd_o)}{J_0(2\sqrt{\alpha}\, kd_o)} = \left(\frac{\varepsilon_1 - \varepsilon_2}{\alpha}\right)^{1/2} \quad . \qquad \text{(B.15)}$$

The graphical solutions (Fig. B.2b) show that there is always a cut-off frequency and the even-odd behavior has disappeared, as is to be expected. The resulting Brillouin diagram (Fig. B.3b) shows each mode of the half space diffusion guide falling in between the corresponding mode-pair of the symmetric guide studied in previous sections. In fact, as $w \to \infty$, a mode pair merges (one from above and the other from below)

with the corresponding half space diffusion guide mode.

A more detailed analysis of the channel diffusion waveguide appears in Ref. 4 and of the half space diffusion guide in Ref. 12.

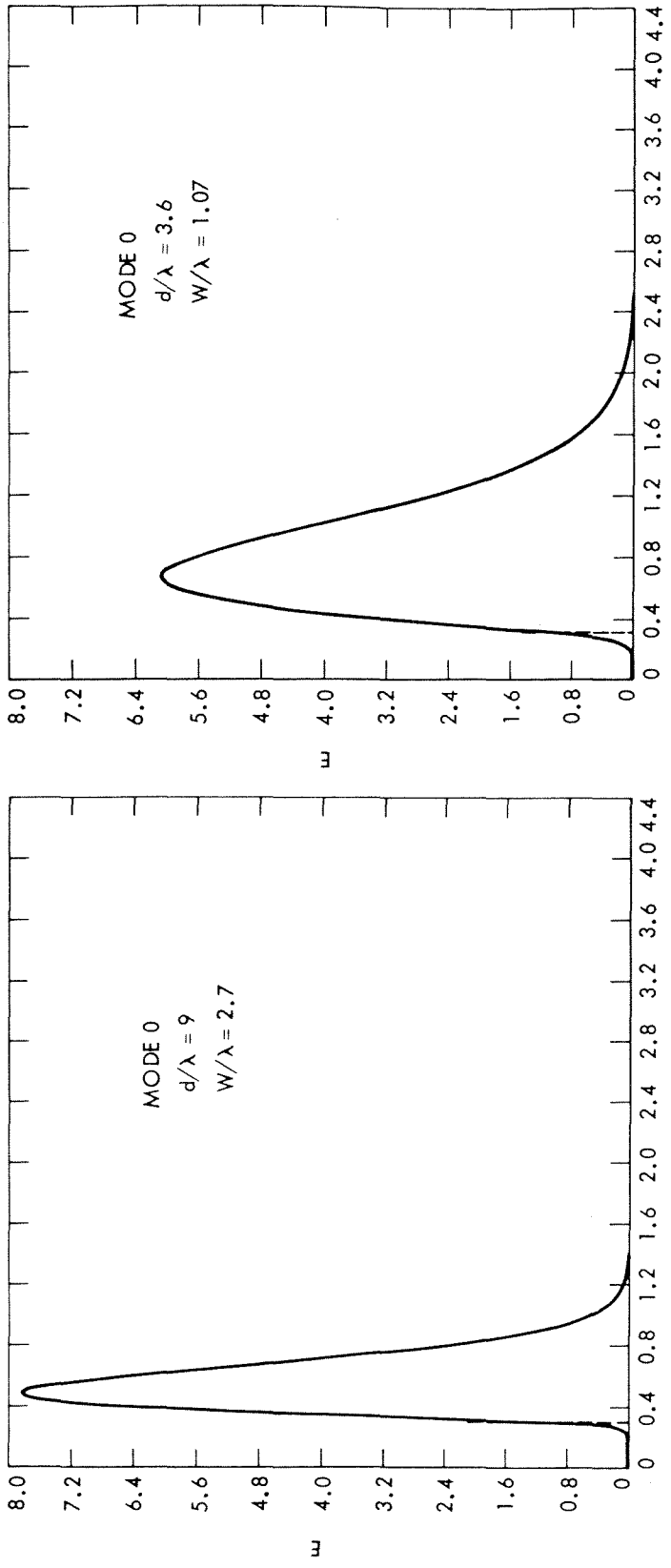

Fig. B.4 Electric field distribution of the 0-mode in a channel waveguide for w/d = 0.3 and α = 0.1. The dashed vertical line is the boundary of the channel. (a) very much above cutoff; (b) somewhat above cutoff.

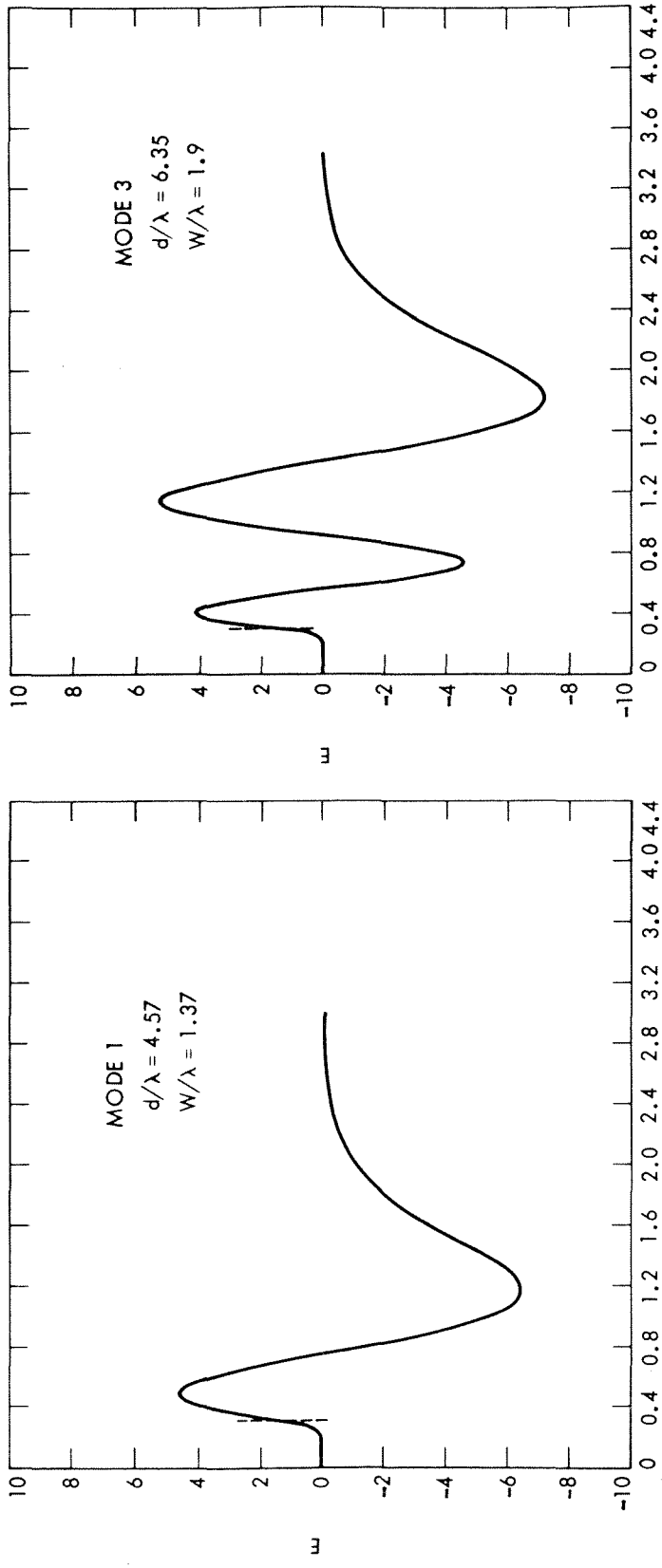

Fig. B.5 Electric field distribution in a channel waveguide for w/d = 0.3 and α = 0.1. (a) mode 1, (b) mode 3.

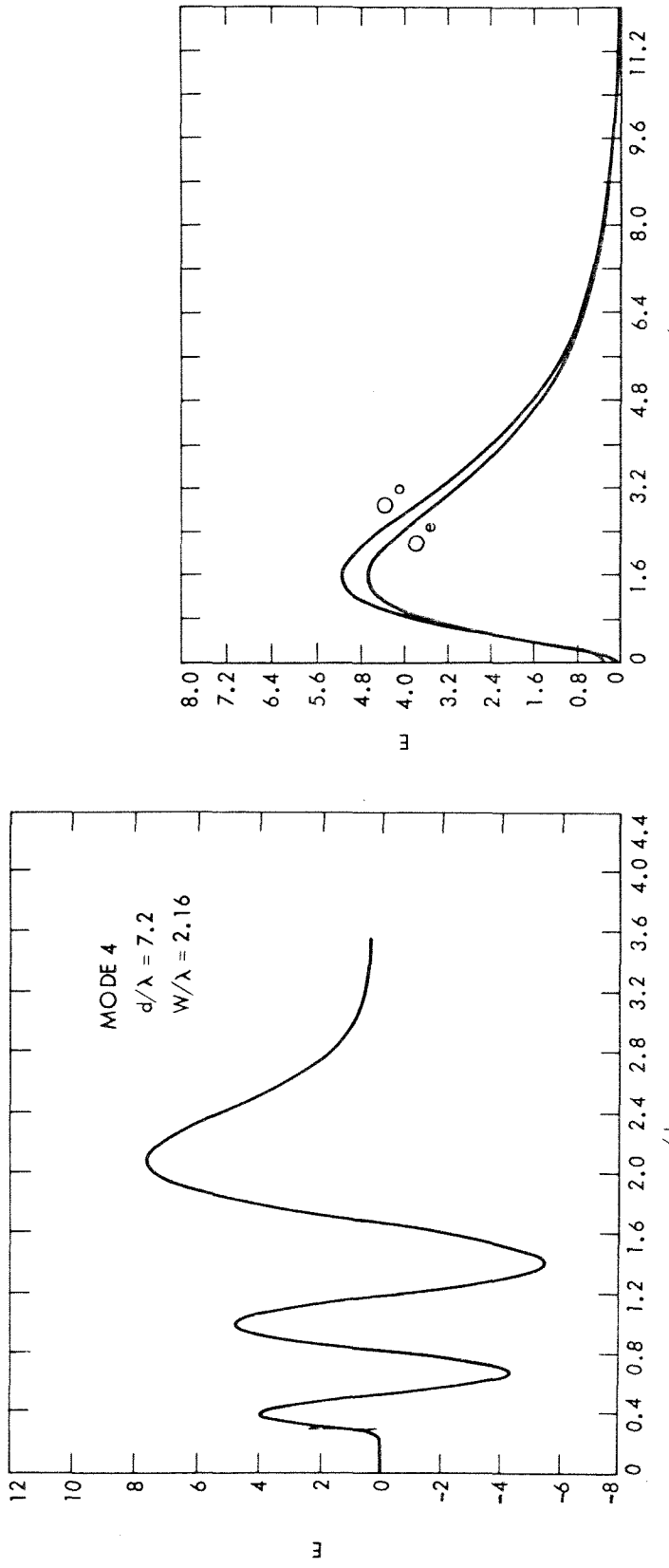

Fig. B.6 Electric field distribution in a channel waveguide for w/d = 0.3 and α = 0.1. (a) Mode 4; (b) distribution of the 0 (even) mode and the 0 (odd) mode for d/λ = 0.9.

Appendix C

FIBER WAVEGUIDES

This appendix derives the dispersion relations and field distributions for the guided modes of a round optical fiber of radius W (Fig. C.1).

Using cylindrical polar coordinates (see Fig. C.2), the wave equations become[28]

$$\frac{\partial^2 E_z}{\partial \rho^2} + \frac{1}{\rho}\frac{\partial E_z}{\partial \rho} + \frac{1}{\rho^2}\frac{\partial^2 E_z}{\partial \phi^2} + (\varepsilon_j k^2 - \beta^2)E_z = 0 \quad , \qquad (C.1)$$

and

$$\frac{\partial^2 H_z}{\partial \rho^2} + \frac{1}{\rho}\frac{\partial H_z}{\partial \rho} + \frac{1}{\rho^2}\frac{\partial^2 H_z}{\partial \phi^2} + (\varepsilon_j k^2 - \beta^2)H_z = 0 \quad , \qquad (C.2)$$

where

$$\rho = \sqrt{x^2 + y^2} \quad , \qquad (C.3)$$

and

$$\varepsilon_j = \begin{cases} \varepsilon_2 & \rho \geq w \\ \varepsilon_1 & \rho \leq w \end{cases} \quad . \qquad (C.4)$$

We assume solutions

$$E_z = \begin{cases} A\, F(\rho) e^{i\nu\phi} e^{i(\beta z - \omega t)} & \rho \leq w \qquad (C.5a) \\ C\, F(\rho) e^{i\nu\phi} e^{i(\beta z - \omega t)} & \rho \geq w \quad , \qquad (C.5b) \end{cases}$$

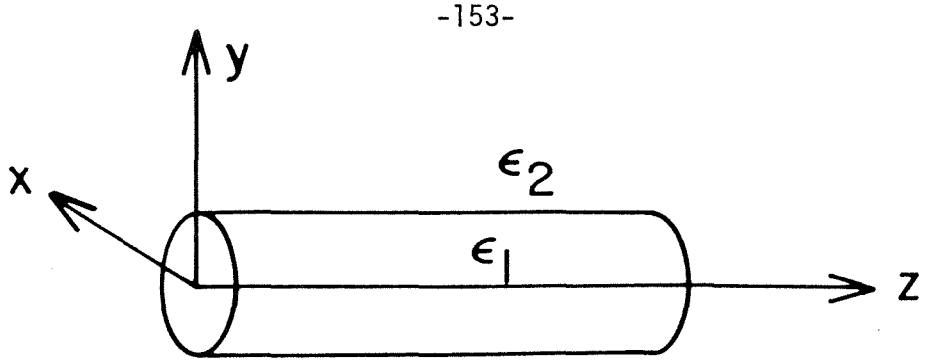

Fig. C.1 Fiber waveguide geometry.

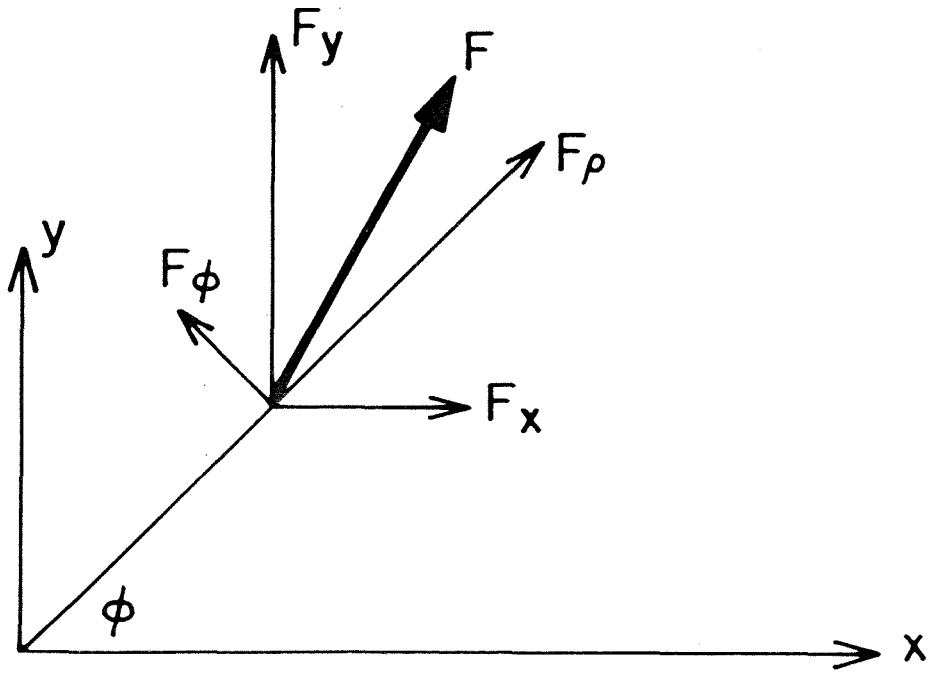

Fig. C.2 Coordinate system.

$$H_z = \begin{cases} B\,F(\rho)e^{i\nu\phi}e^{i(\beta z-\omega t)} & \rho \leq w \qquad (C \quad (C.5c) \\ D\,F(\rho)e^{i\nu\phi}e^{i(\beta z-\omega t)} & \rho \geq w \qquad , \quad (C.5d) \end{cases}$$

and require ν to be a positive or negative integer to ensure that the fields are periodic in ϕ with period 2π.

Substituting (C.5) into (C.1) gives

$$\frac{d^2F}{d\rho^2} + \frac{1}{\rho}\frac{dF}{d\rho} + \left[(\varepsilon_i k^2 - \beta^2) - \frac{\nu^2}{\rho^2}\right] F = 0 \qquad , \quad (C.6)$$

Equation (C.6) is the well known differential equation for Bessel functions.[30] We require different solutions of (C.6) for the regions defined by $\rho \leq w$ and $\rho \geq w$. The solutions inside the core must remain finite at $\rho = 0$, while the solutions outside must decay for $\rho \to \infty$ if we want guided modes. For $\rho \leq w$, the appropriate solutions are

$$E_z = AJ_\nu(s\rho)e^{i\nu\phi} \qquad , \quad (C.7)$$

$$H_z = BJ_\nu(s\rho)e^{i\nu\phi} \qquad , \quad (C.8)$$

where

$$s^2 = \varepsilon_1 k^2 - \beta^2 \qquad , \quad (C.9)$$

and J_ν is the Bessel function of the first kind.

From co-ordinate transformation considerations,[28]

$$E_\rho = \frac{i}{\varepsilon_j k^2 - \beta^2}\left(\beta\frac{\partial E_z}{\partial \rho} + \omega\mu\frac{1}{\rho}\frac{\partial H_z}{\partial \phi}\right) \qquad , \quad (C.10)$$

$$E_\phi = \frac{i}{\varepsilon_j k^2 - \beta^2}\left(\beta \frac{1}{\rho}\frac{\partial E_z}{\partial \phi} - \omega\mu \frac{\partial H_z}{\partial \rho}\right) , \qquad (C.11)$$

$$H_\rho = \frac{i}{\varepsilon_j k^2 - \beta^2}\left(\beta \frac{\partial H_z}{\partial \rho} - \omega\varepsilon_j\varepsilon_o \frac{1}{\rho}\frac{\partial E_z}{\partial \phi}\right) , \qquad (C.12)$$

$$H_\phi = \frac{i}{\varepsilon_j k^2 - \beta^2}\left(\beta \frac{1}{\rho}\frac{\partial H_z}{\partial \phi} + \omega\varepsilon_j\varepsilon_o \frac{\partial E_z}{\partial \rho}\right) . \qquad (C.13)$$

Thus for $\rho \leq w$,

$$E_\rho = \frac{i}{s^2}\left[\beta s\, A\, J_\nu'(s\rho) + \frac{i\omega\mu_o}{\rho} B\, J_\nu(s\rho)\right] e^{i\nu\phi} , \qquad (C.14)$$

$$E_\phi = \frac{i}{s^2}\left[\frac{i\beta\nu}{\rho} A\, J_\nu(s\rho) - \omega\mu_o s B J_\nu'(s\rho)\right] e^{i\nu\phi} , \qquad (C.15)$$

$$H_\rho = \frac{i}{s^2}\left[\beta s B J_\nu'(s\rho) - \frac{i\omega\varepsilon_1\varepsilon_o\nu}{\rho} A\, J_\nu(s\rho)\right] e^{i\nu\phi} , \qquad (C.16)$$

$$H_\phi = \frac{i}{s^2}\left[\frac{i\nu\beta}{\rho} B\, J_\nu(s\rho) + \omega\varepsilon_1\varepsilon_o s\, A\, J_\nu'(s\rho)\right] e^{i\nu\phi} . \qquad (C.17)$$

The prime indicates differentiation with respect to the argument $s\rho$ of the Bessel function.

The fields for $\rho \geq w$ are given by

$$E_z = C\, K_\nu(\delta\rho) e^{i\nu\phi} , \qquad (C.18)$$

$$H_z = D\, K_\nu(\delta\rho) e^{i\nu\phi} , \qquad (C.19)$$

$$E_\rho = \frac{-i}{\delta^2}\left[\delta\beta\ C\ K_\nu'(\delta\rho) + \frac{i\omega\mu\nu}{\rho}\ D\ K_\nu(\delta\rho)\right] e^{i\nu\phi} \quad , \qquad (C.20)$$

$$E_\phi = \frac{-i}{\delta^2}\left[\frac{i\nu\beta}{\rho}\ C\ K_\nu(\delta\rho) - \omega\mu\delta\ D\ K_\nu'(\delta\rho)\right] e^{i\nu\phi} \quad , \qquad (C.21)$$

$$H_\rho = \frac{-i}{\delta^2}\left[\beta\delta\ D\ K_\nu'(\delta\rho) - \omega\varepsilon_2\varepsilon_o\ \frac{i\nu}{\rho}\ C\ K_\nu(\delta\rho)\right] e^{i\nu\phi} \quad , \qquad (C.22)$$

$$H_\phi = \frac{-i}{\delta^2}\left[\frac{i\nu\beta}{\rho}\ D\ K_\nu(\delta\rho) + \omega\varepsilon_2\varepsilon_o\ \delta C\ K_\nu'(\delta\rho)\right] e^{i\nu\phi} \quad . \qquad (C.23)$$

Again, the prime indicates differentiation with respect to the argument $\delta\rho$. We have defined

$$\delta^2 = \beta^2 - \varepsilon_2 k^2 \quad , \qquad (C.24)$$

and K_ν is the modified Bessel function.[30]

Applying the boundary conditions for the E and H field and considering the special case $\nu = 0$, we obtain the dispersion relation for TE waves[28,31]:

$$sw\ \frac{J_o(sw)}{J_1(sw)} + \delta w\ \frac{K_o(\delta w)}{K_1(\delta w)} = 0 \quad , \qquad (C.25)$$

and combining (C.9) and (C.24)

$$(sw)^2 + (\delta w)^2 = (\varepsilon_1 - \varepsilon_2)(kw)^2 \quad . \qquad (C.26)$$

Equations (C.25) and (C.26) can be solved simultaneously[28,31] for s and δ for given k, w, ε_1 and ε_2. The resulting Brillouin diagrams are similar to those of Figs. A.2b and B.3b. The corresponding normalized

fields for the TE modes are ($E_z = E_r = 0$)

$$H_z = J_o(s\rho) \qquad (\rho \leq w) \qquad (C.27)$$

$$E_\phi = \frac{-i}{s}\ \omega\mu_o\ J_o'(s\rho) \qquad (\rho \leq w) \qquad (C.28)$$

$$H_\rho = \frac{i\beta}{s}\ J_o'(s\rho) \qquad (\rho \leq w) \qquad (C.29)$$

and

$$H_z = -\frac{\delta}{s}\frac{J_1(sw)}{K_1(\delta w)}\ K_o(\delta\rho) \qquad (\rho \geq w) \qquad (C.30)$$

$$E_\phi = -\frac{i\omega\mu_o}{s}\frac{J_1(sw)}{K_1(\delta w)}\ K_o'(\delta\rho) \qquad (\rho \geq w) \qquad (C.31)$$

$$H_\rho = -\frac{i\beta}{s}\ \frac{J_1(sw)}{K_1(\delta w)}\ K_o'(\delta\rho) \qquad (\rho \geq w) \qquad (C.32)$$

where we have used the condition of continuous E_ϕ at $\rho = w$ to give

$$\frac{D}{B} = -\frac{\delta}{s}\ \frac{J_1(sw)}{K_1(\delta w)} \qquad (C.33)$$

Many detailed treatments of cylindrical dielectric waveguides are available including those by Borgnis and Papas,[31] Marcuse,[28] Collin,[29] and Yeh[32].

Appendix D

SPACE HARMONICS AND COUPLED MODE THEORY -- SOME COMMENTS AND OBSERVATIONS

In this appendix we discuss similarities between the methods of space harmonics and coupled mode theory. In Chapter II, Section A, the space harmonics approach is developed, and in Chapter II, Section B, a coupled mode theory for DFB lasers is developed. In Chapter IV, a coupled-mode-like approach is used to derive coupling coefficients.

Beginning with (2.39) (see Chapter II, Section A),

$$E_y(x,z) = \sum_{n=-\infty}^{\infty} \sum_{r=-R}^{R} d_{n,r}\, a_{n,r}(x) e^{i(\beta_r + nK)z} \tag{D.1}$$

and we can write (2.12) as

$$\sum_{n=-\infty}^{\infty} \sum_{r=-R}^{R} \left[\left(\frac{d^2 a_{n,r}(x)}{dx^2} - a_{n,r}(x) \left\{ (\beta_r + nK)^2 - \varepsilon_1 k^2 \right\} \right) d_{n,r} \right.$$

$$\left. + \varepsilon_1 \frac{n}{2} k^2 \left\{ a_{n-1,r}(x)\, d_{n-1,r} + a_{n+1,r}(x)\, d_{n+1,r} \right\} \right] e^{i(\beta_r + nK)z} = 0 \tag{D.2}$$

Looking only at the n = 0 space harmonic we can write

$$\sum_{r=-R}^{R} \left[\left(\frac{d^2 a_{0,r}(x)}{dx^2} - a_{0,r}(x) \left\{ \beta_r^2 - \varepsilon_1 k^2 \right\} \right) d_{0,r} \right.$$

$$\left. + \varepsilon_1 \frac{n}{2} k^2 \left\{ a_{-1,r}(x)\, d_{-1,r} + a_{1,r}(x)\, d_{1,r} \right\} \right] = 0 \tag{D.3}$$

Similarly, for the n = 1 and n=-1 space harmonics,

$$\sum_{r=-R}^{R} \left[\left(\frac{d^2 a_{-1,r}(x)}{dx^2} - a_{-1,r}(x) \left\{ (\beta_r - K)^2 - \varepsilon_1 k^2 \right\} \right) d_{-1,r} + \varepsilon_1 \frac{n}{2} k^2 \left\{ a_{-2,r}(x)\, d_{-2,r} + a_{0,r}(x)\, d_{0,r} \right\} \right] = 0 \quad (D.4)$$

and

$$\sum_{r=-R}^{R} \left[\left(\frac{d^2 a_{1,r}(x)}{dx^2} - a_{1,r}(x) \left\{ (\beta_r + K)^2 - \varepsilon_1 k^2 \right\} \right) d_{1,r} + \varepsilon_1 \frac{n}{2} k^2 \left\{ a_{0,r}(x) d_{0,r} + a_{2,r}(x) d_{2,r} \right\} \right] = 0 \quad (D.5)$$

If energy is initially flowing in the waveguide structure in the 0^{th} harmonic of the $+p^{th}$ mode at a frequency $\omega = \omega_{pq} + \Delta\omega$ as indicated in Fig. D.1, only the -1^{th} space harmonic of the $-q^{th}$ mode is expected to have significant amplitude (see Chapter II Section A and Refs. 38 and 54). However, in a DFB laser, stimulated emission will excite equally the $+p^{th}$, $-p^{th}$, $+q^{th}$ and $-q^{th}$ modes. For this reason, all eight space harmonics indicated in Fig. D.1 will have significant amplitudes. Equations (D.3), (D.4), and (D.5) thus become

$$\left[\frac{d^2 a_{0,-p}(x)}{dx^2} - a_{0,-p}(x) \left\{ \beta_{-p}^2 - \varepsilon_1 k^2 \right\} \right] d_{0,-p} + \varepsilon_1 \frac{n}{2} k^2 a_{1,q}(x)\, d_{1,q} = 0 \quad (D.6a)$$

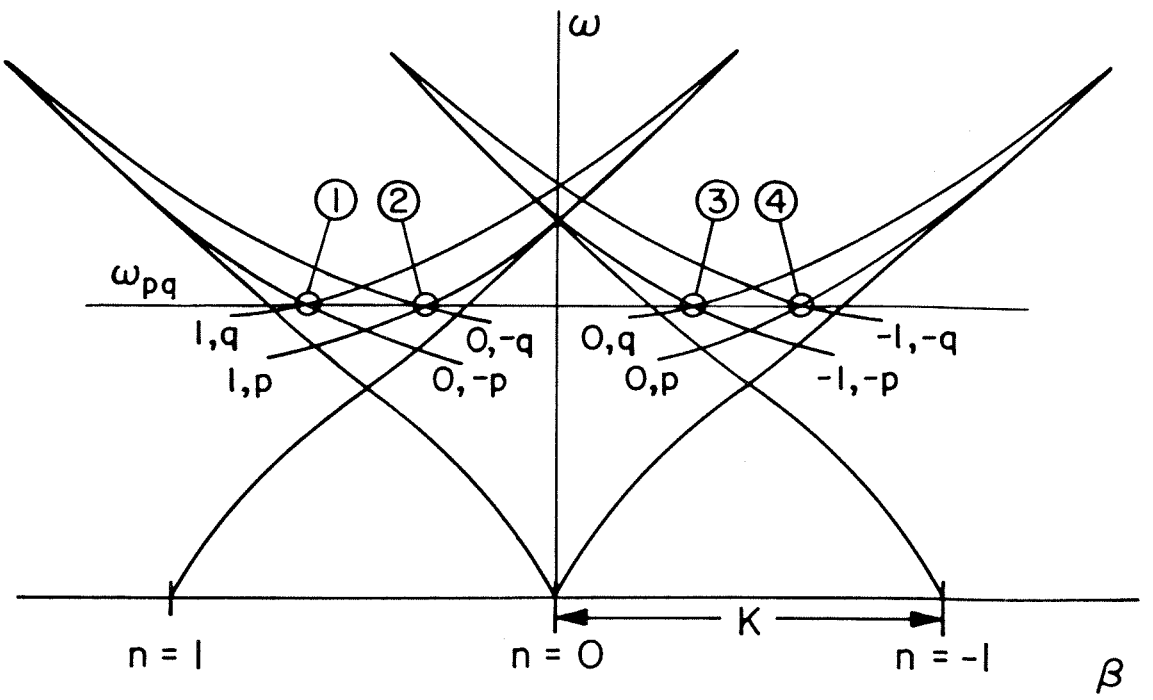

Fig. D.1 For the frequency ω_{pq}, eight space harmonics have significant amplitudes.

$$\left[\frac{d^2a_{1,q}(x)}{dx^2} - a_{1,q}(x)\left\{(\beta_q + K)^2 - \varepsilon_1 k^2\right\}\right] d_{1,q}$$

$$+ \varepsilon_1 \frac{\eta}{2} k^2 a_{0,-p}(x)\, d_{0,-p} = 0 \qquad \text{(D.6b)}$$

$$\left[\frac{d^2a_{0,-q}(x)}{dx^2} - a_{0,-q}(x)\left\{\beta_{-q}^2 - \varepsilon_1 k^2\right\}\right] d_{0,-q}$$

$$+ \varepsilon_1 \frac{\eta}{2} k^2 a_{1,p}(x)\, d_{1,p} = 0 \qquad \text{(D.7a)}$$

$$\left[\frac{d^2a_{1,p}(x)}{dx^2} - a_{1,p}(x)\left\{(\beta_p + K)^2 - \varepsilon_1 k^2\right\}\right] d_{1,p}$$

$$+ \varepsilon_1 \frac{\eta}{2} k^2\, a_{0,-q}(x)\, d_{0,-q} = 0 \qquad \text{(D.7b)}$$

$$\left[\frac{d^2a_{0,q}}{dx^2} - a_{0,q}(x)\left\{\beta_q^2 - \varepsilon_1 k^2\right\}\right] d_{0,q}$$

$$+ \varepsilon_1 \frac{\eta}{2} k^2\, a_{-1,-p}(x)\, d_{-1,-p} = 0 \qquad \text{(D.8a)}$$

$$\left[\frac{d^2a_{-1,-p}}{dx^2} - a_{-1,-p}(x)\left\{(\beta_{-p}-K)^2 - \varepsilon_1 k^2\right\}\right] d_{-1,-p}$$

$$+ \varepsilon_1 \frac{\eta}{2} k^2\, a_{0,q}(x)\, d_{0,q} = 0 \qquad \text{(D.8b)}$$

$$\left[\frac{d^2a_{0,p}(x)}{dx^2} - a_{0,p}(x)\left\{\beta_p^2 - \varepsilon_1 k^2\right\}\right] d_{0,p}$$

$$+ \varepsilon_1 \frac{\eta}{2} k^2\, a_{-1,-q}(x)\, d_{1,q} = 0 \qquad \text{(D.9a)}$$

and

$$\left[\frac{d^2 a_{-1,-q}(x)}{dx^2} - a_{-1,-q}(x)\left\{(\beta_{-q}-K)^2 - \varepsilon_1 k^2\right\}\right] d_{-1,-q}$$

$$+ \varepsilon_1 \frac{n}{2} k^2 a_{0,p}(x) d_{0,p} = 0 \qquad \text{(D.9b)}$$

where $\beta_{-r} = -\beta_r$. Equations (D.6 a,b) describes the coupling of the two space harmonics indicated by 1 in Fig. D.1; (D.7 a,b), (D.8a,b), and (D.9a,b) correspond to the intersections (coupling) indicated by 2, 3, and 4. By inspection of Fig. D.1, we see that at 1 ,

$$\beta_{-p} = \beta_q + K \qquad \text{(D.10a)}$$

at 2 ,

$$\beta_{-q} = \beta_p + K \qquad \text{(D.10b)}$$

at 3 ,

$$\beta_q = \beta_{-p} - K \qquad \text{(D.10c)}$$

at 4 ,

$$\beta_p = \beta_{-q} - K \qquad \text{(D.10d)}$$

Thus all the $n = \pm 1, \pm p^{th}$ space harmonics propagate with phase velocities of the $n = 0, \mp q^{th}$ space harmonics and the $n = \pm 1, \pm q^{th}$ space harmonics propagate with phase velocities of the $n = 0, \mp p^{th}$ space harmonics. Thus the starting point (Chapter II (2.4)):

$$E_{pq}(x,z) = a_p(x)d_p(z)e^{i\beta_{po}z} + a_q(x)d_q(z)\, e^{-i\beta_{qo}z} \qquad \text{(D.11)}$$

for the derivation of the coupled mode theory includes implicitly the $n = \pm 1$ space harmonics. This is an important point, because for n as

large as 0.4, only the n = 0 and the -1^{st} or $+1^{st}$ space harmonic has significant amplitude.[38,54] Neglecting the last two terms in (2.48) corresponds to neglecting higher order space harmonics as was done in going from (D.3), (D.4), and (D.5) to (D.6 a,b), (D.7 a,b), (D.8 a,b). and (D.9 a,b).

In the transversely bounded medium, (D.6 a,b) through (D.9 a,b) correspond to (2.29 a,b) for the infinite medium; all have the same general form as the coupled wave equations (2.53 a,b).

In Chapter II Section A and throughout Chapter IV, the symbol $\Delta\beta$ represents the correction to the unperturbed longitudinal wavevector β. For coupled mode theory (Chpater II, Section B), the corresponding correction term is γ. The dispersion relations for the various perturbed dielectric waveguides in Chapter IV are all of the form (4.32):

$$\frac{\Delta\beta}{K} = (\theta_p - \theta_q)\frac{\Delta\omega}{\omega_{pq}} \pm \sqrt{(\theta_p+\theta_q)^2\left(\frac{\Delta\omega}{\omega_{pq}}\right)^2 - \eta^2(\xi_{pq})^2} \qquad (D.12)$$

A similar relation holds for the transversely infinite medium (2.35):

$$\frac{\Delta\beta}{\beta_o} = \pm\sqrt{\left(\frac{\eta}{4}\right)^2 - \left(\frac{\Delta\omega}{\omega_o}\right)^2} \qquad (D.13)$$

From the coupled wave theory (2.35),

$$\gamma_{1,2} = \left(\frac{C_p(k)-C_q(k)}{2}\right)G + ic\left(\frac{\psi_p(k)-\psi_q(k)}{2}\right)\Delta k \pm \sqrt{\chi_{pq}^2(k) + \left[\left(\frac{C_p(k)+C_q(k)}{2}\right)G + ic\left(\frac{\psi_p(k)+\psi_q(k)}{2}\right)\Delta k\right]^2} \qquad (D.14)$$

Equation (D.14) has the form of (D.12) and (D.13) when the gain G is equal to zero. The resulting behavior of $\gamma_{1,2}$ (or $\Delta\beta$) is the well known dispersive nature of periodic structures discussed in Chapter II and Chapter IV. When gain is introduced into the structure, we can use (D.14) to obtain the normalized shape of the dispersion curve indicated in Fig. D.2. For active interactions between modes where $q \neq p$, the dispersion diagram is similar to Fig. D.2 but slanted in the manner of Fig. 2.6b.

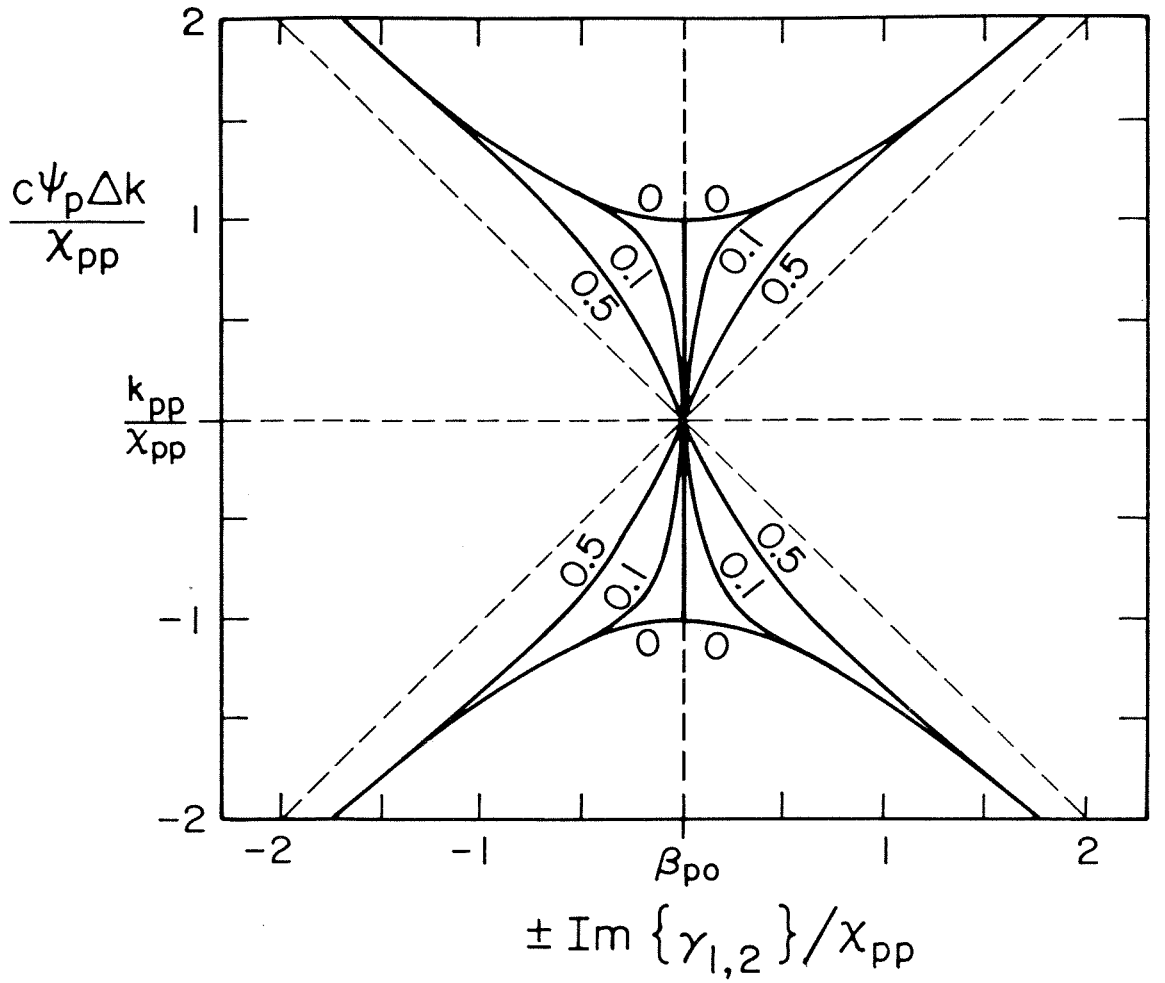

Fig. D.2 Normalized plot of Δk versus $\mathrm{Im}\{\gamma\}$ for ratios of $c_p G/\chi_{pp} = 0, 0.1, 0.5$. (Adapted from Reference 1).

References

1) H. Kogelnik and C. V. Shank, "Coupled-Wave Theory of Distributed Feedback Lasers," J. Appl. Phys., Vol. 43, No. 5 (May 1972), p. 2327.

2) D. Marcuse, "Hollow Dielectric Waveguide for Distributed Feedback Lasers," IEEE JQE, Vol. QE-8, No. 7 (July 1972), p. 661.

3) A. E. Siegman, An Introduction to Lasers and Masers, McGraw-Hill Book Co., New York 1971.

4) C. Elachi, G. Evans, and G. Franceschetti, "Diffused Optical Waveguides," to be published in Alta Frequenzia.

5) S. Wang, "Proposal of Periodic Layered Waveguide Structures for Distributed Lasers," J. Appl. Phys., Vol. 44, No. 2 (February 1973), p. 767.

6) S. Wang, "Principles of Distributed Feedback (DFB) and Distributed Bragg-Reflector (DBR) Lasers," Topical Meeting on Integrated Optics, New Orleans, Louisiana, January 1974.

7) R. E. DeWames and W. F. Hall, "Conditions for Laser Oscillations in Distributed Feedback Waveguides," Appl. Phys. Lett., Vol. 23, No. 1 (1 July 1973), p. 28.

8) S. Chinn, "Effects of Mirror Reflectivity in a Distributed Feedback Laser," IEEE JQE, Vol. QE-9, No. 6 (June 1973), p. 574.

9) R. Shubert and D. B. Anderson, "Characteristics of Nonuniform Distributed Feedback Waveguide Lasers," IEEE/OSA Conference on Laser Engineering and Applications, Washington, D. C., May 1973.

10) R. Shubert, "Generalized Theory of Thin Film Distributed-Feedback

Lasers," Topical Meeting on Integrated Optics, New Orleans, Louisiana, January 1974.

11) C. Elachi, G. Evans, and C. Yeh, "Parametric Optimization of Thin Film DFB Lasers," Topical Meeting on Integrated Optics, New Orleans, Louisiana, January 1974.

12) E. Conwell, "Modes in Optical Waveguides Formed by Diffusion," Appl. Phys. Lett., Vol. 23, No. 6 (15 September 1973), p. 328.

13) Laser Focus, Vol. 9, No. 5 (May 1973), p. 10.

14) Laser Focus, Vol. 9, No. 12 (December 1973), p. 3.

15) F. Grunthaner, "Characterization, Site Analysis, and Surface Reactivity of Transition Metal Complexes and Metalloproteins by X-Ray Photoelectron Spectroscopy," Ph.D. Thesis, California Institute of Technology, 1974.

16) B. Batterman and H. Cole, "Dynamical Diffraction of X-Rays by Perfect Crystals," Rev. Mod. Phys., Vol. 36, No. 3 (July 1964), p. 681.

17) C. F. Quate, C. D. Wilkinson, and D. K. Winslow, "Interaction of Light and Microwave Sound," Proc. IEEE, Vol. 53, No. 10 (October 1965), p. 1604.

18) E. I. Gordon and M. G. Cohen, "Electro-optic Diffraction Grating for Light Beam Modulation and Diffraction," IEEE JQE, Vol. QE-1, No. 5 (August 1965), p. 191.

19) H. Kogelnik, "Coupled Wave Theory for Thick Hologram Gratings," B.S.T.J., Vol. 48, No. 9 (November 1969), p. 2909.

20) C. Elachi and C. Yeh, "Periodic Structures in Integrated Optics," J. Appl. Phys., Vol. 44, No. 7 (July 1973), p. 3146.

21) C. Elachi, "Electromagnetic Wave Propagation and Source Radiation in Space-Time Periodic Media," Ph.D. Thesis, California Institute of Technology, 1971.

22) C. Elachi and C. Yeh, "Mode Conversion in Period Structures," to be published in J. Appl. Phys., August 1974.

23) E. A. Coddington, An Introduction to Ordinary Differential Equations, Englewood Cliffs, N. J., Prentice-Hall, Inc. 1961.

24) M. Born and E. Wolf, Principles of Optics, Oxford, Pergamon Press, 4th edition 1970.

25) R. Shubert, "Theory of Optical Waveguide Distributed Lasers with Nonuniform Gain and Coupling," J. Appl. Phys., Vol. 45, No. 1 (January 1974), p. 209.

26) R. Ulbrich and M. H. Pilkuhn, "Longitudinal Photon Flux Distribution in Low-Q Semiconductor Lasers," Appl. Phys. Lett., Vol. 16, No. 12 (15 June 1970), p. 516.

27) J. W. Crowe and R. M. Craig, Jr., "Small Signal Amplification in GaAs Lasers," Appl. Phys. Lett., Vol. 4, No. 3 (1 February 1964), p. 57.

28) D. Marcuse, Light Transmission Optics, New York, Van Nostrand Reinhold Company, 1972.

29) R. E. Collin, Field Theory of Guided Waves, New York, McGraw-Hill Book Company, Inc. 1960.

30) M. Abramowitz and A. Segun, editors, Handbook of Mathematical Functions, New York, Dover Publications, Inc. 1968.

31) F. Borgnis and C. H. Papas, "Electromagnetic Waveguides and Resonators," appearing in Handbuch der Physik, Vol. 16: Elektrische

Felder und Wellen, edited by S. Flügge, Springer-Verlag, Berlin, 1958.

32) C. Yeh, "Electromagnetic Surface-Wave Propagation Along a Dielectric Cylinder of Elliptical Cross Section," Ph.D. Thesis, California Institute of Technology, 1961.

33) R. Chu and T. Tamir, "Guided-Wave Theory of Light Diffraction by Acoustic Microwaves," IEEE Transactions, Vol. MTT-18, No. 8 (August 1970), p. 486.

34) D. Marcuse, "Mode Conversion Caused by Surface Imperfections of a Dielectric Slab Waveguide," B.S.T.J., Vol. 48, No. 10 (December 1969), p. 3187.

35) D. Marcuse, Theory of Dielectric Optical Waveguides, Academic Press, Inc. New York, 1974.

36) C. H. Papas, Theory of Electromagnetic Wave Propagation, McGraw-Hill, New York, 1965.

37) A. Hessel, "General Characteristics of Travelling-Wave Antennas," appearing in Antenna Theory Part II, edited by R. E. Collin and F. J. Zucker, McGraw-Hill, New York, 1969.

38) E. S. Cassedy, "Waves Guided by a Boundary with Time-Space Periodic Modulation," Proc. IEEE, Vol. 112, No. 2 (February 1965), p. 269.

39) E. S. Cassedy and A. A. Oliver, "Dispersion Relations in Time-Space Periodic Media: Part I - Stable Interactions," Proc. IEEE, Vol. 51, No. 10 (October 1963), p. 1342.

40) P. Bernardi and A. Salsamo, "Wave Propagation in Rectangular Waveguides Having a Time-Space Periodically Modulated Side-Wall,"

URSI Symposium on Electromagnetic Waves 1968, Alta Frequenza, p. 77.

41) F. Odeh and J. Keller, "Partial Differential Equations with Periodic Coefficients and Bloch Waves in Crystals," J. Math. Phys., Vol. 5, No. 11 (November 1964), p. 1499.

42) E. L. Ince, Ordinary Differential Equations, Dover Publications, Inc., New York, 1956.

43) F. Bloch, "Über die Quantenmechanik der Elektronen in Kristallgittern," Z. Physic, Vol. 52 (1928), p. 555.

44) R. Shubert and J. H. Harris, "Optical Surface Waves on Thin Films and their Applications to Integrated Data Processors," IEEE Transactions, Vol. MTT-16, No. 12 (December 1968), p. 1048.

45) J. R. Pierce, "Coupling of Modes of Propagation," J. Appl. Phys., Vol. 25, No. 2 (February 1954), p. 179.

46) J. R. Pierce, Almost Everything About Waves, MIT Press, Cambridge, Massachusetts, 1974.

47) L. Brillouin, Wave Propagation in Periodic Structures, McGraw-Hill, New York, 1946.

48) Lord Rayleigh, "On the Maintenance of Vibrations by Forces of Double Frequency, and on the Propagation of Waves through a Medium Endowed with a Periodic Structure," Phil. Mag., Vol. 24 (1887), p. 145.

49) M. J. O. Strutt, "Zur Wellenmechanik der Atomgitters," Ann. Der. Phys., Vol. 87, No. 10 (1928), p. 319.

50) B. Van der Pol and M. J. O. Strutt, "On the Stability of the Solutions of Mathieu's Equations," Phil. Mag., Vol. 5, No. 27, (January 1928), p. 18.

51) C. Kittel, Introduction to Solid State Physics, 4th edition, John Wiley and Sons, Inc., New York 1971.

52) Y. Ninomiya, "Recording Characteristics of Volume Holograms," J.O.S.A., Vol. 63, No. 9,(September 1973), p. 1124.

53) F. W. Dabby, A. Kestenbaum, and U. C. Paek, "Periodic Dielectric Waveguides," Opt. Comm., Vol. 6, No. 2 (October 1972), p. 125.

54) A. Hessel, "Guiding and Scattering by Sinusoidally Modulated Reactance Surfaces," Microwave Res. Inst. Rept. R-825-60, Polytechnic Institute of Brooklyn, June 1960.

55) W. S. C. Chang, "Periodic Structures and their Application in Integrated Optics," IEEE Transactions, Vol. MTT-21, No. 12 (December 1973), p. 775.

56) L. Kuhn, P. F. Heidrich, and E. G.Lean, "Optical Guided Wave Mode Conversion by an Acoustic Surface Wave," Appl. Phys. Lett., Vol. 19, No. 10 (15 November 1971), p. 428.

57) T. P. Sosnowski, "Polarization Mode Filters for Integrated Optics," Opt. Comm., Vol. 4, No. 6 (February 1972), p. 408.

58) S. Wang, M. Shaw, and J. D. Crow, "Studies of the Use of Gyrotropic and Anisotropic Materials for Mode Conversion in Thin-Film Optical-Waveguide Applications," J. Appl. Phys., Vol. 43, No. 4 (April 1972), p. 1861.

59) J. E. Bjorkholm, T. P. Sosnowski, and C. V. Shank, "Distributed-Feedback Lasers in Optical Waveguides Deposited on Anisotropic Substrates," Appl. Phys. Lett., Vol. 22, No. 4 (15 February 1973), p. 132.

60) H. Kogelnik, C. V. Shank, and J. E. Bjorkholm, "Hybrid Scattering in Periodic Waveguides," Appl. Phys. Lett., Vol. 22, No. 4 (15 February 1973), p. 135.

61) B. B. Snavely, "Flashlamp-Excited Organic Dye Lasers," Proc. IEEE, Vol. 57, No. 8 (August 1969), p. 1374.

62) A. Hessel, M. H. Chenn, R. C. M. Li, and A. A. Oliver, "Propagation in Periodically Loaded Waveguides with Higher Symmetries," Proc. IEEE, Vol. 61, No. 2 (February 1973), p. 183.

63) J. M. Ortega, W. C. Rinebolt, Iterative Solutions of Nonlinear Equations in Several Variables, Academic Press, New York, 1970.

64) W. J. Cody, A. J. Strecok, and H. C.Thacher, Jr., "Chebyshev Approximation for the Psi Function," Math. Comp., Vol. 27, No. 121 (January 1973), p. 123.

65) J. R. Airey, "The Bessel Function Derivatives $\partial/\partial\nu\ J_\nu(x)$ and $\partial^2/\partial\nu^2 J_\nu(x)$," Phil. Mag., Vol. 19, No. 125 (February 1935), p. 236.

66) J. R. Airey, "Tables of the Bessel Function Derivative $\partial/\partial\nu\ J_\nu(x)$; $\nu = \pm 1/2, \pm 3/2$," Report of the Math. Tables Comm., British Association, 1928.

67) S. E. Miller, E.A.J. Marcatili, and T. Li, "Research Towards Optical-Fiber Transmission Systems," Proc. of the IEEE, Vol. 61, No. 12 (December 1973), p. 1703.

68) H. Kogelnik and C. V. Shank, "Stimulated Emission in a Periodic Structure," Appl. Phys. Lett., Vol. 18, No. 4 (15 February 1971), p. 152.

69) C. V. Shank, J. E. Bjorkholm, and H. Kogelnik, "Tunable Distributed-Feedback Dye Laser," Appl. Phys. Lett., Vol. 18, No. 9 (1 May 1971), p. 395.

70) K. O. Hill and A. Watanabe, "A Distributed Feedback Side-Coupled

Laser," Opt. Comm., Vol. 5, No. 5 (August 1972), p. 389.

71) D. P. Schinke, R. G. Smith, E. G. Spencer, and M. F. Galvin, "Thin Film Distributed Feedback Laser Fabricated by Ion Milling," Appl. Phys. Lett., Vol. 21, No. 10 (15 November 1972), p. 494.

72) J. E. Bjorkholm and C. V. Shank, "Higher-Order Distributed Feedback Oscillators," Appl. Phys. Lett., Vol. 20, No. 8 (15 April 1972), p. 306.

73) M. Nakamura, A. Yariv, H. W. Yen, S. Somekh, and H. L. Garvin, "Optically Pumped GaAs Surface Laser with Corrugation Feedback," Appl. Phys. Lett., Vol. 22, No. 10 (15 May 1973), p. 515.

74) J. W. S. Rayleigh, The Theory of Sound, Vol. II, Dover, New York, 1945.

75) R. F. Millar, "On the Rayleigh Assumption in Scattering from a Periodic Surface," Proc. Camb. Phil. Soc., Vol. 65, Part 3 (May 1969), p. 773.

76) R. F. Millar, "On the Rayleigh Assumption in Scattering from a Periodic Surface II" Proc. Camb. Phil. Soc., Vol. 69, Part I (January 1971), p. 217.

77) A. Yariv, Quantum Electronics, John Wiley and Sons, Inc., New York, 1967.

78) A. Yariv, Introduction to Optical Electronics, Holt, Rinehart, and Winston, Inc., New York, 1971.

Postscript:

I would hate to tell you what this lousy little book cost me in money and anxiety and time...I've finished my war book now. The next one I write is going to be fun.

Kurt Vonnegut, Jr.

Slaughterhouse--five